



**The ESS Project  
Volume IV**

**Instruments  
and User Support**



The ESS Council thanks ENSA, ESF and CEC for stimulating this study and gratefully acknowledges the support from the CEC (Infrastructure Cooperation Network HPRI-CT-2001-40027 and Neutron Round-Table HPRI-CT-1999-40007) and the ongoing encouragement and support from the laboratories and organisations throughout Europe, which have been involved in this phase of the Project.

Publisher: ESS Council

Distribution: ESS Central Project Team  
c/o Forschungszentrum Jülich  
D – 52425 Jülich, Germany  
Phone: + 49 2461 61 2244  
Fax: + 49 2461 61 4155  
E-mail: [esscpt@fz-juelich.de](mailto:esscpt@fz-juelich.de)  
Web site: <http://www.ess-europe.de>

Cover Layout: Andreas Henrich, Kunsthochschule für Medien Köln  
Mediengestaltung, Peter-Welter-Platz 2, 50676 Köln, Germany

Printing: Druckerei Plump OHG, Postfach 1569, 53585 Bad Honnef, Germany

Copyright: ESS Council 2002

ISBN 3-89336-299-1 Complete Edition  
ISBN 3-89336-300-9 Volume I: Quelle des Wissens (German)  
ISBN 3-89336-301-7 Volume I: European Source of Science (English)  
ISBN 3-89336-302-5 Volume II: New Science and Technology for the 21<sup>st</sup> Century  
ISBN 3-89336-303-3 Volume III: Technical Report

ISBN 3-89336-304-1 Volume IV: Instruments and User Support

ISSN 1443-559X

May 2002

Editorial Board: K Clausen, R Eccleston , P Fabi, T Gutberlet, F Mezei, H Tietze-Jaensch

The ESS Council does not accept any responsibility for loss or damage arising from the use of information contained in this report. Reproduction including extracts is permitted subject to crediting the source.

**The European Spallation Source Project**

---

# **The ESS Project**

**Volume IV**

Instruments and User Support

# The European Spallation Source Project

---

## ESS Council

F Barocchi, INFN, Univ. Firenze  
A Belushkin, JINR, Dubna  
R Cywinski, ENSA, Univ. Leeds  
R Eichler, PSI, Villigen  
R Feidenhans'l, Risø, Roskilde  
F Gounand, CEA, Saclay  
H Klein, Univ. Frankfurt/Main  
E Koptelov, INR, Moscow  
H Rauch, Atominstytut, TU Wien  
D Reistad, Univ. Uppsala  
D Schildt, CCLRC, Oxfordshire  
U Steigenberger (*Secretary*), CCLRC, Oxfordshire

M Steiner, HMI, Berlin  
P Tindemans (*Chairman*), The Hague  
A Verkooijen, IRI, Delft  
R Wagner, FZJ, Jülich  
F Yndurain, CIEMAT, Madrid  
M Zoppi, CNR, Firenze  
**Observers:**  
C Carlile, ILL, Grenoble  
A Fontaine, CNRS, Univ. Paris Sud  
T Mason, SNS, Oak Ridge  
S Nagamiya, JSNS, Tsukuba  
G Ricco, INFN, Univ. Genova  
N Williams, ESF, Strasbourg

## ESS Project Directorate

K Clausen, Risø, Roskilde  
I Gardner, RAL, Didcot

J-L Laclare (*Project Director*), CEA Saclay  
D Richter, FZJ, Jülich

## ESS Task Leaders and Deputies

### **Instrumentation:**

F Mezei, HMI, Berlin  
R Eccleston, CCLRC, Oxfordshire

### **Target Systems:**

G Bauer, FZJ, Jülich  
T Broome, CCLRC, Oxfordshire

### **Ring & Achromat:**

C Prior, CCLRC, Oxfordshire

### **Linac:**

A Mosnier, CEA, Saclay

### **Beam Transport:**

R Maier, FZJ, Jülich

### **Conventional Facilities:**

P Giovannoni, CEA, Saclay

## ESS Central Project Team

F H Bohn  
F Carsughi  
A Claver  
K Clausen (*Director*)  
C Desailly\*

P Fabi  
Ch Hake  
S Palanque\*  
H Tietze-Jaensch

---

\* members of the staff supporting the project chairman in Saclay.

# The European Spallation Source Project

---

## ESS Scientific Advisory Committee

J Colmenero, Univ. of the Basque Country  
R Cywinski, Univ. Leeds  
W I F David, CCLRC, Oxfordshire  
C Fermon, CEA, Saclay  
A Furrer, ETHZ & PSI, Villigen  
J R Helliwell, CLRC, Daresbury  
S Ikeda, KENS/KEK, Tsukuba  
G H Lander, IfT, Karlsruhe  
H Jobic, Univ. Lyon  
T Lorentzen, DanStir ApS,  
Frederiksborgvej (until Autumn 2001)  
T Mason, SNS, Oak Ridge

R L McGreevy, Univ. Uppsala - CCLRC,  
Oxfordshire  
F M Mulder, Univ. Delft  
H Rauch, Atominstut, TU Wien  
D Richter (*Chairman*), FZJ, Jülich  
R Rinaldi, Univ. Perugia  
W G Stirling, ESRF, Grenoble  
C Vettier, ILL, Grenoble  
A Wischnewski (*SAC Assistant*), FZJ, Jülich  
H Zabel, Univ. Bochum

## ESS Technical Advisory Committee

### **Target:**

J Carpenter, Argonne National Lab.  
M Furusaka, KENS/KEK, Tsukuba  
K Jones, Los Alamos National Lab.  
J Knebel, FZK, Karlsruhe

### **Linac:**

R Garoby, CERN, Geneva  
D Proch, DESY, Hamburg  
J Stovall, Los Alamos National Lab.  
Y Yamazaki, JAERI/KEK, Tsukuba

### **Instruments:**

M Arai, KENS/KEK, Tsukuba  
P Böni, TU, München  
G H Lander (*Chairman*), IfT, Karlsruhe  
D Myles, EMBL, Grenoble  
W Press, ILL, Grenoble

### **Rings:**

H Schönauer, CERN, Geneva  
W T Weng, Brookhaven National Lab.

### **Conventional Facilities:**

J Lawson, SNS, Oak Ridge  
J-P Magnien, ESRF, Grenoble

**The European Spallation Source Project**

---

# **The ESS Project**

Volume I  
**European Source of Science**

Volume II  
**New Science and Technology  
for the 21<sup>st</sup> Century**

Volume III  
**Technical Report**

Volume IV  
**Instruments and User Support**

## Contents of Volume IV

---

### Instruments and User Support

|      |  |        |
|------|--|--------|
| I    | <b>Introduction</b>  | I - 1  |
| 1.   | <b>ESS Neutron Instrument Suite and Layout</b>                           | 1 - 1  |
|      | Tables of Instruments  | 1 - 10 |
| 2.   | <b>ESS Reference Instrument Performance Sheets</b>                       | 2 - 1  |
| -    | Thermal chopper spectrometer (medium resolution)                         | 2 - 4  |
| -    | High resolution single crystal diffractometer (chemical crystallography) | 2 - 6  |
| -    | Liquids and amorphous material diffractometer                            | 2 - 8  |
| -    | High resolution protein single crystal diffractometer                    | 2 - 10 |
| -    | Single pulse diffractometer  | 2 - 12 |
| -    | High energy chopper spectrometer (high resolution, low Q)                | 2 - 14 |
| -    | Tomography / Radiography instrument                                      | 2 - 16 |
| -    | Engineering diffractometer   | 2 - 19 |
| -    | Magnetic powder diffractometer   | 2 - 22 |
| -    | High resolution powder diffractometer                                    | 2 - 24 |
| -    | High resolution backscattering spectrometer (0.8 $\mu\text{eV}$ )        | 2 - 26 |
| -    | High resolution backscattering spectrometer (1.5 $\mu\text{eV}$ )        | 2 - 28 |
| -    | High resolution reflectometer  | 2 - 30 |
| -    | Cold chopper spectrometer (low resolution)                               | 2 - 32 |
| -    | Variable resolution cold neutron chopper spectrometer                    | 2 - 36 |
| -    | High intensity SANS instrument   | 2 - 38 |
| -    | Wide angle NSE spectrometer / Diffuse scattering (D7 – type)             | 2 - 40 |
| -    | Particle physics beam lines  | 2 - 44 |
| -    | High intensity reflectometer   | 2 - 46 |
| -    | Focussing mirror low q SANS instrument                                   | 2 - 48 |
| -    | High resolution NSE spectrometer   | 2 - 50 |
| 3.   | <b>Flight Simulators for Neutrons: Virtual Instruments for the ESS</b>   | 3 - 1  |
| 4.   | <b>Non-neutron Scattering Applications</b>                               | 4 - 1  |
| 4.1. | Radioactive Beam Facility at ESS   | 4 - 3  |
| 4.2. | Ultra-Cold Neutron Source at ESS   | 4 - 8  |
| 4.3. | Muon Scattering Facility at the ESS                                      | 4 - 10 |
| 5.   | <b>Sample Environment and Scientific Utilisation</b>                     | 5 - 1  |

## Authors and Contributors

### ESS Instrumentation Task Group:

Ferenc Mezei (Leader), HMI  
Roger Eccleston (Deputy), ISIS  
Thomas Gutberlet (Assistant), HMI  
Holger Tietze-Jaensch (CPT Coordinator) ESS / FZJ

### Direct Geometry Spectrometer:

Roger Eccleston,\* ISIS  
Rob Bewley, ISIS  
Ruep E. Lechner, HMI  
Feri Mezei, HMI  
Hannu Mutka, ILL  
Heloisa Nunes Bordallo HMI  
Henrik Ronnow, ILL  
Werner Schweika, FZJ

### Indirect Geometry Spectrometer:

Ken Andersen,\* ISIS  
Peter Allenspach, PSI  
Danielle Colognesi, ISIS  
Bjoern Fak, ISIS  
Oliver Kirstein, FZJ  
Marco Zoppi, CNR

### Engineering:

Philip J. Withers,\* Manchester  
Mark Daymond, ISIS  
Eberhard Lehmann, PSI  
Torben Lorentzen, Riso  
Walter Reimers, HMI  
Burghard Schillinger, TUM  
Axel Steuwer, Manchester

### SANS:

Richard Heenan,\* ISIS  
Bob Cubitt, ILL  
Kell Mortensen, Riso  
Dietmar Schwahn, FZJ  
Albrecht Wiedenmann, HMI

### Reflectometry:

Helmut Fritzsche,\* HMI  
Claude Fermon, LLB  
John Webster, ISIS

### MC Simulation:

Geza Zsigmond,\* HMI  
Klaus Lieutenant, HMI  
Kim Lefmann, Riso

### Single Crystal Diffraction:

Chick Wilson,\* ISIS  
Wolfgang Jauch, HMI  
Gary McIntyre, ILL  
Dean Myles, EMBL  
Judith Peters, HMI

### Powder Diffraction:

Paolo Radaelli,\* ISIS  
A.M. Balagurov, JINR  
Hans-Jürgen Bleif, HMI  
Steve Hull, ISIS  
J. Rodriguez Carvajal, LLB  
Emmanuelle Suard, ILL

### NSE:

Michael Monkenbusch,\* FZJ  
Bela Farago, ILL  
Goerg Ehlers, ILL  
Catja Pappas, HMI  
Ross Stewart, ILL

### S(q):

Alan Soper,\* ISIS  
Robert McGreevy, Studsvik

### Particle Physics:

Hartmut Abele,\* Heidelberg  
Hans Boerner, ILL  
Manfred Daum, PSI  
W. Heil, Mainz  
Anatoli Serebrov, PNPI

### Non-neutron Scattering

Hans Boerner, ILL  
Robert Cywinski, Leeds  
Helmut Rauch, AI Wien  
Gary Simpson, ILL

\*group convenor



# **INTRODUCTION**



## I INTRODUCTION

This volume of ESS Project 2002 aims at giving a preliminary taste of the first ESS "user guide" that the neutron research community will be provided with in about 10 years from now in order to help to prepare their first research proposals to do experiments at ESS. Of course, the chapter on important practicalities, such as where to submit the proposals, travel information how to reach the ESS site and guest facilities is missing – for the obvious reason that the decision on site preference is not yet made. It is also obvious, furthermore, that the first half of the ESS instruments, which will gradually come on line for full user operation by 2013, with commissioning (at first without neutrons) starting in 2010, will mostly be refined versions of what can be conceived today – and is described in this provisional user guide. Nevertheless with the detail design work to start for the first batch of about 10 instruments around 2005, we can have a reasonable first idea of how these instruments will look.

Within the construction phase of ESS, planned to last until the end of 2011, about 20 neutron scattering instruments and beam facilities will be in more or less advanced stage of manufacturing and installation, following a carefully staggered time schedule. This timeline foresees the technical completion of on average 5 instruments a year between mid 2010 and mid 2014. After this date 3 instruments will come on line each year to achieve a total of 40 to be built and operated by ESS. Further 8 beam lines are envisaged for instruments to be built and run by external co-operating research groups. The scope of ESS project construction phase includes funding of the costs incurring before 2012 for the building of the first neutron scattering instruments. These will amount according to the above schedule to the equivalent of 15 instruments fully completed, while more than 20 will have been started, at least with detailed design, by this date. Further funding for completion of the full instrument suite, as well as modernising and rebuilding on longer term will be part of ESS operational budget.

The selection of the suite of instruments described in this volume is based on the recommendations of the ESS Scientific Advisory Council (SAC) as compiled in November 2001 as a results of a statistical evaluation of the priority research needs expressed by the various science groups of the SAC. A subsequent workshop of the SAC in March 2002 was specifically dedicated to review the outstanding opportunities offered by ESS for applied research, health care and technology development missions and the corresponding instrumental needs. It was found that these overwhelmingly coincide with the experimental priorities defined in November 2001 on the basis of the evaluation of basic scientific opportunities.

The instrumental capabilities detailed in this guide convincingly fulfil the ESS project goal to decisively advance the power of neutron scattering as a versatile research tool in all areas of condensed matter science and technology, compared to that currently available at the most advanced continuous and/or pulsed neutron sources. Achieving this goal will also make ESS provide the community with unique, unprecedented research opportunities, complementary to other important foreseeable advances in large-scale facilities for condensed matter science. These two aspects of ESS based science can be illustrated by the following examples.

Small angle neutron scattering (SANS) is currently one of the main strengths of continuous reactor sources, which thus provide unique potentials in the study of nano-scale structures in solid-state physics, polymer and material research and life sciences. SANS is a very important area in neutron science where pulsed spallation sources are by now in general dominated by continuous ones and it was therefore one of the particular priorities in ESS design optimisation. Indeed, as much as by its enhanced accelerator power as by its innovative target configuration ESS will offer an order of magnitude gain in sensitivity in this crucial research field not only compared to the currently leading reactor sources but also relative to the 2 MW SNS pulsed spallation source facility now being built in Oak Ridge, Tennessee (cf. Fig. I-1).

Another representative and crucial application of neutron scattering is to explore the atomic and molecular dynamics on the mesoscopic time scale  $10^{-12} - 10^{-7}$  s, characteristic for many fundamental phenomena in soft and complex matter. Here ESS will offer 3 orders of magnitude enhanced sensitivity as a result of combining source power and innovative beam delivery and instrument design (cf. the description of cold neutron spectrometers in chapter 2 of this volume). This will make possible to study many to date inaccessible phenomena, for example exploring the endemically small dynamic signals in all kinds of non-crystalline matter.

Neutron and X-ray scattering experiments are primarily complementary by the information they deliver due to the different properties of the two kinds of radiation. For example neutrons offer uniquely high sensitivity for observing light elements in the presence of heavy ones, magnetic disorder and dynamics, isotopically labelled parts of large molecules, etc. In addition, with the power of ESS in many experiments the data collection rates will also be superior to those attainable at advanced synchrotron radiation facilities, notorious for their high beam intensities. In particular, in the kind of inelastic spectroscopy mentioned in the previous paragraph, the sheer beam intensity of ESS will be orders of magnitude superior to that of the most brilliant synchrotron sources today and also superior to the projected, most powerful X-ray free electron lasers (X-FEL). Indeed, the spectral density of the neutron beam over the typically  $10 \text{ cm}^2$  beam

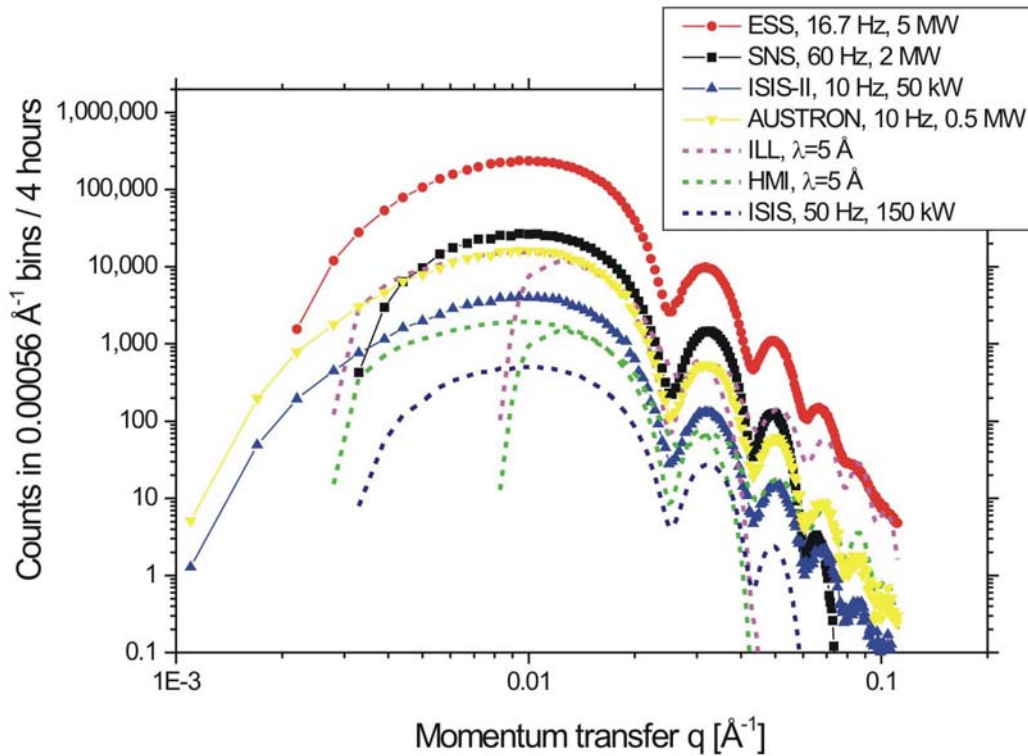


**Figure I-1:** Simulated data collected on a isotropic colloidal model sample by virtual SANS instruments of equal angular resolution, sample size, detector area and detector pixel size at various existing (dashed lines) and projected (symbols) neutron sources. The settings are chosen to optimally explore the  $q$  range  $0.005$  to  $0.05 \text{ \AA}^{-1}$ . For the two reactor sources, ILL and HMI two settings with different collimations and sample to detector distances were assumed ( $12 \text{ m} + 12 \text{ m}$  for 90 % of the data collection time and  $4 \text{ m} + 4 \text{ m}$  for 10 %), in order to cover a  $q$  domain similarly broad to that at the spallation sources in a single setting ( $12 \text{ m} + 12 \text{ m}$ , single source frame data collection).

area will reach at ESS peak values of  $2 \cdot 10^{11}$  neutrons/s/meV (the relevant intensity parameter in neutron time-of-flight spectroscopy with repetition rate multiplication) compared to  $10^8 - 10^9$  photons/s/meV at ESRF and  $10^{10} - 10^{11}$  photons/s/meV expected at the most powerful X-FEL. Of course, the some  $0.1 \text{ mm}^2$  beam cross section of these X-ray sources is a major advantage for very small samples, but many samples, in particular in soft matter research can be produced in sufficient quantity to take full advantage of the large beam cross sections typical for neutron scattering instruments. In the  $10^{-9}$  eV resolution range (corresponding to about  $10^{-7}$  s in time) the beam intensity advantage of neutrons is even bigger: The ESS high resolution neutron spin echo instrument will deliver  $10^8$  neutrons/s to typical samples compared to  $10^{5-6}$  photons/s at the X-FEL (using  $\gamma$  resonance techniques).

In contrast to the study of dynamics by inelastic scattering experiments, in elastic diffraction work the advanced X-ray sources deliver orders of magnitude

higher beam intensities than any thinkable neutron source. However, the high X-ray intensities over a very small beam cross section can actually lead to the rapid deterioration of the sample, in contrast to the fundamentally non-destructive character of the neutron radiation in diffraction studies even at sources as powerful as ESS. Indeed, for samples of substantial size in the several cm<sup>2</sup> range the number of neutrons impinging in an experimental run of about an hour will reach as much as 10<sup>15</sup> at ESS without any damage to the sample. This is about the same as the number of photons which are expected to impinge on a sample in one single pulse on a projected X-FEL instrument, before the sample is fully destroyed.

In order to help to better appreciate the performance and hence the scientific capabilities of the first ESS instruments, comparisons to neutron intensities on similar, top of the line, popular user instruments currently in operation are included in this provisional ESS user guide. Such information, of course, will be by no means part of the real user guide to come at a time, when thousands of users will be given the chance to experience first hand and make their scientific work benefit from the unprecedented opportunities ESS will bring to the broadest research and development community.

Ferenc Mezei  
ESS Instrumentation Task Leader

**Chapter 1**

**ESS NEUTRON  
INSTRUMENT SUITE  
AND LAYOUT**





## 1. ESS NEUTRON INSTRUMENT SUITE AND LAYOUT

In this volume a first set of 21 first priority neutron scattering instruments and beam facilities are described in detail. The ESS Scientific Advisory Council has selected them on the basis of an evaluation of the broad scientific impact. The two target stations, however, will accommodate 48 beam lines (or a few more if it is found feasible during the detailed engineering design to diminish the angle of neighbouring beam lines). In order to establish a reference instrument layout which better represents the completed status of ESS for the purpose of facility planning, the list of the priority instruments has been extended by another 16 spectrometers, which reflect the current state-of-the-art in neutron scattering for a fairly full coverage of the broadest experimental needs. This extended suite (see Table 1-1 and 1-2, below), with particular weight on the requirements of the priority set, has been used as reference to choose the types and number of moderators for each target station and to establish a reference lay-out of the target stations and their environment.

The reference geometry of the moderators for both the short and long pulse target stations (cf. Vol III, chapter 4) consists of two large size moderator positions ( $\sim 20 \times 12 \text{ cm}^2$ ), each viewed from both sides, i.e. four extended viewing fans per target station with different moderator characteristics:

- a) short pulse target station (SPTS):
  - a conventional thin decoupled cold  $\text{H}_2$  moderator viewed from one side, back-to-back to a decoupled thermal  $\text{H}_2\text{O}$  moderator viewed from the opposite side,
  - a novel type, so-called multi-spectral moderator with the combined spectra of a coupled thermal  $\text{H}_2\text{O}$  and a coupled cold  $\text{H}_2$  moderator placed side by side to one another. At the SPTS, one viewing fan faces the multi-spectral side, while the opposite viewing fan faces the coupled cold part of the moderator, only,
  - the use of advanced cold moderators (solid methane like) is being considered. A decision to replace some of the above moderators at a later stage by such an advanced one will eventually be made after detailed studies of feasibility, performance, stability and maintenance.

- b) long pulse target station (LPTS):
- a coupled cold H<sub>2</sub> moderator viewed from both sides,
  - a novel type, so-called multi-spectral moderator with the combined spectra of a coupled thermal H<sub>2</sub>O and a coupled cold H<sub>2</sub> moderator placed side by side to one another and viewed from both sides
  - the use of advanced cold moderators (solid methane like) is being considered, as the SPTS.

Common features both target stations:

- straight viewing fans with opening angles of ~60 deg each
- the total number of beam-lines at each target station is 24 at minimum, i.e. 6 per viewing fan,
- angular separation of the beam-lines: 11 deg or less (space for additional beam lines),
- each beam-line will have its own individual shutter and no bundled guides are foreseen (splitting of guides possible)
- the distance between the moderators and neutron guides front-end is ~1.5m,
- net open cross-section for the neutron guide inserts in the 2.8 m diameter shutter wheels is 23 x 17 cm<sup>2</sup> to give sufficient space for curved guides, beam splitters and multi-spectral beam extraction.

Figs. 1-1 and 1-2 illustrate the schematic geometries of the short pulse target station (SPTS) of the ESS:

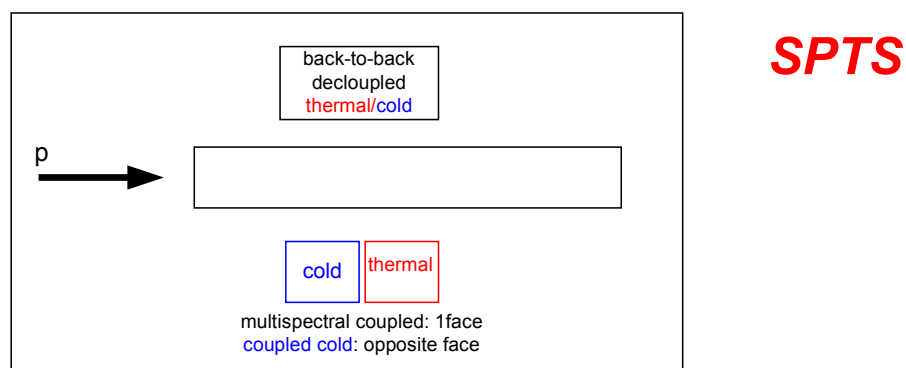


**Figure 1-1:** Short pulse target station: schematic cross section

For the reference design conventional, established moderators technique have been adopted. The replacement of conventional moderators by advanced cold moderators will be considered once they become established, technologically proven and extensively tested for performance and stability. The fairly short pulse moderator with a decoupled thermal H<sub>2</sub>O side and a decoupled cold (20K) liquid hydrogen side placed back-to-back with a Cd-decoupler sheet in between

is located on the top of the lq. Hg-target. Spectral and pulse width properties are described in detail in Vol. III, chapter 4. Thus, one viewing fan of 6 beam ports provides a thermal neutron spectrum, whereas the opposite side serves for the short pulsed cold moderator (see Fig. 1-2). There will be no poisoned moderator at the SPTS because of too short burn-out times of the poison at the high beam intensity of ESS. The newly conceived multi-spectral moderator with combined spectral properties of both a thermal and a cold coupled moderator [Mezei, 2002] is placed below the lq. Hg-target. At the short pulse station, however, the multi-spectral beam will be extracted on one side only. The viewing fan on the other side will face a purely coupled cold moderator, which provides rather short pulses in the thermal energy range. The top and bottom moderators can be exchanged according to engineering demands if requested. The footprint of the SPTS geometry is sketched in Fig. 1-2.

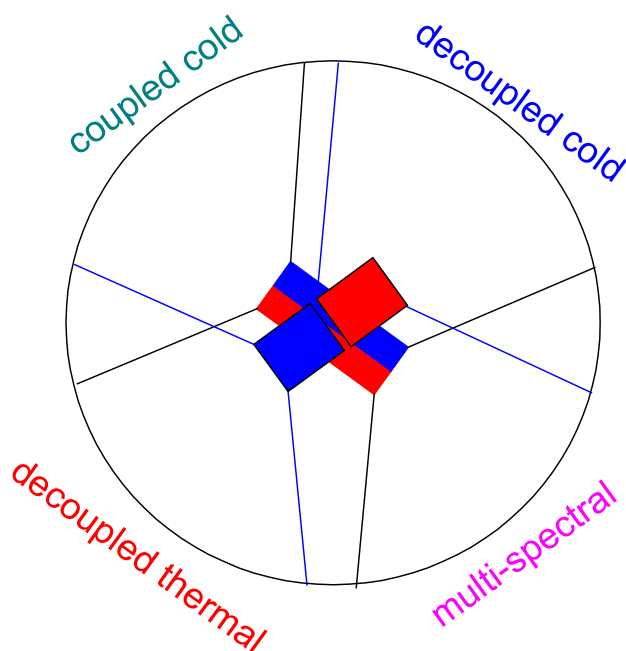
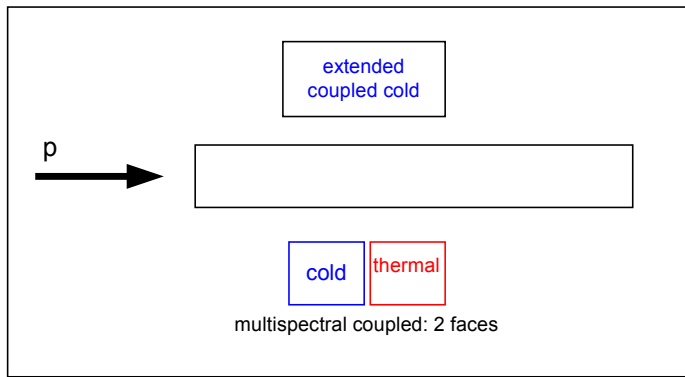


**Figure 1-2:** *SPTS footprint and neutron fan spectral properties*

The geometry of the LPTS is similar to that of the SPTS. Only the back-to-back moderators are replaced by a conventional pre-moderated and fully coupled, super-critical liquid H<sub>2</sub>-moderator, optimized for high neutron current leakage. The multi-spectral moderator at the bottom of the lq. Hg-target is viewed from both sides (Fig. 1-3).

The neutron spectrum requirements of the instruments, the target station geometries and moderator constraints allow for a number of possibilities to shuffle the instruments around one or the other target station. Fig. 1-4 shows a scaled draft of the long and short pulse target stations with all the neutron



**LPTS**

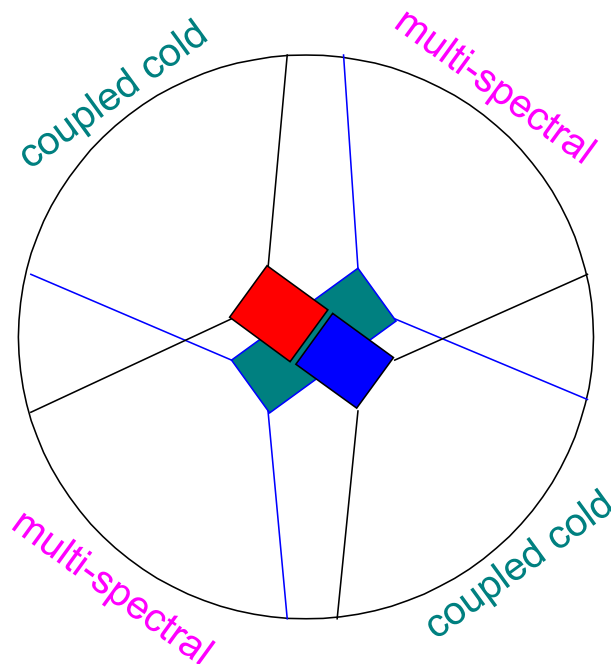


**Figure 1-3:** *LPTS geometry and spectral properties of neutron beam extraction fans*

beam ports named and numbered throughout. The inner circle is scaled to the real size of the reflector, all 24 of the 2.8 m diameter wheel shutters are drawn at a separation angle of 11 deg. All the beam-line front-ends start 1.5 m from the moderators. The outer circle at a radius of 6 m illustrates the approx. size of the target shielding. The beam port number comprises the type of the target station, S or L, respectively. The second character stands for the moderator type followed by a consecutive port no. This number links the neutron beam port with a specific neutron instrument identified in Tab. 1-1 or Tab. 1-2, respectively.

Several geometrical constraints must be satisfied to fit the instrument suite into the anticipated angular sectors and a given moderator beam-port fan. The individual footprints of the instruments need to be accommodated in accordance with the optimised layout of all neutron instruments. The result of this instrument shuffle is compiled in Tab. 1-1 for the SPTS and Tab. 1-2 for the LPTS. The footprint of this arrangement is illustrated in Fig. 1-5. Fig. 1-6

displays the general site layout of the whole ESS facility visualizing the reference instrument placement and space allocation.

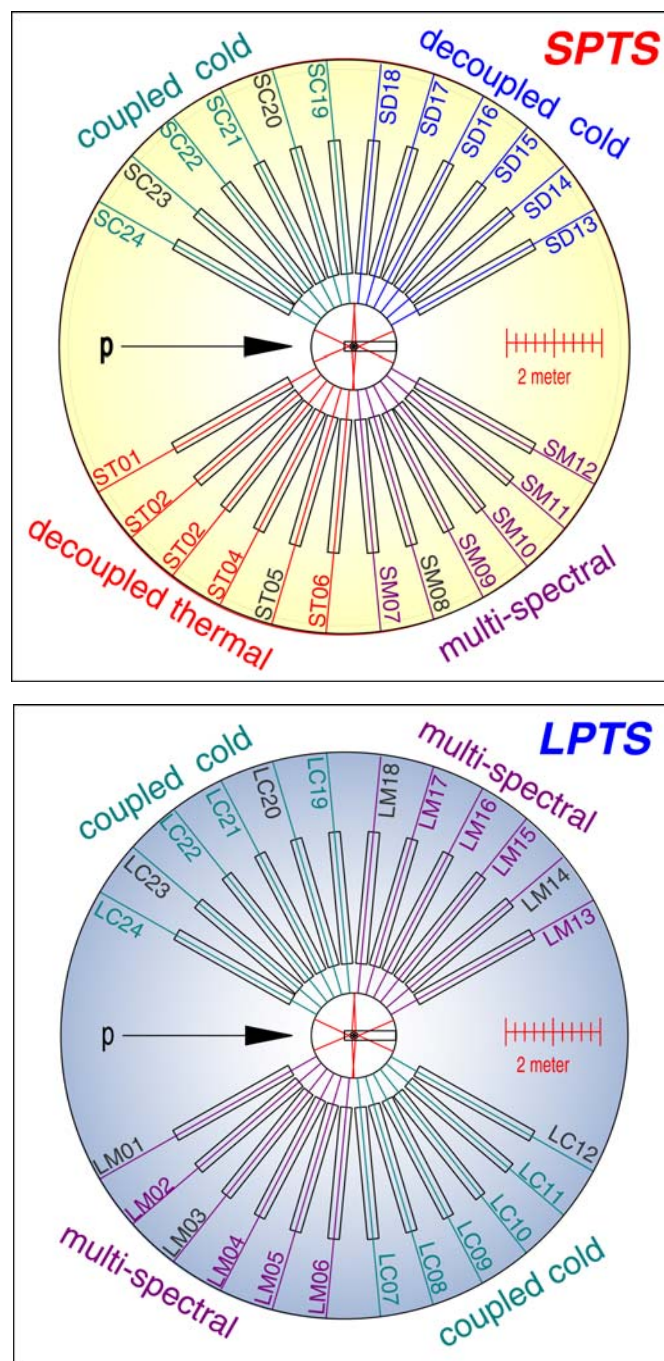


**Figure 1-4:** Scaled draft of the short pulse target station SPTS (top) and long pulse target station (bottom: reflector vessel (inner circle), set of 24 beam shutters of 2.8 m diameter with beam front-end 1.5 m from the moderators, beam port no., size of target shielding (outer circle)).

## REFERENCES

- [Mezei, 2002] F. Mezei, M. Russina, Patent application of 23.01.2002, Deutsches Patent- u. Markenamt, 102 03 591.1

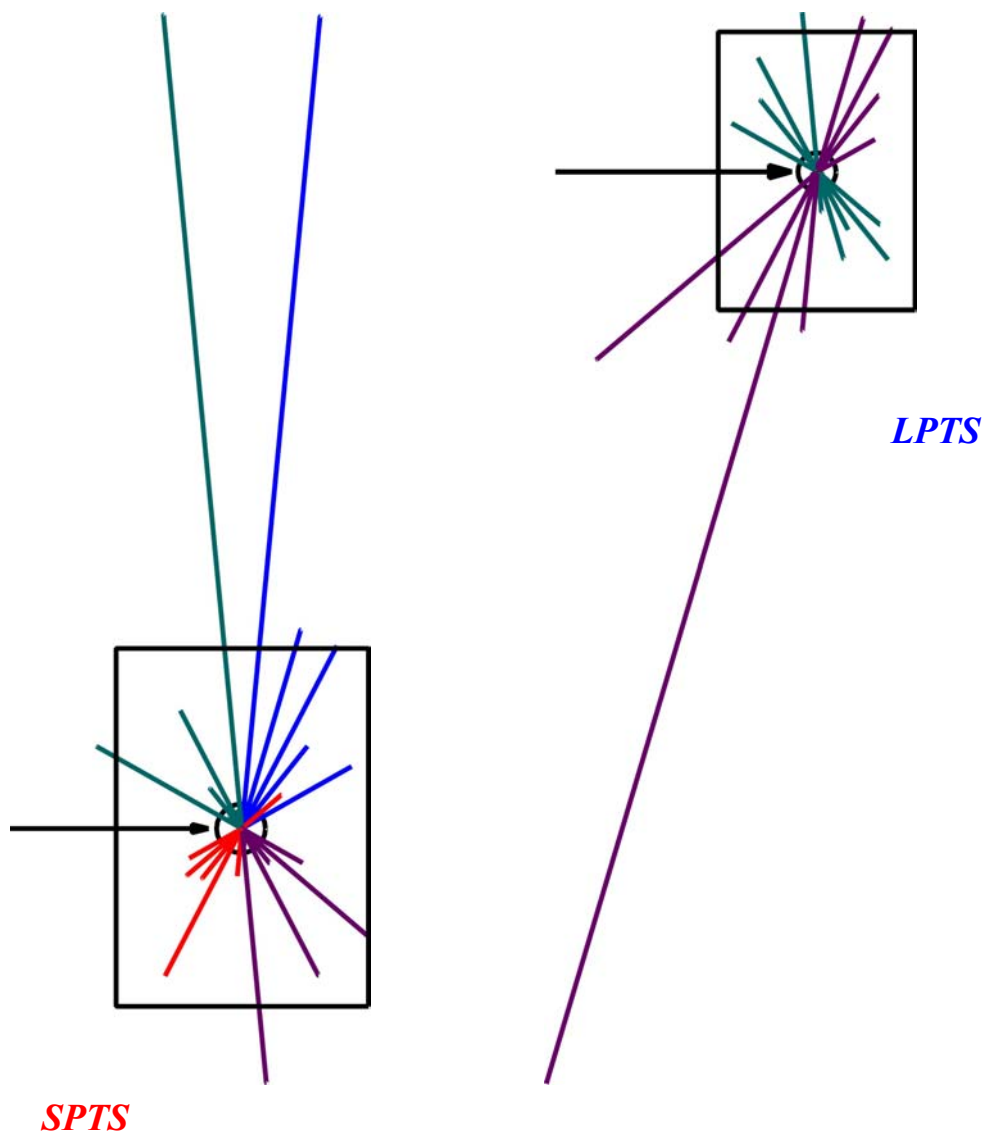


**Figure 1-5:** Scaled footprints of the SPTS (left) and LPTS (right) target stations. The proton beam is incident from the left, the rectangle shows the size of the individual target station hall ( $62 \times 88 \text{ m}^2$ ).

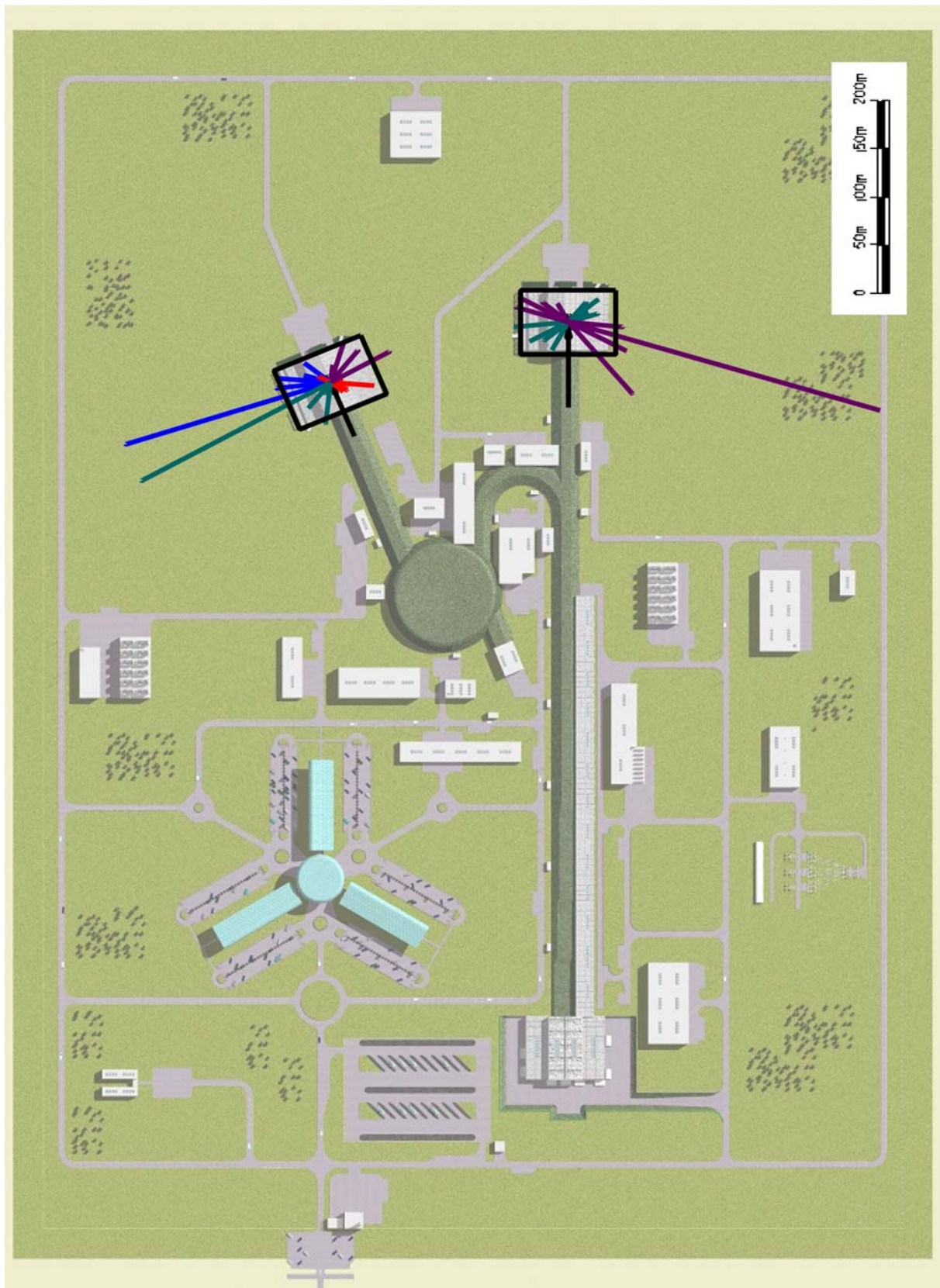


**Figure 1-6:** Footprint of the ESS neutron instrument suite and site layout at the short pulse target station (top left) and long pulse target station (top right).

**Tab. 1-1: Instruments at the Short Pulse Target Station (SPTS)**  
Reference instruments are in red.

| Port no. | Instrument   | Acronym | Moderator         | Flight Path Length (m)<br>(prim.L <sub>i</sub> , sec. L <sub>p</sub> ) | Incident Energy (meV) | $\lambda$ -range (Å) |
|----------|--|---------|-------------------|--|-----------------------|----------------------|
| ST01     | <b>Thermal Chopper Spectrometer (medium resolution)</b>                      | MET     | TDC               | 14, 2.5  | 15-1500               | 0.23-2.5             |
| ST02     | <b>Molecular Spectroscopy</b>  | TOSCA   | TDC               | 17, 1.5  | 3-2000                | 0.2-5                |
| ST03     | <b>High Resolution Single Crystal Diffractometer (chemical crystallogr.)</b> | CHRSXD  | TDC               | 15, 3  | 3-1300                | 0.25-5               |
| ST04     | <b>High Q Powder Diffractometer</b>  | HQP     | TDC               | 40, 2  | 1-10                  | 3-8                  |
| ST05     | –  | –       | –                 | –  | –                     | –                    |
| ST06     | <b>Liquids and Amorphous Materials Diffractometer</b>                        | LAD     | TDC               | 11, 6  | 3-33000               | 0.05-5               |
| SM07     | <b>Particle Physics Beam Line S</b>  | PPS     | MS                | 40, x  | –                     | –                    |
| SM08     | –  | –       | –                 | –  | –                     | –                    |
| SM09     | <b>High Resolution Protein Single Crystal Diffractometer</b>                 | HRPSXD  | MS                | 40, 2  | 3-25                  | 1.8-5                |
| SM10     | <b>Single Pulse Diffractometer</b>   | SPD     | MS                | 10, 2  | 1-250                 | 0.5-8                |
| SM11     | <b>Medium Resolution Backscattering Spectrometer (5 <math>\mu</math>eV)</b>  | MRBS    | MS                | 40, 2  | 1.6-20                | 2-7                  |
| SM12     | <b>High Energy Chopper Spectrometer (high resolution, low Q)</b>             | HET     | MS                | 15, 8  | 15-1500               | 0.23-2.5             |
| SD13     | <b>Backscattering Spectrometer (17 <math>\mu</math>eV)</b>                   | LRBS    | CDC               | 30,2   | 1 – 80                | 1 - 9                |
| SD14     | <b>eV Spectrometer</b>   | EVS     | CDC<br>(hot mod.) | 12, 1  | 5000-64000            | 0.04-0.11            |
| SD15     | <b>Tomography / Radiography Instr.</b>                                       | TOMO    | CDC               | 25, 4  | 1.6-82                | 1-7                  |
| SD16     | <b>Engineering Diffractometer</b>  | ENGIN   | CDC               | 50, 3  | 1.6-170               | 0.7-7                |
| SD17     | <b>Magnetic Powder Diffractometer</b>  | MagP    | CDC               | 50, 2  | 0.1-82                | 1.0-30               |
| SD18     | <b>High Resolution Powder Diffractometer</b>                                 | HRPD    | CDC               | 200, 2   | 0.3-170               | 0.7-15               |
| SC19     | <b>High Resolution Backscattering Spectrometer (0.8 <math>\mu</math>eV)</b>  | HRBS    | CC                | 200, 3   | 1-20                  | 2-10                 |
| SC20     | –  | –       | –                 | –  | –                     | –                    |
| SC21     | <b>High <math>\lambda</math> Resolution SANS Instrument</b>                  | HR-SANS | CC                | 12, 20   | 0.2-20                | 2-20                 |
| SC22     | <b>High Resolution Reflectometer</b>   | HRRf    | CC                | 12, 3  | 1.6-20                | 2-7                  |
| SC23     | –  | –       | –                 | –  | –                     | –                    |
| SC24     | <b>Cold Chopper Spectrometer (low resolution)</b>                            | LET     | CC                | 40, 3  | 0.5-80                | 1-12                 |

Moderator: TDC thermal decoupled, MS multi-spectral, CDC cold decoupled, CC cold coupled



**Tab. 1-2: Instruments at the Long Pulse Target Station (LPTS)**  
Reference instruments are in red.

| Port no. | Instrument   | Acronym      | Moderator | Flight Path Length (m)<br>(prim. L <sub>i</sub> , sec. L <sub>p</sub> ) | Incident Energy (meV) | $\lambda$ -range (Å) |
|----------|--|--------------|-----------|---|-----------------------|----------------------|
| LM01     | –  | –            | –         | –   | –                     | –                    |
| LM02     | <b>Variable Resolution Cold Neutron Chopper Spectrometer</b>       | VarChop      | MS        | 90,3  | 0.2-80                | 1-20                 |
| LM03     | –  | –            | –         | –   | –                     | –                    |
| LM04     | <b>High Intensity SANS Instrument</b>                              | HiSANS       | MS        | 21,30   | 0.2-20                | 2-20                 |
| LM05     | <b>Ultra-high Resolution Powder Diffractometer</b>                 | URPD         | MS        | 300,3   | 1-100                 | 0.9-10               |
| LM06     | <b>High Pressure Diffractometer</b>                                | HiPD         | MS        | 40,6  | 1-300                 | 0.5-10               |
| LC07     | <b>Neutron Depolarisation Instrument</b>                           | n-DEPOL      | CC        | 12,2  | –                     | –                    |
| LC08     | <b>Grazing Incident SANS Instrument</b>                            | GISANS HiRef | CC        | 20,8  | 0.2-80                | 1-20                 |
| LC09     | <b>Single Peak Diffractometer (CryoPAD)</b>                        | SPAD         | CC        | 20, 2   | 3-330                 | 0.5-5                |
| LC10     | <b>Very High Intensity SANS Instrument</b>                         | SANS         | CC        | 21,15   | 0.1-20                | 2-25                 |
| LC11     | <b>Fourier Diffractometer</b>                                      | FourDif      | CC        | 25,2  | 0.2-80                | 1-20                 |
| LC12     | –  | –            | –         | –   | –                     | –                    |
| LM13     | <b>Low Resolution Single Crystal Protein Diffractometer</b>        | LRPD         | MS        | 20,2  | 0.3-3.3               | 5-15                 |
| LM14     | –  | –            | –         | –   | –                     | –                    |
| LM15     | <b>Coherent Excitation Spectrometer (TAS)</b>                      | TAS          | MS        | 30,2  | 1-170                 | 0.7-10               |
| LM16     | <b>Wide Angle NSE Spectrometer / Diffuse Scattering Instrument</b> | WanNSE       | MS        | 50,4  | 0.1-20                | 2-25                 |
| LM17     | <b>High Magnetic Field Instrument</b>                              | HiMag        | MS        | 50,2  | 1- 80                 | 1 - 9                |
| LM18     | –  | –            | –         | –   | –                     | –                    |
| LC19     | <b>Particle Physics Beam Line L</b>                                | PPL          | CC        | 40, x   | 0.1-20                | 2-25                 |
| LC20     | –  | –            | –         | –   | –                     | –                    |
| LC21     | <b>High Intensity Reflectometer</b>                                | HiRef        | CC        | 37,3  | 1-20                  | 2-9                  |
| LC22     | <b>Focusing Mirror Low Q SANS Instrument</b>                       | FocSANS      | CC        | 20,8  | 0.7-3.3               | 5-12                 |
| LC23     | –  | –            | –         | –   | –                     | –                    |
| LC24     | <b>High Resolution NSE Spectrometer</b>                            | HRNSE        | CC        | 30,6  | 0.1-20                | 2-25                 |

Moderator: MS multi-spectral, CC cold coupled



# **Volume IV Instruments and User Support**

---

## **Chapter 2**

# **ESS REFERENCE INSTRUMENT PERFORMANCE SHEETS**



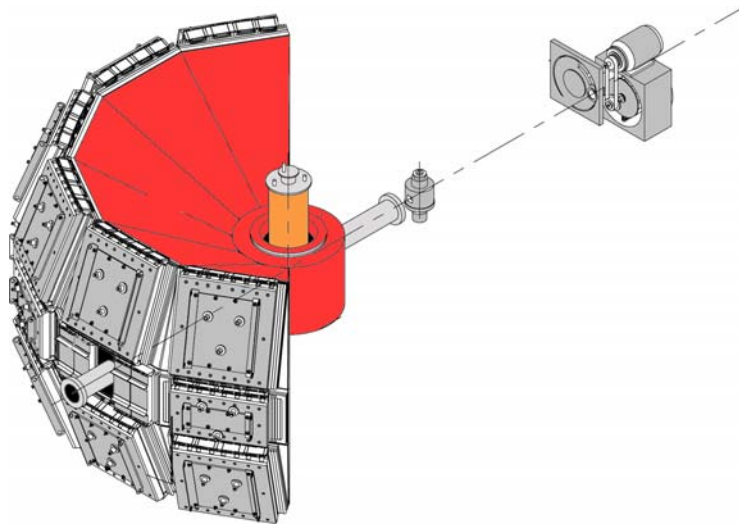
## 2. ESS REFERENCE INSTRUMENT PERFORMANCE SHEETS

- Thermal chopper spectrometer (medium resolution) (ST01)
- High resolution single crystal diffractometer (chemical crystallography) (ST03)
- Liquids and amorphous material diffractometer (ST06)
- High resolution protein single crystal diffractometer (SM09)
- Single pulse diffractometer (SM10)
- High energy chopper spectrometer (high resolution, low Q) (SM12)
- Tomography / Radiography instrument (SD15)
- Engineering diffractometer (SD16)
- Magnetic powder diffractometer (SD17)
- High resolution powder diffractometer (SD18)
- High resolution backscattering spectrometer (0.8  $\mu\text{eV}$ ) (SC19)
- High resolution backscattering spectrometer (1.5  $\mu\text{eV}$ ) (SC19)
- High resolution reflectometer (SC22)
- Cold chopper spectrometer (low resolution) (SC24)
- Variable resolution cold neutron chopper spectrometer (LM02)
- High intensity SANS instrument (LM04)
- Wide angle NSE spectrometer / Diffuse scattering (D7 – type) (LM16)
- Particle physics beam lines (LC19, SM07)
- High intensity reflectometer (LC21)
- Focussing mirror low q SANS instrument (LC22)
- High resolution NSE spectrometer (LC24)

## THERMAL CHOPPER SPECTROMETER

**Location:** SPTS, ST01  
**Moderator:** decoupled thermal water

Schematic setup:



### **Instrument description:**

A medium resolution, high-count-rate chopper spectrometer. A large position sensitive detector array provides broad angular coverage. A converging supermirror guide provides enhanced flux in the thermal neutron region.

An oscillating collimator will reduce scattering from sample environment equipment, allowing the use of pressure cells magnets, furnaces etc..

It will be possible to install polarising filters in the incident and scattered beams to provide polarisation analysis

## Applications:

The high flux of the ESS will allow this instrument to be used for parametric studies, studies of weak signals and small samples. The oscillating collimator will effectively enhance the range of parameter space that can be accessed.

The spectrometer will be well suited to measurements of magnetic excitations and fluctuations in a wide range of materials. The wide Q range will also be appropriate for phonon measurements and molecular spectroscopy.

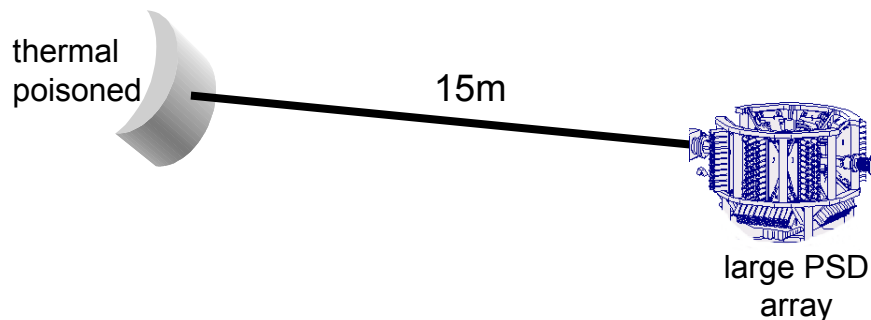
## Instrument data:

|                        |   |
|------------------------|---|
| moderator:             | decoupled thermal water   |
| neutron guide:         | converging m=3 guide<br>L <sub>1</sub> :12 m<br>L <sub>2</sub> : 2.5 m<br>L <sub>3</sub> : 1 m                        |
| choppers               | Fermi chopper at 11 m, 50-600Hz<br>range of slit packages<br>nimonic chopper at 6 m, 50-100 Hz                        |
| Detectors              | Llrge PSD array   |
| incident energy range: | 15 meV - 1.5 eV   |
| resolution:            | E <sub>i</sub> =20meV $\eta\omega=0, 5\% E_i$ to 2.5 % E <sub>i</sub>   |
| flux at sample:        | 9 x10 <sup>5</sup> n cm <sup>-2</sup> s <sup>-1</sup>   |
| sample environment:    | standard sample environment<br>equipment, bespoke top-loading closed<br>cycle refrigerator<br>oscillating collimator. |
| polarisation analysis  | <sup>3</sup> He filters in incident and scattered<br>beams  |

## HIGH RESOLUTION SINGLE CRYSTAL DIFFRACTOMETER

**Location:** SPTS, ST03  
**Moderator:** decoupled thermal water

Schematic setup:



### Instrument description:

Single crystal chemical crystallography is a "high resolution" technique, typically requiring the measurement of d-spacings to as low as 0.35-0.4Å, while for physics applications in harder materials this can extend as low as 0.2Å. This also requires good Q-space resolution to allow for peaks to be separated and therefore integrated accurately. A short pulse is therefore required, around 30µs pulse length or better. To maximise the flux in the region of interest a decoupled thermal water moderator is chosen (with the option of intermediate 130K moderator - the advanced cold moderator), with high flux at 1Å and below but also retaining significant flux in the region up to and beyond 2-3Å. Sharp pulses are required for good Q-space resolution to high Q, so the moderator is decoupled. To match the pulse length requirements dictated by the problem dependent parameters  $d_{\min} (\equiv Q_{\max})$ ,  $\sim 0.4 \text{ \AA}$ , and a (maximum cell edge),  $\sim 30 \text{ \AA}$ , this instrument type should have a medium path length (15 m) on the SPTS, where the band-width will be adequate. The instrument will use the time-of-flight Laue diffraction technique.

*We note also here that such an instrument could also serve for the measurement of magnetisation densities from flipping ratios if an efficient white-beam spin polariser is available. At 15 m provision of a guide can be beneficial, and this will be particularly relevant if the option of focusing for the study of very small samples is pursued. With many of the anticipated samples having linear dimensions of 0.5-3 mm, the possible gains from focused beams should be evaluated further.*



## Applications:

The single crystal diffractometer will find widespread applications in chemical crystallography and materials science. The instrument will provide an ideal facility for rapid structure determination for unit cells up to 30 Å cell edge. The very rapid data collections to be offered (in favourable cases under one hour for a full 3D single crystal data set) will open up exciting new possibilities in parametric studies, for example as a function of temperature and pressure. The high flux offered at the ESS will also allow the study of small single crystal samples of volume  $<0.1 \text{ mm}^3$ . The instrument will allow for the full determination of a wide range of structures, allowing information to be obtained on hydrogen atom positions, atomic disorder, thermal parameters including anharmonicity, charge and spin density studies etc. The instrument will also be capable of undertaking reciprocal space surveying in the areas of diffuse scattering, quasicrystals and incommensurate structures, though at relatively modest  $\Delta Q/Q$  resolution.

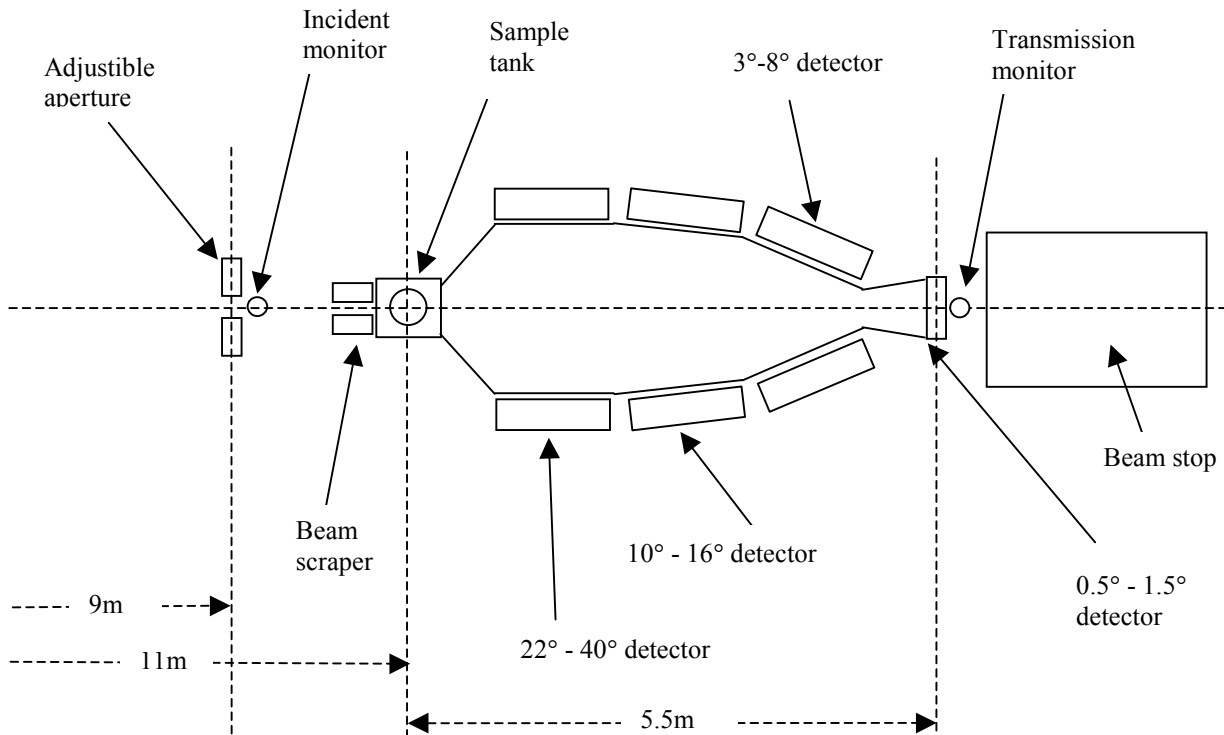
## Instrument data:

|                          |  |
|--------------------------|--|
| moderator:               | decoupled thermal water  |
| neutron guide:           | to be finalised, option for focusing for small samples   |
| chopper distance:        | none   |
| polarizer:               | efficient wide-band polariser for spin density studies   |
| wavelength range:        | $0.25 < \lambda < 5 \text{ \AA}$   |
| diffraction resolution:  | $d_{\min} \sim 0.2 \text{ \AA}$ , $\sin\theta/\lambda \leq 2.5 \text{ \AA}^{-1}$ , $Q \leq 31 \text{ \AA}^{-1}$                |
| resolution               | $\Delta Q/Q \sim 2.5 \cdot 10^{-3}$ (in three dimensions)  |
| flux at sample:          | dependent on guide choice  |
| scattering angle:        | PSDs covering range $15^\circ < 2\theta < 165^\circ$   |
| diffractometer:          | restricted rotation stages, pseudo-vertical geometry for sample environment  |
| distance sample detector | 500-750 mm   |
| detector                 | large area PSDs, $>2\pi$ solid angle, resolution 1-2 mm, high efficiency at 1 Å, shield for operation in stray magnetic field. |
| sample environment       | full range of cryostats, furnaces, high pressure gas cells and DACs, cryomagnet  |

# LIQUIDS AND AMORPHOUS MATERIAL DIFFRACTOMETER

**Location:** SPTS, ST06  
**Moderator:** decoupled thermal water

Schematic setup:



## Instrument description:

The liquids diffractometer is purpose built for studying liquids and other disordered materials, particularly when significant intermediate range order is present. In the present design the detectors are confined to low scattering angles ( $<40^\circ$ ) to ensure that recoil corrections are minimised, but back scattering detectors can be included if higher resolution is required. Within this angle range, solid angle coverage is maximised, to give a total solid angle of around 1sr. The planned instrument will offer a count rate some 20 times greater (averaged over  $Q$  range) than existing facilities at ILL and ISIS, and will provide an unprecedented momentum transfer range, estimated to be  $0.03 \text{ \AA}^{-1}$  to  $70 \text{ \AA}^{-1}$ , with excellent resolution ( $\Delta Q/Q \sim 2\%$  or better) over most of this range. The instrument requires a large vacuum tank to obtain low backgrounds, and the design leaves many options for future upgrades when these are deemed necessary. Particularly important in this regard is the provision of a Fermi chopper to allow approximate determinations of the inelastic scattering from samples with low atomic mass content. The proposed instrument has an incident flight path of 11m, with the secondary flight path up to 5.5m at low angles to

optimise the lowest Q capability. A longer flight path version of this instrument can be envisaged (with corresponding increased secondary flight path), with improved resolution and low-Q capability.

### Applications:

The high count rate and good resolution offered by the Liquids Diffractometer will be exploited in a number of scientific areas:-

- Liquids and solids under extremes of temperature and pressure. This work typically requires small samples, often as little as 2mm in diameter. Current neutron sources are really not able to tackle such small systems in the liquid or disordered state.
- Small isotope differences. A number of isotopes are difficult or impossible to exploit with current neutron sources because the available contrast is close to or below the current limits of detectability. Particularly important in this regard are carbon and sulphur, which occur widely in many systems of chemical and biological interest.
- Dilute systems. Much important chemistry and biology takes place in dilute systems – much lower concentrations than are traditionally available to neutron diffraction experiments.
- Phase diagram mapping. The requirement here is to map out structures as a function of state variables – this has always been hard at current sources because of the amount of time required. With the liquids diffractometer at the ESS this becomes feasible.

### Instrument data:

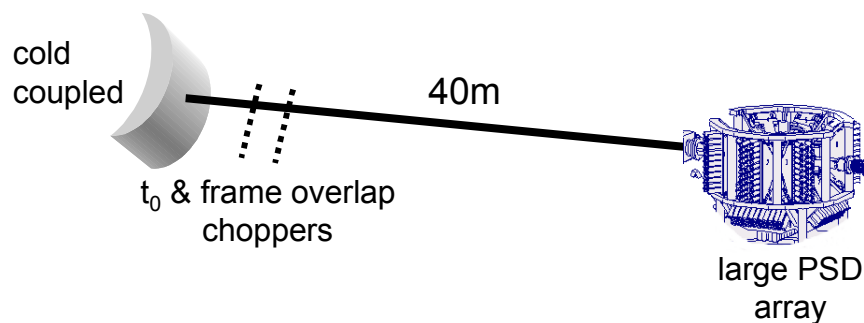
|   |   |
|---|---|
| moderator:  | decoupled thermal water   |
| incident flight path:                                 | 11m   |
| adjustable apertures:                                 | at approximately 6.5m and 9m  |
| wavelength range:                                     | $0.05 < \lambda(\text{\AA}) < 3$  |
| Q range:  | $0.03 < Q(\text{\AA}^{-1}) < \sim 70$   |
| Q resolution:   | $\Delta Q/Q \sim 1-2\%$ ( $2\theta=10^\circ-40^\circ$ )<br>$\Delta Q/Q \sim 10\%$ ( $2\theta=3^\circ$ )                                       |
| flux at sample, C-number:                             | $3 \times 10^5$ n/s/0.05 $\text{\AA}^{-1}/\text{cm}^3\text{V}$ (peak)<br>(compared to $5 \times 10^2$ for D4C at $\lambda = 0.7\text{\AA}$ ). |
| scattering angle:                                     | $0.5 < 2\theta(^{\circ}) < 40$ (expandable to 160)  |
| detector:   | 5 or 10 mm wide scintillators   |
| sample environment:                                   | all standard items, including sample changer  |
| <i>Flux comparison with existing diffractometers:</i> | $5 \times 10^2$ for D4C at $\lambda = 0.7\text{\AA}$  |

# HIGH RESOLUTION PROTEIN SINGLE CRYSTAL DIFFRACTOMETER

**Location:** SPTS, SM09

**Moderator:** multi-spectral, coupled thermal cold combination

Schematic setup:



## Instrument description:

Single crystal macromolecular crystallography is a "medium resolution" technique, typically requiring the measurement of d-spacings to around  $d_{\min}=1.5-1.8\text{\AA}$ , on unit cell edges of up to 150-200 $\text{\AA}$ . Also requires reasonably good Q-space resolution to allow for peaks to be separated and therefore integrated accurately. To match the pulse length requirements dictated by the problem dependent parameters  $d_{\min}$  ( $\equiv Q_{\max}$ ),  $\sim 1.2/1.5\text{\AA}$ , with a (the maximum cell edge),  $\sim 100/200\text{\AA}$ , this instrument type should have a path length of 40m using the coupled cold moderator on the SPTS, where the band-width will be adequately matched to the range of diffraction information available. In this case frame-overlap choppers will be required, particularly to reduce incoherent background levels. However, in terms of moderator options, the advanced cold moderator with a shorter  $L_1$  (15-20m) is also feasible for this instrument, and significant gains can be made in the d-spacing range of most interest using the advanced cold moderator. Then instrument will use the time-of-flight Laue diffraction technique.

*It is also now well established that many important hydrogen/deuterium positions in proteins can also be established reliably at lower resolution if necessary, say  $d_{\min}$  of  $2.4\text{\AA}$ , which greatly facilitates the experiment. We note also here that such a MacroSX instrument on a cold moderator will also allow for the measurement of lower resolution diffraction patterns of larger macromolecular complexes. The Q-range able to be accessed will also allow for medium resolution studies of small crystals of large chemical structures and complexes.*

## Applications:

The macromolecular single crystal diffractometer will find widespread applications in studies of biomolecular systems. The instrument will allow the study of macromolecular (protein) crystallography from materials of unit cells up to 150-200 Å, using crystals of order 1 mm<sup>3</sup>. The instrument will allow for the determination of H/D positions in active sites, specification of mobile protons, detailed structural studies of H/D exchange, and the full determination of solvent structure around biological macromolecules. The instrument will also be capable of studying larger unit cell complexes to lower d-spacing resolution, and may also have a role in studying large, possibly disordered, chemical and supramolecular complexes.

## Instrument data:

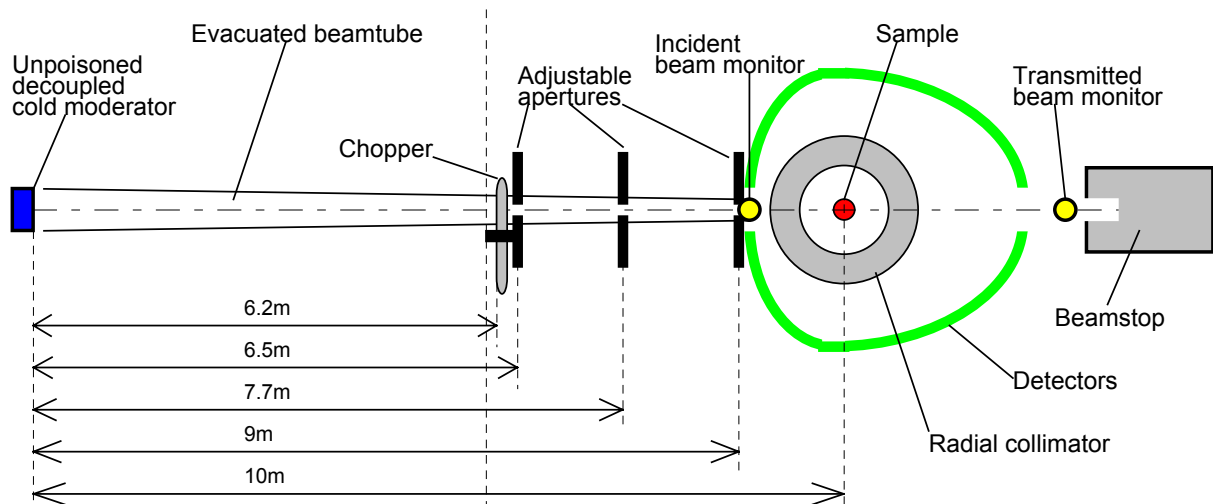
|                          |   |
|--------------------------|---|
| moderator:               | multi-spectral, coupled thermal cold combination  |
| neutron guide:           | to be finalised, option for focusing for small samples normally used in this area   |
| chopper distance:        | Nimonic 7m (or curved guide)<br>25/50Hz frame overlap disks 8m, 12m   |
| polarizer:               | none  |
| wavelength range:        | $1.8 < \lambda < 5 \text{ \AA}$   |
| diffraction resolution:  | $d_{\min} \sim 1.2\text{-}2.4 \text{ \AA}$ , $\sin\theta/\lambda \leq 0.4 \text{ \AA}^{-1}$ , $Q \leq 5.0 \text{ \AA}^{-1}$ |
| flux at sample:          | dependent on guide choice   |
| scattering angle:        | PSDs covering range $15^\circ < 2\theta < 165^\circ$  |
| diffractometer:          | restricted rotation stages, pseudo- vertical geometry for sample environment  |
| distance sample detector | 500-750 mm  |
| detector                 | large area PSDs, $>2\pi$ solid angle, resolution 1-2 mm, high efficiency at $>\sim 2 \text{ \AA}$ .                         |
| sample environment       | simple, open geometry cold (CCR/N <sub>2</sub> flow?)   |

## SINGLE PULSE DIFFRACTOMETER

**Location:** SPTS, SM10

**Moderator:** multi-spectral, coupled thermal cold combination

Schematic setup:



### Instrument description:

The Single Pulse Diffractometer is optimised for ultra high countrates and its principal design features are, therefore, a short incident flightpath ( $L_1=10$  m) and a large solid angle of detector coverage ( $\sim 6$  steradians). The planned instrument will offer a countrate approximately 500 times that of the current GEM diffractometer at ISIS. Neutrons from the multi-spectral decoupled cold hydrogen moderator reach the sample position through a series of adjustable collimating slits, allowing the beamsize at the sample to be matched to the sample dimensions. Further reductions in the background contributions from complex sample environments (pressure cells, in-situ chemical reaction vessels, etc.) will be achieved by incorporating an oscillating radial collimator around the sample position. A wavelength range of  $0.5 < \lambda(\text{\AA}) < 7.9$  will be used. Due to the space limitations, a single 50Hz chopper situated at 6.2m performs the dual purpose of eliminating the prompt neutron pulse ('t-zero' chopper) and those neutrons at  $\lambda > 7.9$  \AA which might otherwise cause frame overlap problems. The large, continuous detector array covers the scattering angle range  $5 < 2\theta(^{\circ}) < 175$  and extend above and below the horizontal plane by  $\pm 45^{\circ}$ . The use of 5mm wide detector elements provides an estimated best resolution of  $\Delta d/d=0.5\%$  at backscattering, whilst the low angle region will provide access to  $d$ -spacings in excess of 50 \AA.

## Applications:

The uniquely high count rate offered by the Single Pulse Diffractometer will be exploited in a number of novel scientific areas :

- The opportunity to collect a good quality diffraction pattern in a single ESS frame will allow the kinetics of, for example, rapid chemical reactions to be studied in-situ. Indeed, in some favourable cases the ability to combine data collected simultaneously over the continuous  $2\theta$  range of the detector will allow the evolution of the structure(s) to be investigated at several times within a single frame.
- Extensive, detailed studies of the evolution of structural changes over multi-dimensional space (temperature, pressure, composition, etc.) will become possible.
- Alternatively, the high incident neutron flux and large solid angle of detector coverage will be used to investigate ultra-small sample volumes ( $\sim 0.001\text{mm}^3$ ) in reasonable timescales. This has applications for the studies of materials which are rare or difficult to prepare and also for structural investigations of materials under extreme conditions of pressure and/or temperature.

## Instrument data:

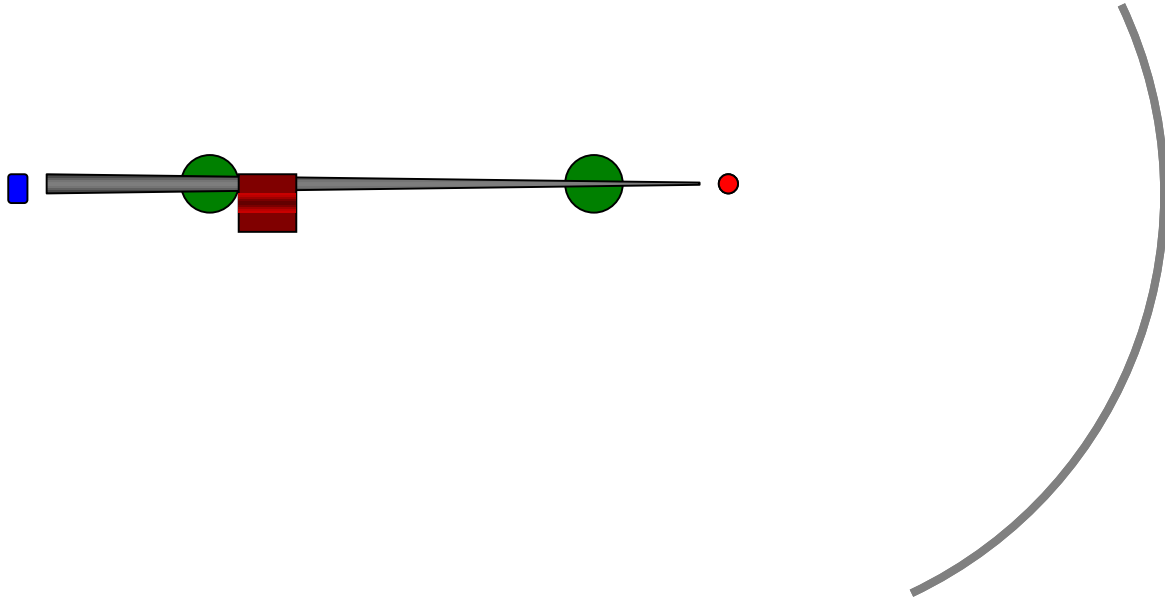
|   |  |
|---|--|
| moderator:  | multi-spectral, coupled thermal cold combination   |
| incident flightpath:                                  | 10 m   |
| chopper distance:                                     | 6.2 m  |
| chopper speed:  | 50Hz   |
| adjustable apertures:                                 | at approximately 6.5 m, 7.7 m and 9 m  |
| wavelength range:                                     | $0.5 < \lambda(\text{\AA}) < 7.9$  |
| $d$ -spacing range:                                   | $0.25 < \lambda(\text{\AA}) < \sim 50$   |
| $d$ -spacing resolution:                              | $\Delta d/d=0.5\%$ (backscattering), $\Delta d/d=0.9\%$ ( $2\theta=90^\circ$ ),<br>$\Delta d/d\sim 5\%$ ( $2\theta=10^\circ$ )               |
| flux at sample:                                       | $1.0 \times 10^9$ n/cm <sup>2</sup> /sec   |
| scattering angle:                                     | $5 < 2\theta(^\circ) < 175$ , $\pm 45^\circ$ from horizontal plane   |
| distance sample detector:                             | $\sim 1$ m (backscattering),<br>$\sim 1.5$ m ( $2\theta=90^\circ$ ),<br>$\sim 2$ m ( $2\theta=10^\circ$ )                                    |
| detector:   | 5 mm wide scintillators  |
| sample environment:                                   | in-situ chemical reaction vessels cryostat and furnace (fast cooling/ heating), sample changer, high pressure (+ variable temperature) cells |
| <i>Flux comparison with existing diffractometers:</i> | <i>GEM (ISIS): <math>1-2 \cdot 10^6</math> n /cm<sup>2</sup>/sec</i>   |

## HIGH ENERGY CHOPPER SPECTROMETER

**Location:** SPTS, SM12

**Moderator:** multi-spectral, coupled thermal cold combination

Schematic setup:



### Instrument description:

A chopper spectrometer optimised for high resolution studies in the thermal to high-energy regimes. Under normal operating conditions, a single Fermi chopper will be used to monochromate the incident beam. For high-resolution applications a second chopper, 6 m from the moderator, will be used to decrease the equivalent of the moderator pulse shape to provide high resolution. Energy resolutions of order 0.5%  $E_i$  will be achievable for  $\eta\omega=0$  falling to half this value at approximately 75%  $E_i$  energy transfer. A range of slit packages will be available to provide optimum flexibility in the selection of flux-resolution characteristics. The second chopper (at 6 m) will be mounted on a lift mechanism to make the transition between modes of operation as efficient as possible.



## Applications:

Magnetic excitations in single crystals for example detailed studies of spin wave dispersion relations.

High-resolution studies of excitations in a broad range of fields including, quantum fluids, lattice dynamics and molecular spectroscopy.

Collimation of the incident beam will allow access to sufficiently low angles to facilitate Brillouin scattering.

## Instrument data:

|                        |   |
|------------------------|---|
| moderator:             | multi-spectral, coupled thermal cold combination  |
| neutron guide:         | converging m=3 guide<br>L <sub>1</sub> (mod-sample) 12 m<br>L <sub>2</sub> (sample-det): 8 m<br>L <sub>3</sub> (chop-sample): 1 m                                     |
| choppers:              | Fermi chopper at 11 m, 50-600Hz<br>optional Fermi chopper at 6 m, 50-600Hz<br>range of slit packages for both choppers<br>nimonic chopper at 6.3 m, 50-100 Hz         |
| detectors:             | large PSD array   |
| incident energy range: | 15 meV - 1.5 eV   |
| resolution:            | E <sub>i</sub> =20meV $\eta\omega=0$ , 1.5% E <sub>i</sub> to 0.5% E <sub>i</sub><br>E <sub>i</sub> =500meV $\eta\omega=0$ , 2% E <sub>i</sub> to 1.5% E <sub>i</sub> |
| flux at sample:        | 2 x10 <sup>5</sup> n cm <sup>-2</sup> s <sup>-1</sup> , low resolution<br>4 x10 <sup>4</sup> n cm <sup>-2</sup> s <sup>-1</sup> , high resolution                     |
| polarisation analysis: | <sup>3</sup> He spin filters can be installed in the incident and scattered beam.   |
| sample environment:    | standard sample environment equipment, mounted on a bespoke goniometer  |

## TOMOGRAPHY / RADIOGRAPHY INSTRUMENT

**Location:** SPTS, SD15 or LPTS (to be discussed)  
**Moderator:** decoupled cold hydrogen

### Introduction

Neutron imaging is a very important tool for non-destructive and non-invasive testing at many sites world-wide [Domanus, 1992, Schillinger, 1996, Fujine, 1999, Lehmann, 1998]. Most of the neutron sources are based on a fission reactor, only one facility has so far been built at a spallation neutron source [Lehmann]. High performance systems in respect to high spatial and time resolution need as high neutron intensity as possible.

At the ESS, it would be possible to select the applied neutron energy during the neutron imaging process, giving many advantages. Using a tight energy window, resonance structures or edges (strong slopes) in the neutron cross-section can be used to vary elemental contrast and transmission properties dramatically (by orders of magnitude). An example is given in Fig. 1 for the four technically relevant materials Cu, Fe, Al and Pb.

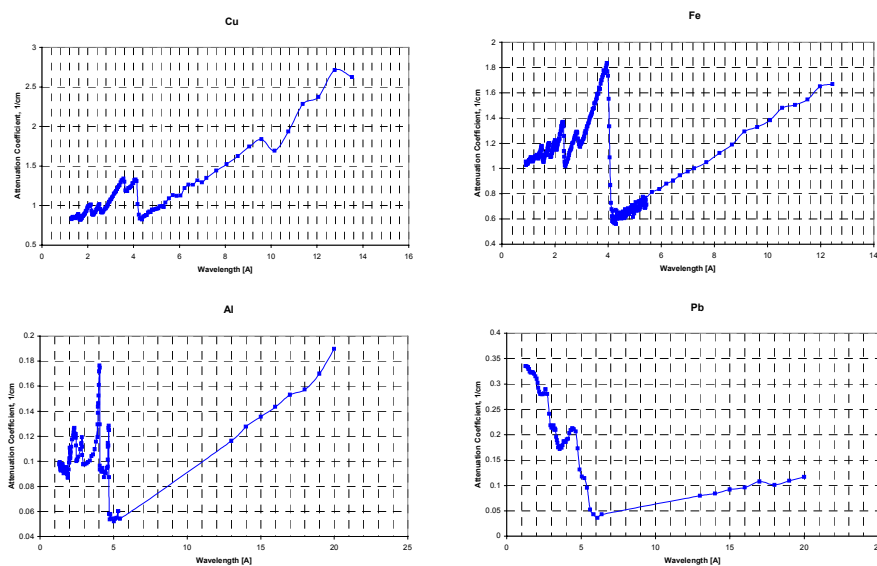


**Figure 2-1:** Total neutron interaction cross-sections in the low energy range for Cu, Fe, Al and Pb

While steady state radiography with high total fluences can also be performed at ILL or FRM-II, the main advantage of ESS will be this time- and thus energy resolved radiography and tomography.

## Radiography station

The beam design containing collimator, sample, detector and beam dump can be copied from the FRM-II facility [Schillinger, 2001], which again is based on the PSI design. For high resolution imaging, a high value ( $>500$ ) of the collimation parameter  $L/D$  must be achieved, which is only possible with a diaphragm plus consecutive flight tube, but not with a neutron guide. A beam-adapted collimator converging from square opening to round diaphragm and diverging to square opening again will provide a square beam with minimum background and penumbra.

As a detector, no counting system can be employed, as the dynamics, spatial resolution and total count rate on the detector area are not sufficient for imaging. The time resolution can be achieved by gating the image intensifier of a cooled CCD camera. Gating times can be as low as 3 ns, but time resolution is determined by the decay time of the scintillator employed.

A typical ZnS(Ag)+LiF scintillator decays to 10% in 85  $\mu\text{s}$ , which is sufficient for the time spread of the neutron pulse (FWHM 25  $\mu\text{s}$  originally) after a flight path of 10 meters.

**Table 2-1:** Flight time for neutrons of different wavelength for 10 meters flight path

| $\lambda[\text{\AA}]$ | 1   | 1.8 | 2   | 3   | 4    | 5    | 6    | 7    | 8    | 9    |
|-----------------------|-----|-----|-----|-----|------|------|------|------|------|------|
| $t_{10m}[\text{ms}]$  | 2.5 | 4.5 | 5.0 | 7.6 | 10.1 | 12.6 | 15.1 | 17.7 | 20.2 | 22.7 |

As Table 2-1 shows, a frame overlap will occur for 1  $\text{\AA}$  and 9  $\text{\AA}$  neutrons if the facility is installed at the short pulse target station with 50 Hz repetition rate and thus 20 ms between pulses. Since the interesting wavelength range is between 2  $\text{\AA}$  and 6  $\text{\AA}$  and the intensity drops heavily for longer wavelengths, this may be acceptable. Another problem is the fact that the radiography facility must allow for big samples and massive shielding, which may require a larger radial distance from the target due to the space used up by neighbouring experiments.

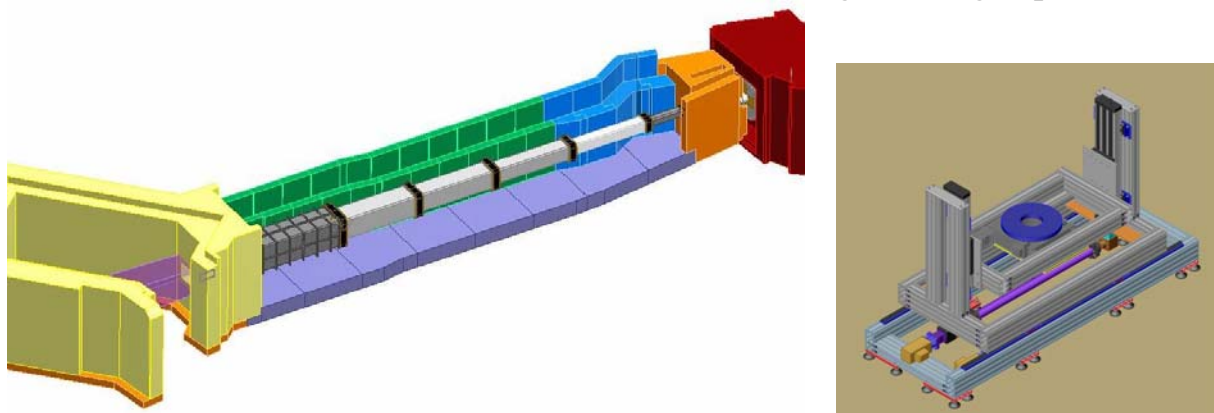


**Figure 2-2:** Beam design for FRM-II with 17 m length outside the reactor wall and sample manipulator

To avoid frame overlap, either a chopper must be used, or the radiography facility should be built at the long pulse target station. This would allow for a larger radial distance, more space for the sample position, a larger beam area and better time resolution with no frame overlap, but would lose 80% of the time-averaged flux available at the short pulse target station.

## REFERENCES

- [Domanus, 1992] J.C. Domanus (ed.), Practical Neutron Radiography, Kluwer Academic Publ., 1992
- [Schillinger, 1996] B. Schillinger, R. Gebhard, B. Haas, W. Ludwig, C. Rausch, U. Wagner: "3D Neutron Tomography in Material Testing and Archaeology", Proc. 5<sup>th</sup> World Conf. Neutron Radiography Berlin 1996
- [Fujine, 1999] S. Fujine et al. (ed.), Proc. 6<sup>th</sup> World Conf. on Neutron Radiography, Osaka, 1999
- [Lehmann, 1998] E. Lehmann et al. (ed.), Proc. 3<sup>rd</sup> Int. Topical Meeting on Neutron Radiography, Lucerne, 1998
- [Lehmann] E. Lehmann, P. Vontobel, L. Wiesel, Properties of the radiography facility NEUTRA at SINQ and its potential use as European reference facility, Nondestr. Test Eval. Vol.16, pp. 191-202
- [Schillinger, 2001] B. Schillinger, E. Calzada, F. Grünauer, E. Steichele, "The design of the neutron radiography and tomography facility at the new research reactor FRM-II at Technical University Munich", 4<sup>th</sup> Int. Topical Meeting on Neutron Radiography, Penn State Univ., 2001

## Instrument data:

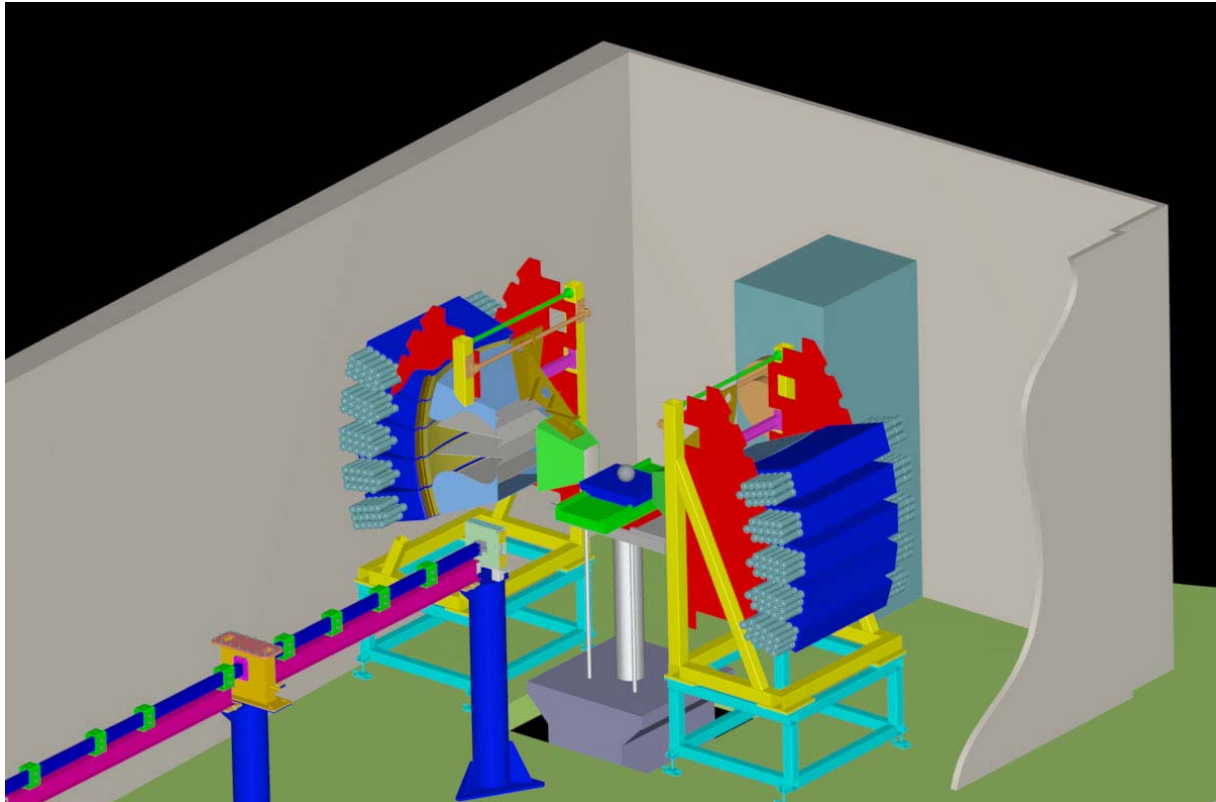
|                     |  |
|---------------------|--|
| moderator:          | decoupled cold hydrogen  |
| wavelength range:   | required wavelength range is 1 to 7 Å  |
| neutron guide:      | 5-25 m flight path   |
|                     | 100-600 collimation ratios   |
| choppers:           | counter-rotating, frame definition choppers:<br>7 & 10.5 m   |
| detectors:          | ideally 500 mm (0.5 mm resolution) time of flight sensitive detector, 100 mm (100 micron resolution) time of flight sensitive detector, traditional imaging detector                           |
| sample environment: | large footprint 'open access' sample area. 2x2 m sample area for <i>in situ</i> studies, high capacity positioner (500 kg, 10 micron), furnaces, processing plants, <i>in situ</i> loading rig |



## ENGINEERING DIFFRACTOMETER

**Location:** SPTS, SD16  
**Moderator:** decoupled thermal water

Schematic setup:



Schematic showing high capacity positioner at sample position, 90° detector banks and tuneable resolution super-mirror guide.

### Instrument description:

Substantial gains are possible in performance for an Engineering Diffractometer for Strain Measurement at the ESS, compared with existing sources. For such an instrument, the overriding requirement is the accurate measurement of a lattice parameter at a known location within the sample. The instrument is thus a powder diffractometer, modified to meet these specific requirements. Other issues include the requirement for considerable space and flexible prior setup of the instrument to allow for alignment of large samples as well as complicated sample environments.

The Engineering diffractometer would require a high resolution moderator (decoupled). Neither the proposed H<sub>2</sub> or H<sub>2</sub>O moderator options so far presented fully meet the needs of a strain measurement diffractometer. The possibility of obtaining higher resolutions using methane or hybrid moderators should be investigated.

The instrument should be situated on the 50Hz target. Two broad classes of experiment use the instrument, on a wide range of materials. Firstly, measurement of lattice separation changes as a function of position in an actual component providing maps of the stresses remaining after production, joining or use. Secondly studies of the effect of stress, temperature and other environmental variables on the deformation of materials, providing a fundamental understanding of the mechanics of materials. Both types of experiments provide information for process modelling, and materials development. In the former class, intensity is more important than monitoring a large range of peaks, hence would be run at 50Hz. The second class requires a greater wavelength window, hence would be run at 25 or even 16.67Hz.

To enable different instruments to be compared we define a Figure of Merit (FOM), proportional to the inverse of the time taken to measure a d-spacing to a given uncertainty. This approach has been used in the design of instruments presently under construction, which it is anticipated will be best-in-class e.g. [Johnson, 2002]. Undoubtedly, once these instruments have been commissioned, further lessons will be learnt and the ESS design modified accordingly.

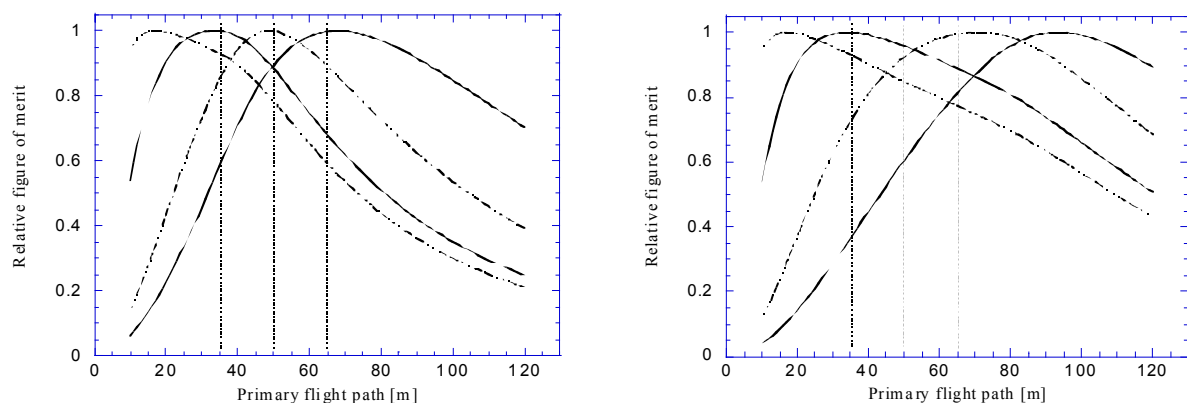


**Figure 2-3:** *Relative figure of merit [Johnson, 2002] for different samples, as a function of flight path, with running at (a) 50Hz, and (b) 25Hz. A reduced sample contribution to peak broadening leads to a longer optimum flight path. The curves, peaking from left to right in each figure, correspond to sample broadening comparable to martensite, heavily worked steel, steel and ceramic respectively. The instrument resolution has been tuned to match the sample resolution. Vertical lines indicate measurement band. The absolute values of the FOM increase with reduced sample broadening, being some factor of 4 larger for the 'ceramic' compared to the 'martensite'.*

The optimum instrument thus requires an ~50 m flight path, a variable resolution, and several square metres of space for large components and sample environments. These requirements can only be properly achieved with a dedicated instrument. Variable resolution would be achieved by allowing the sides of the guide to be switchable for absorbing material for approximately the last 10 m of guide. This allows horizontal divergence (and hence resolution) to be improved at the expense of neutron flux, 'tuning' the instrument resolution to match the sample resolution maximising performance.

Based on the criteria of the FOM, the basic instrument will perform from ~15 to 30 times better than best in class instruments presently under construction, with gain dependent on the sample resolution. If an improved, higher resolution moderator than detailed so far can be obtained, this would improve to ~x30 for all samples. By improving detector coverage, rapid mapping of strain tensors will provide improvements for some types of experiment, by a further factor of x2 to x3.

**REFERENCES:**

[Johnson, 2002] M.W. Johnson and M.R. Daymond, J. Appl. Cryst., (2002), **35** p.49-57.

**Instrument data:**

|                      |  |
|----------------------|--|
| moderator:           | high resolution decoupled thermal moderator  |
| wavelength range:    | $0.5 < \lambda < 7 \text{ \AA}$  |
|                      | $0.2\% < \Delta\lambda/\lambda < 0.7\%$ in $90^\circ$  |
| neutron guide:       | 40-60 m flight path, curved guide<br>20x60 mm cross section, m=3 supermirror.<br>tuneable resolution by 'switching' guide  |
| beam characteristics | Divergence variable $2E-2 \Rightarrow 2E-3$ vertical;<br>variable $7E-3 \Rightarrow 7E-4$ horizontal   |
| choppers:            | 6 and 9 m counter-rotating, large diameter, frame definition choppers required (50, 25 and 16.7Hz running).  |
| detectors:           | $90^\circ$ and backscatter detector banks, + transmission detector. $70 < 2\theta < 110^\circ$ ; $140 < 2\theta < 175^\circ$ . $\pm 45^\circ$ from horizontal Sample-detector distance ~1.5m<br>3mm wide scintillator elements for scattering, 0.2x0.2mm resolution for transmission   |
| sample environment:  | large footprint 'open access' sample area; 6 x 8 m, centred on measurement position, long axis parallel to beam. A preparation facility of similar size is required close by. If the flight path is long enough to require its own building, this would require a minimum footprint of ~13 x 13 m, and a crane hook height of >5 m. High capacity positioner (1500 kg, 10 micron accuracy), <i>in situ</i> loading rig (250 kN) with furnace and cryo-attachments, goniometer. |

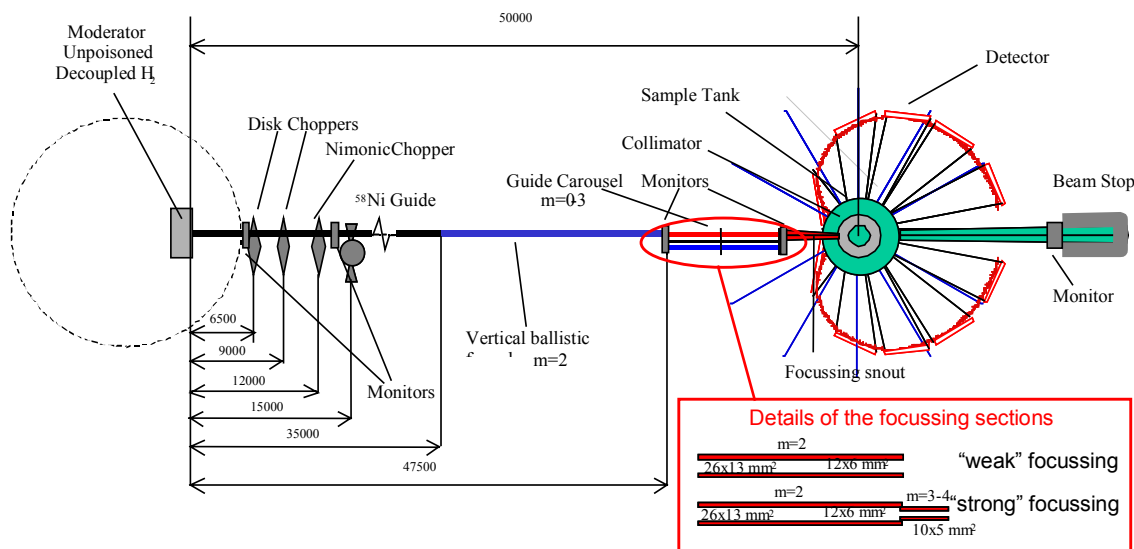




# MAGNETIC POWDER DIFFRACTOMETER

**Location:** SPTS, SD17  
**Moderator:** decoupled cold hydrogen

Schematic setup:



## Instrument description:

A straight  $^{58}\text{Ni}$  guide (tall  $(20 \times 80 \text{ mm}^2)$ ) delivers a chopper-selected bandwidth ( $1.6 \text{ \AA}$  at  $50 \text{ Hz}$ ) to a point  $35 \text{ m}$  away from the from the high-flux, decoupled  $\text{H}_2$  moderator. Here, the beam is vertically compressed by a super-mirror ( $m=2$ ) ballistic funnel ( $l=12.5 \text{ m}$ ). A guide carousel enables to select the final values of the horizontal and vertical divergence. A final focussing snout is provided for ultra-small sample and high-pressure experiments. The extended detector is designed for both narrow-bandwidth (angle-dispersive) and broad-bandwidth (wavelength-dispersive) operations, the latter achieved by repetition-rate reduction and/or chopper “slewing”. MAGPOW will have a top resolution comparable to GEM and OSIRIS ( $0.2\%$  in back-scattering), with count rate gains of  $\times 100$  and  $\times 30$ , respectively. In addition, MAGPOW will have a much-reduced beam divergence with respect to OSIRIS, which is essential to make use of the low-angle detectors. The *unfocussed* beam from MAGPOW will be twice as intense as the *focussed* beam of the new dedicated high-pressure magnetic diffractometer MICRO at LLB. Enhancement up to  $\times 10$  can be obtained by means of interchangeable focussing sections (see schematic drawing).

## Applications:

This instrument combines extremely high flux (maximising the count rate has been the guiding design principle) with good back-scattering resolution and low but tuneable beam divergence, and will provide excellent performances in all branches of magnetic powder diffraction. MAGPOW will excel in the study of ultra-small samples (<0.1 mg) at applied pressures in excess of 1 Mbar or in very high magnetic fields. The decoupled moderator delivers superb flux, but offers good resolution performances at 50 m, especially at long wavelengths. This is essential to study low-symmetry magnetic structures and magnetic domain size effects.

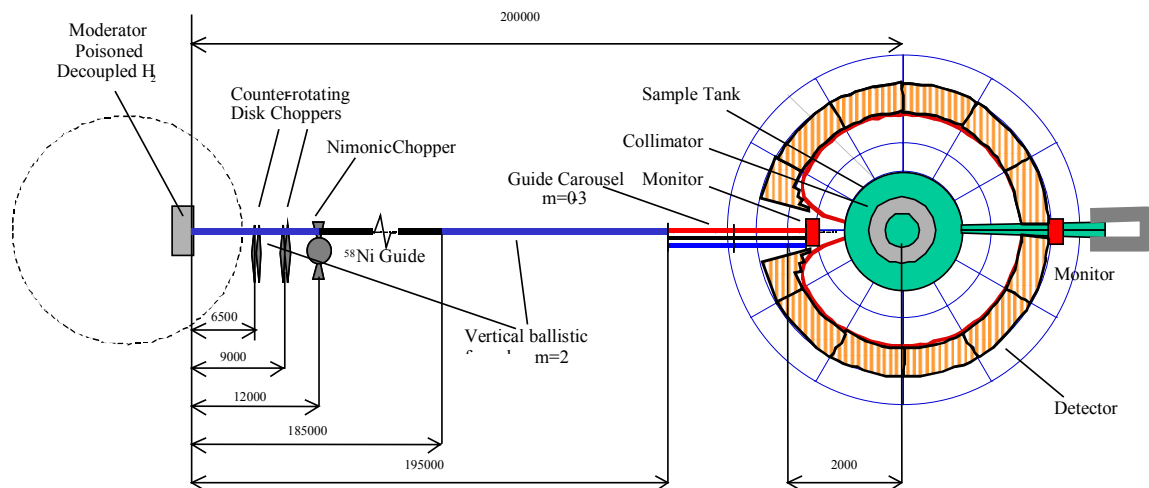
## Instrument data:

|   |   |
|---|---|
| moderator:  | decoupled hydrogen  |
| neutron guide:  | straight $^{58}\text{Ni}$ + focussing sections.   |
| neutron guide cross section:                          | 20×80 mm <sup>2</sup> (straight section).   |
| chopper distance:                                     | 6.3m, 10m, 12m, 15m   |
| chopper windows:                                      | 6.5 m: 42°@50 Hz<br>10.0 m: 69°@50 Hz<br>12.0 m 85°@ 50 Hz<br>15 m: 500 μsec raise time.  |
| chopper speed range:                                  | 5-50 Hz (disks), 100 Hz (nimonic)   |
| wavelength range:                                     | 1.0 < $\lambda$ < 30 Å  |
| bandwidth:  | 1.6 Å @ 50 Hz   |
| <i>d</i> -spacing resolution:                         | 0.2 % (backscattering)<br>0.3 % (2 $\theta$ =90°)<br>2.5% (2 $\theta$ =10°)   |
| flux at sample:                                       | 2×10 <sup>8</sup> n/cm <sup>2</sup> /sec @3.0 Å (unfocussed beam)<br>1×10 <sup>9</sup> n/cm <sup>2</sup> /sec @3.0 Å (“weak” focussing)<br>2×10 <sup>9</sup> n/cm <sup>2</sup> /sec @3.0 Å (“strong” focussing) |
| beam divergences:                                     | 0.25°×0.60° (uf)<br>0.7°×1.40° (wf)<br>1.1°×2.0° (sf)   |
| scattering angle:                                     | 2≤2 $\theta$ ≤175°, ±45 from horizontal plane   |
| distance sample detector:                             | 0.8-2.5m  |
| detector solid angle:                                 | 5 sterad  |
| detector elements:                                    | 3mm wide Ce:Li6Gd(BO <sub>3</sub> ) <sub>3</sub> scintillators  |
| sample environment:                                   | Cryostats, cryomagnets, high-pressure diamond-anvil cells.  |
| <i>Flux comparison with existing diffractometers:</i> | <i>GEM (ISIS): 1-2·10<sup>6</sup> n/cm<sup>2</sup>/sec</i><br><i>OSIRIS (ISIS): 1·10<sup>7</sup> n/cm<sup>2</sup>/sec</i>   |

# HIGH RESOLUTION POWDER DIFFRACTOMETER

**Location:** SPTS, SD18  
**Moderator:** decoupled cold hydrogen

Schematic setup:



## Instrument description:

A tall ( $20 \times 80 \text{ mm}^2$ ) straight  $^{58}\text{Ni}$  guide delivers the chopper-selected bandwidth ( $0.4 \text{ \AA}$  at  $50 \text{ Hz}$ ) to a point  $185 \text{ m}$  away from the moderator. Here, the beam is vertically compressed by a super-mirror ( $m=2$ ) ballistic funnel ( $l=10 \text{ m}$ ; a true ballistic guide may be considered to improve chopper performances). The final interchangeable guide section either homogenises the beam whilst maintaining the vertical divergence (top-bottom  $m=3$  section) or further focuses it to the sample position. This innovative design enables the vertical divergence to be matched precisely to the out-of-plane detector coverage, and leaves room for further focussing downstream. The extended detector is designed for both narrow-bandwidth (angle-dispersive) and broad-bandwidth (wavelength-dispersive) operations, the latter achieved by repetition-rate reduction and/or chopper “slewing”. ESS-HRPD will have a top resolution comparable to the best existing neutron diffractometers ( $0.04\%$  in back-scattering), but offers an increase in count rate by a factor of 300 with respect to HRPD at ISIS (with proportionately much bigger gains at shorter wavelengths) and D2B at the ILL (these figures also reflect the large potential for improvement of existing instruments). The flux at the sample position will be 5-10 times greater than that of GEM at ISIS with 5 times better resolution, making it possible to collect data on small samples (e.g.,  $1 \text{ mm}$  capillaries) in a few minutes and on normal-size neutron samples in seconds.

## Applications:

This instrument covers all the traditional applications of both pulsed and reactor high-resolution powder diffraction, including Rietveld refinement on low-symmetry structures, strain analysis and magnetism. The resolution function can be tailored to best suit each problem. The much-enhanced flux of ESS-HRPD will enable multi-dimensional phase diagrams to be explored at high resolution in a variety of sample environments. In wavelength-dispersive mode, ESS-HRPD will be suitable for solving crystal and magnetic structures of moderate complexity.

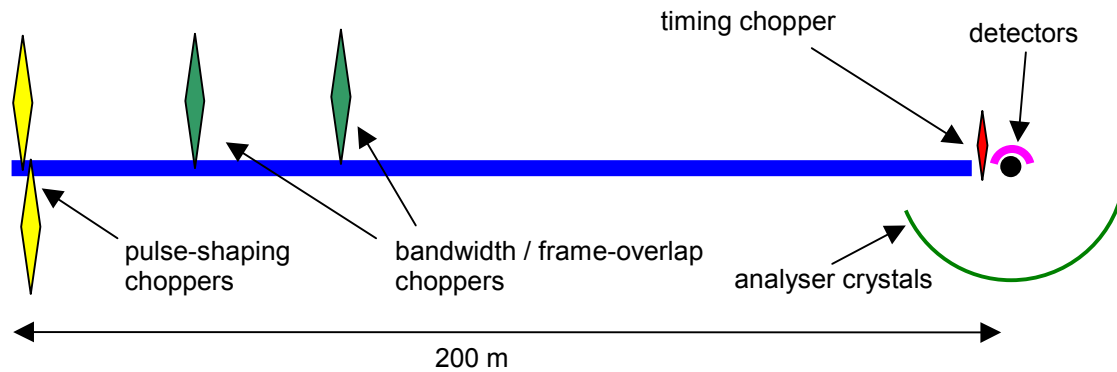
## Instrument data:

|   |  |
|---|--|
| moderator:  | decoupled cold hydrogen  |
| neutron guide:  | straight $^{58}\text{Ni}$ + focussing sections.  |
| neutron guide cross section:                          | $20 \times 80 \text{ mm}^2$ (straight section).  |
| chopper distance:                                     | 6.5m, 9m, 12m  |
| chopper windows:                                      | 6.5 m: $11^\circ$ - $118^\circ$ @ 50-5 Hz<br>9.0 m: $16^\circ$ - $164^\circ$ @ 50-5 Hz<br>12 m: 500 $\mu\text{sec}$ raise time.                      |
| chopper speed range:                                  | 5-50 Hz (disks), 100 Hz (nimonic). Large-diameter counter-rotating choppers are required for narrow-band operation (0.4 $\text{\AA}$ )               |
| wavelength range:                                     | $0.4 < \lambda < 15 \text{ \AA}$   |
| bandwidth:  | 0.4 $\text{\AA}$ @ 50 Hz   |
| $d$ -spacing resolution:                              | 0.04% (backscattering)<br>0.15% ( $2\theta=90^\circ$ )<br>1.7% ( $2\theta=10^\circ$ )  |
| flux at sample:                                       | $1\text{-}2 \times 10^7 \text{ n/cm}^2/\text{sec}$ @ 1.5 $\text{\AA}$ , depending on choice of final guide section                                   |
| beam divergence:                                      | $0.17^\circ \times 0.50^\circ$ (unfocussed)  |
| scattering angle:                                     | $5 \leq 2\theta \leq 175^\circ$ , $\pm 45$ from horizontal plane   |
| distance sample detector:                             | 1.0-2m   |
| detector solid angle:                                 | 5 sterad   |
| detector elements:                                    | mm wide Ce:Li <sub>6</sub> Gd(BO <sub>3</sub> ) <sub>3</sub> scintillators   |
| sample environment:                                   | Cryostats and furnaces, both standard and optimised for small-samples/fast equilibration time, variable pressure/ temperature cells, cryomagnets.    |
| <i>Flux comparison with existing diffractometers:</i> | <i>HRPD (ISIS): <math>1 \cdot 10^5 \text{ n/cm}^2/\text{sec}</math><br/>GEM (ISIS): <math>1\text{-}2 \cdot 10^6 \text{ n/cm}^2/\text{sec}</math></i> |

## HIGH RESOLUTION QUASIELASTIC BACKSCATTERING (0.8 $\mu\text{eV}$ )

**Location:** SPTS, SC19  
**Moderator:** coupled cold hydrogen

Schematic setup:



### Instrument description:

An inverse-geometry instrument for quasielastic measurements using Si 111 crystals arranged in direct backscattering to give an energy resolution of 0.8  $\mu\text{eV}$ . The instrument is 200 m long and uses a ballistic supermirror guide.

A pulse-shaping chopper is used to provide a very sharp time structure, while benefitting from the high peak flux of the coupled cold moderator. Slowing down the pulse-shaping chopper allows about a factor of 4 to be gained in flux by relaxing the resolution up to about 4  $\mu\text{eV}$ .

A wavelength band of  $\Delta\lambda = 0.3 \text{ \AA}$  is used, centred on the elastic wavelength for the Si 111 reflection of 6.27  $\text{\AA}$ . This gives a dynamic range of about 200  $\mu\text{eV}$  in energy transfer.

A timing chopper is used to discriminate against neutrons scattering directly into the detectors from the sample. Decoupling the frequency of the timing chopper from the source frequency allows the full incident wavelength band to be used. The factor of two loss in flux arising from the timing chopper is compensated for by the large solid-angle coverage of the analyser crystals, similarly to present-day reactor-source instruments.

## Applications:

Dynamics of polymer and glassy materials, phase transitions, disordered magnetic systems and transport phenomena.

## Instrument data:

|                              |   |
|------------------------------|---|
| moderator:                   | coupled cold hydrogen   |
| neutron guide:               | $m=2$ ballistic with $m=4$ converging section   |
| neutron guide cross section: | $11 \times 12$ cm   |
| chopper distance:            | 6.3 m   |
| wavelength range:            | $6.0 < \lambda < 6.3 \text{ \AA}$   |
| energy range:                | $\pm 100 \text{ \mu eV}$  |
| energy resolution:           | $0.8 \text{ \mu eV}$ adjustable up to $4 \text{ \mu eV}$  |
| $Q$ range:                   | $0.1 < Q < 1.9 \text{ \AA}^{-1}$  |
| flux at sample:              | $1.7 \times 10^7 \text{ n/cm}^2/\text{s}$ adjustable up to $9 \times 10^7 \text{ n/cm}^2/\text{s}$ by relaxing resolution |
| beam size at sample:         | $2 \times 3$ cm   |
| distance sample-detector:    | 4 m sample-analysers-detectors  |

The figures below shows the calculated flux at the elastic line and the dynamic range, compared to IN16 and HFBS (NIST). The flux at the elastic line can be dramatically increased on a steady-state source by switching off the monochromator Doppler drive. There is no such option for this instrument. However, even with the Doppler drive off, the ESS instrument still has a factor of two higher flux than IN16 at the same resolution. The dynamic range is 1-2 orders of magnitude greater.

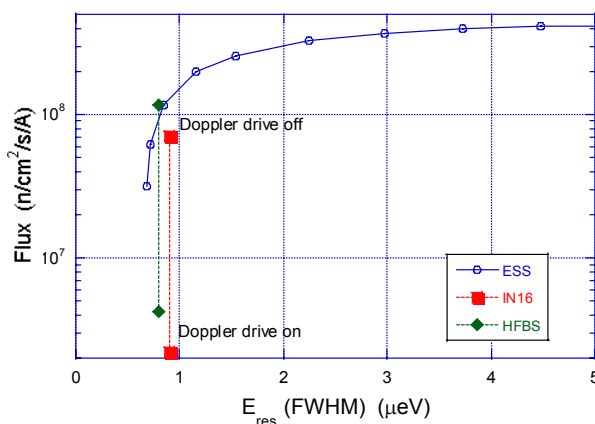


**Figure 2-4:** Flux Comparison

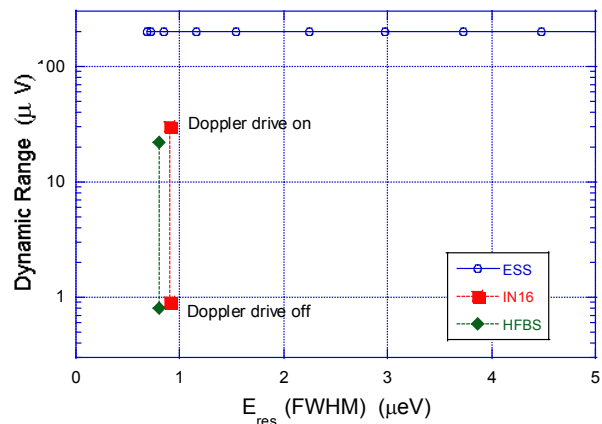
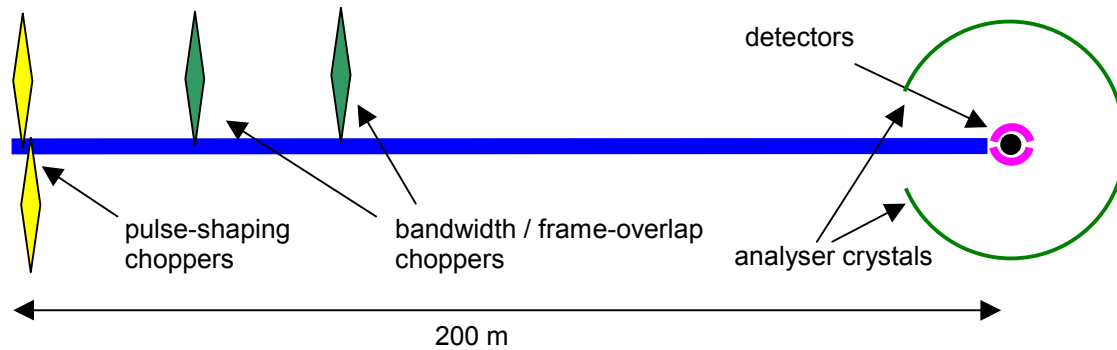


**Figure 2-5:** Dynamic Range

## HIGH RESOLUTION INELASTIC BACKSCATTERING (1.5 $\mu\text{eV}$ )

**Location:** SPTS, SC19  
**Moderator:** coupled cold hydrogen

Schematic setup:



### Instrument description:

An inverse-geometry instrument for inelastic measurements using Si 111 crystals arranged in near-backscattering to give an energy resolution of 1.5  $\mu\text{eV}$ . The instrument is 200 m long and uses a ballistic supermirror guide.

A pulse-shaping chopper is used to provide a very sharp time structure, while benefitting from the high peak flux of the coupled cold moderator.

Placing the detectors in near-backscattering allows the clean measurement of inelastic scattering far from the elastic peak and improves the signal-to-noise ratio.

Resolution can be tuned by adjusting the speed of the pulse-shaping chopper. Varying the chopper phases allows energy transfers of up to 10 meV to be accessed with energy resolutions between 1.1 and about 20  $\mu\text{eV}$ . A wavelength band of  $\Delta\lambda = 0.3 \text{ \AA}$  is used. This gives a dynamic range of about 200  $\mu\text{eV}$  in energy transfer around the elastic peak and about 3 meV at 10 meV energy transfer.

Energy transfers around 10 meV can be reached with a resolution of 5  $\mu\text{eV}$ . Such a combination of energy transfer and resolution is not presently accessible on any instrument.

### Applications:

Dynamics of polymers, glassy materials, and disordered magnetic systems, high-resolution structural and magnetic excitations such as rotational tunnelling of larger molecular systems (molecular ratchets), crystal-field splitting, magnetic cluster splitting of molecular magnets



### Instrument data:

|                              |   |
|------------------------------|---|
| moderator:                   | coupled cold hydrogen   |
| neutron guide:               | $m=2$ ballistic with $m=4$ converging section   |
| neutron guide cross section: | $11 \times 12$ cm   |
| chopper distance:            | 6.3 m   |
| wavelength range:            | $2 < \lambda < 10 \text{ \AA}$  |
| energy range:                | $-1 < \eta\omega < 10$ meV  |
| energy resolution:           | 1.1 $\mu\text{eV}$ adjustable up to 4 $\mu\text{eV}$ at the elastic line<br>up to 20 $\mu\text{eV}$ at energy transfers up to 10 meV      |
| $Q$ range:                   | $0.1 < Q < 1.9 \text{ \AA}^{-1}$ at the elastic line  |
| flux at sample:              | $7 \times 10^7$ n/cm <sup>2</sup> /s at the elastic peak, adjustable up to<br>$5 \times 10^8$ n/cm <sup>2</sup> /s by relaxing resolution |
| beam size at sample:         | $2 \times 3$ cm   |
| distance sample-detector:    | 4 m sample-analysers-detectors  |

The figures below shows the calculated flux at the elastic line, compared to IN16, IN13 and HFBS (NIST). At comparable resolution, the ESS instrument gives between one and two orders of magnitude more flux than IN16 and IN13. In addition, energy transfers of up to 10 meV can be accessed with  $\mu\text{eV}$  resolution.

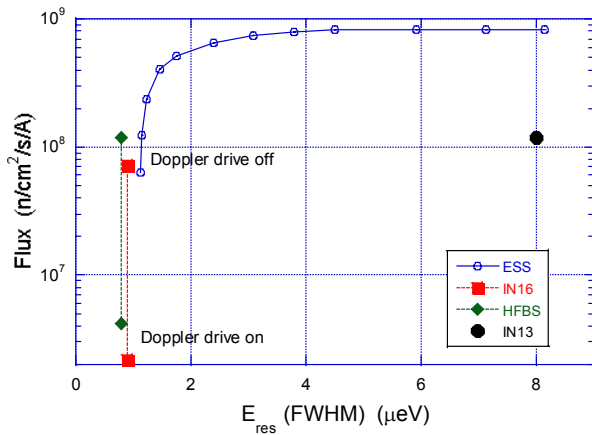


Figure 2-6: Flux Comparison

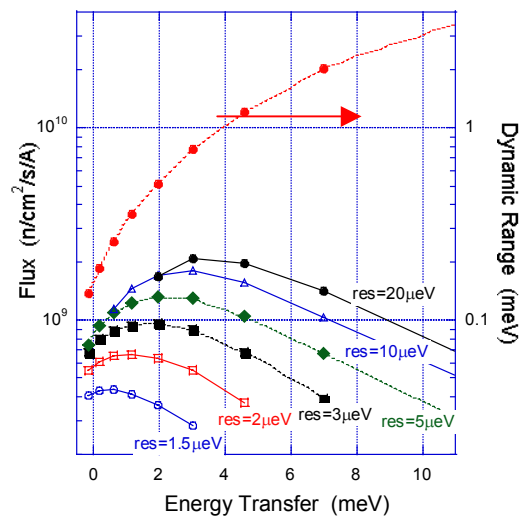
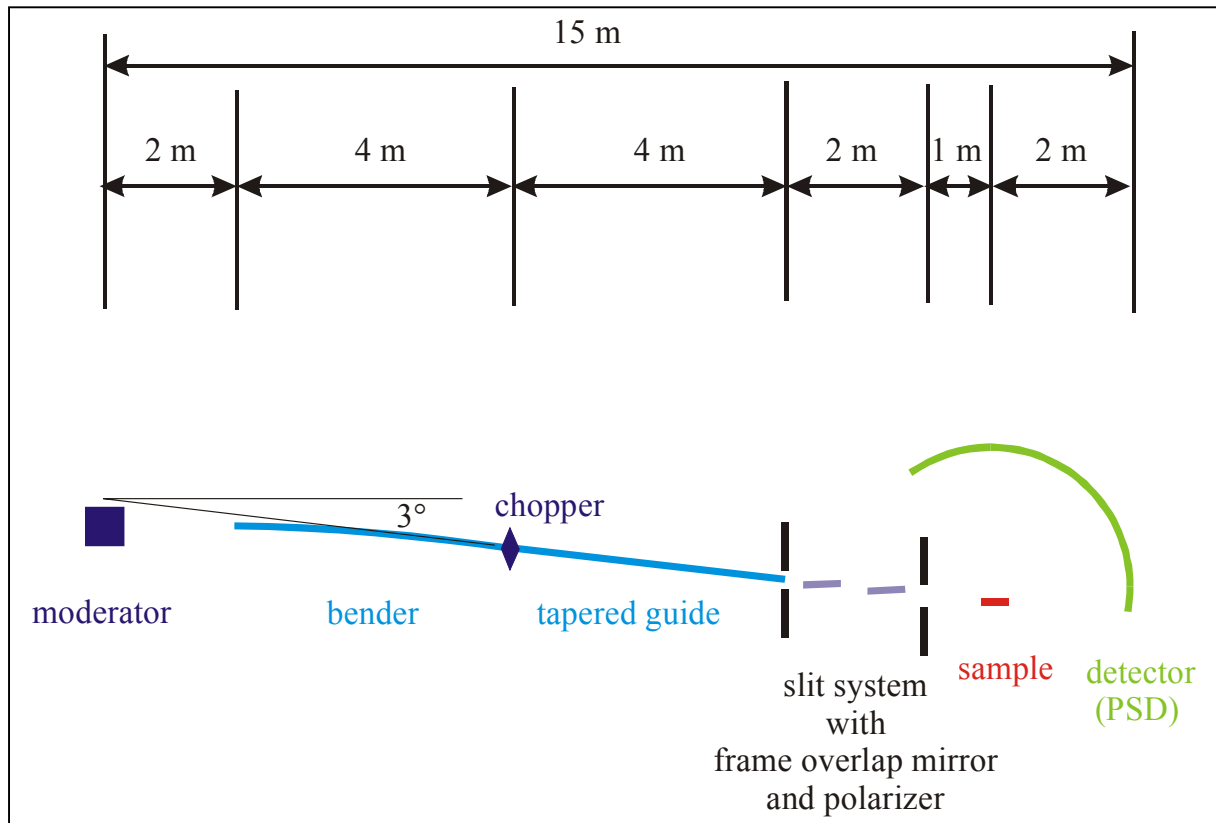


Figure 2-7: Inelastic Performance

## HIGH RESOLUTION REFLECTOMETER

**Location:** SPTS, SC22  
**Moderator:** coupled cold hydrogen

Schematic setup (side view):



### Instrument description:

A bender with 4 channels is used to avoid the direct line-of-sight to the moderator and to get rid of the background produced by the fast neutrons and the  $\gamma$  rays. The used wavelength range between 0.2 nm and 0.72 nm is defined by the bender and the chopper. To avoid a crosstalk from the slow neutrons of the previous pulse a frame overlap mirror has to be inserted.

In order to be able to investigate solid as well as liquid samples a vertical scattering plane is realised. The exit of the bender has an inclination of  $3^\circ$  with respect to the horizontal and the tapered guide delivers a divergence of about  $6^\circ$ . Hence a range from  $0^\circ$  to  $6^\circ$  can be achieved for the angles of incidence by changing the height of the slits and the sample.

The position sensitive detector (PSD) covering a range of the scattering vector of  $150^\circ$  as well as the sample holder consisting of two tilt stages ( $\omega$ - and  $\chi$ -rotation) are novel design features. It is not only possible to investigate off-specular scattering but because of the large angular range covered by the PSD it is also possible to perform reflectometry and diffractometry on the same

instrument, i.e. to determine e.g. the ferromagnetic and crystalline properties and their dependencies at exact the same values for all sample environment parameters.

### Applications:

This reflectometer is dedicated to samples which need a high resolution in  $q$  of 3%. Because of the vertical scattering plane solid as well as liquid samples can be investigated. The high intensity provides the possibility to measure down to reflectivities of about  $10^{-9}$  and  $q$ -values corresponding to Bragg peaks of 1 nm thick layers.

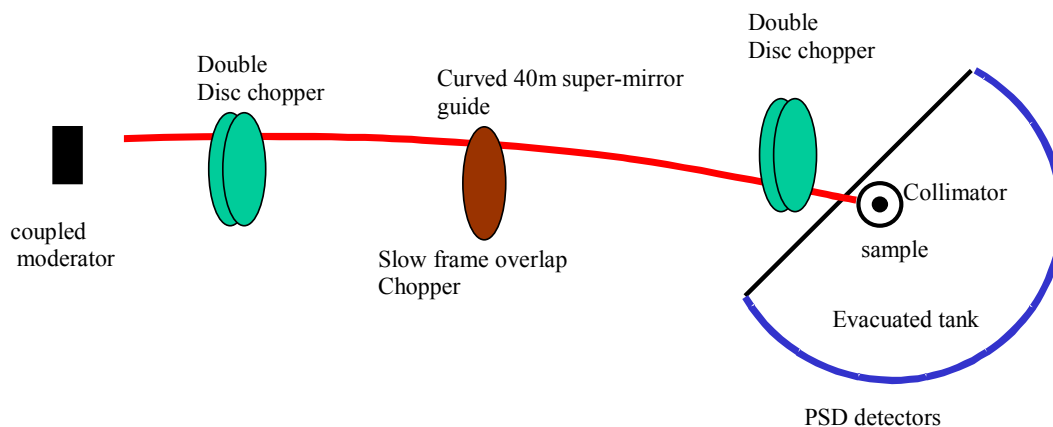
### Instrument data:

|  |   |
|--|---|
| moderator:   | coupled cold hydrogen   |
| neutron guide:   | bender (bending angle $1.5^\circ$ ) and tapered guide   |
| neutron guide cross section:   | <u>bender:</u><br>width: tapered 15 cm - 10 cm; height: 10 cm.<br><u>tapered guide:</u><br>width 10 cm - 5cm; height: 10 cm - 3 cm.                           |
| chopper distance:  | 6 m from moderator  |
| chopper windows:   | $146^\circ$   |
| chopper speed range:   | 3000 rpm  |
| polarizer:   | Fe/Co supermirrors  |
| wavelength range:  | $0.2 \text{ nm} < \lambda < 0.72 \text{ nm}$  |
| $q$ -range for solids:   | $0.003 \text{ \AA}^{-1} - 4.5 \text{ \AA}^{-1}$   |
| $q$ -range for liquids:  | $0.003 \text{ \AA}^{-1} - 0.3 \text{ \AA}^{-1}$   |
| flux at sample:  | approx. $1 \cdot 10^8 \text{ n/s/cm}^2$ at a collimation of 1 mrad  |
| scattering angle:  | $0^\circ$ - $150^\circ$ for solids, $0^\circ$ - $12^\circ$ for liquids  |
| distance sample detector:  | 2 m   |
| detector:  | PSD covering an angular range of $150^\circ$  |
| sample environment:  | Langmuir trough, magnet, cryostat, furnace  |
|  |   |
| <i>Flux comparison to existing liquids reflectometers:</i>                           | <i>V6 (HMI, PG monochromator): <math>3 \cdot 10^4 \text{ n/s/cm}^2</math> ;<br/>SURF (ISIS; estimated): <math>8 \cdot 10^5 \text{ n/s/cm}^2</math></i>        |
| <i>Flux comparison to existing reflectometers with a horizontal scattering plane</i> | <i>ADAM (ILL; PG monochromator) <math>2 \cdot 10^6 \text{ n/s/cm}^2</math> ;<br/>D17 (ILL; velocity selector): <math>2 \cdot 10^7 \text{ n/s/cm}^2</math></i> |
| <i>Performance gain factors</i>  | <i>V6: 3300; SURF: 120; ADAM: 50; D17: 5</i>  |

## COLD CHOPPER SPECTROMETER

**Location:** SPTS, SC24  
**Moderator:** coupled cold hydrogen

Schematic setup:



### Instrument description:

LET is a direct geometry time of flight spectrometer. It will have a wide dynamic range with incident energies ranging from less than 1 meV to around 80 meV making it excellent for both quasi-elastic and inelastic scattering. The large angular coverage of the detector bank ensures a large region of  $Q$ ,  $\omega$  space is accessed in a single scan. The instrument offers total flexibility over the incident energy and the resolution thanks to the multiple chopper system. The initial pair of counter-rotating choppers control the component of the resolution arising from the moderator whereas the final pair of counter rotating choppers, just before the sample, control the chopper resolution component. Apart from giving total flexibility over the resolution it also allows one to optimise the flux by 'matching' the different resolution components. Having control over the moderator component also enables the use of a coupled moderator, which also enhances the flux and has the additional benefit of allowing one to relax the resolution if necessary and gain considerably in flux. Another advantage of using multiple choppers is one gets a better lineshape (very close to triangular) as the initial chopper cuts the long tail off the moderator. A frame overlap chopper is needed to ensure there is no overlap of neutrons from different frames when measuring at very incident energies.

The 40 m guide is curved such that the sample does not view the moderator directly. This ensures the ‘prompt’ pulse from the next frame does not affect the measurements. Provision will be made for a He3 spin polariser in the incident beam and analyser in the scattered beam for when the technology becomes feasible.

The whole detector tank will be pumped down to cryogenic vacuums as with the MAPS spectrometer at ISIS. This reduces the background scattering because no Aluminium windows are necessary between the sample and detector tank. The cryogenic vacuum also allows one to design cryogenics with less Aluminium in the beam. For example, at ISIS we have designed a cryostat which can cool samples to 4K in an exchange gas with a total of only 0.2 mm thickness of Aluminium in the beam from the cryostat. A rotating radial collimator on a jacking system for easy removal will reduce the background from more extreme sample environment equipment such as pressure cells.

The detectors will all be position sensitive He3 detector tubes. This gives the user total flexibility to ‘slice and dice’ reciprocal space within the software making the instrument ideal for both powder and single crystal communities. The detectors will span a wide angular range,  $-30^\circ$  to  $140^\circ$ , which is necessary to give a large enough Q range at low incident energies. Ideally squashed detector tubes will be used as this improves the best resolution achievable by reducing the detector contribution.

### Instrument data:

| <b>Primary Spectrometer:</b>        |   |
|-------------------------------------|---|
| moderator                           | coupled cold hydrogen                                     |
| choppers                            | two double disk choppers<br>frame overlap chopper         |
| chopper Speed                       | 6000 – 20000 rpm  |
| incident $\lambda$                  | 12 – 1 Å  |
| incident energy $E_0$               | 0.5-80 meV  |
| moderator to sample distance        | 40 m  |
| He3 spin polariser                  |   |
| elastic energy resolution           | 7 $\mu$ eV at $E_0=1$ meV<br>900 $\mu$ eV at $E_0=80$ meV |
| max energy loss of neutrons         | $\approx 0.8 \times E_0$                                  |
| max energy gain of neutrons         | 2.5 $k_B T$ of sample                                     |
| max momentum transfer<br>$Q_{\max}$ | $0.037 \times E_0^{1/2}$                                  |
| min momentum transfer $Q_{\min}$    | $1.32 \times E_0^{1/2}$                                   |

|   |   |
|---|---|
| beam size at sample                             | 3x5 cm  |
| flux at the sample at 5meV<br>and 2% resolution | $4.2 \times 10^6 \text{ n cm}^2 \text{ s}^{-1}$ |
| <b>Secondary spectrometer</b>                   |   |
| detector type                                   | position sensitive detectors                    |
| sample to detector distance                     | 4 m   |
| angular range                                   | - 30° – 140°                                    |
| He3 spin analyser                               |   |
| oscillating radial collimator                   |   |



## VARIABLE RESOLUTION COLD CHOPPER SPECTROMETER

**Location:** LPTS, LM02

**Moderator:** multi-spectral, coupled thermal cold combination

The instrument lay-out similar to the cold neutron chopper spectrometer, p. 2-32.

This instrument offers optimal flexibility for trading intensity for resolution and vice versa, in particular to provide high neutron counting rates to explore very small inelastic and quasielastic signals from non-crystalline matter in the most relevant  $q$  range for observing collective phenomena  $q < 1.5 \text{ \AA}^{-1}$ . At the same time the wide incoming wavelength range provided by the cold and thermal multi-spectral beam also allows experimenters to obtain an overview over the whole picture, including high  $q$  values up to  $10 \text{ \AA}^{-1}$  and energies up to 60 meV in down-scattering. The instrument combines a series of features aimed at achieving maximal neutron counting rates:

- using the LPTS for highest number of neutrons per pulse
- pulse repetition rate on the sample up to 333 Hz by repetition rate multiplying chopper system
- beam delivery by supermirror ballistic guide
- trapezoidal, close to rectangular chopper line shapes to maximize intensity for a given pulse duration

The 90 m moderator to sample distance assures good efficiency for repetition rate multiplication operation with  $0.15 \text{ \AA}$  wavelength difference between subsequent pulses on the sample at 300 Hz (optimal e.g. for down-scattering experiments at low temperatures) and  $< 2.5 \text{ \AA}$  difference between the shortest and the longest wavelengths used in one run. Typical effective pulse repetition rate at 5 meV incoming energy or higher with up-scattering allowed for: 150 Hz.

The ballistic neutron guide is 70 mm wide and 180 mm high in the middle, Ni coated section, it is compressed to a 25 mm x 65 mm cross section before the sample. It transmit neutrons with high efficiency for wavelengths  $> 1 \text{ \AA}$ .

The 3 m sample to detector distance favors high solid angle coverage with position sensitive detectors with 2 cm x 2 cm pixel size and provide  $-140^\circ$  to  $140^\circ$  angular coverage. Oscillating radial collimator is used to reduce the background. The sample chamber is evacuated.

A part of the Ni coated middle guide section can be optionally replaced by a broad band supermirror cavity polarizer, and similar polarization analyzers can be placed in front of the a small fraction of the detectors in the equatorial plane.



The repetition rate multiplying chopper system consists of 2 double disc choppers and 5 frame overlap and repetition rate adjustment choppers. The pulse length are primarily adjusted by choosing between different slit widths at high choppers speeds with the help of the relative phasing of the choppers compared to each other or by stopping a chopper in the open position. The two double choppers defining the primary and secondary resolution are always operated > 60 % of maximum speed to assure nearly rectangular pulse shapes in the highest intensity mode.

### Instrument data:

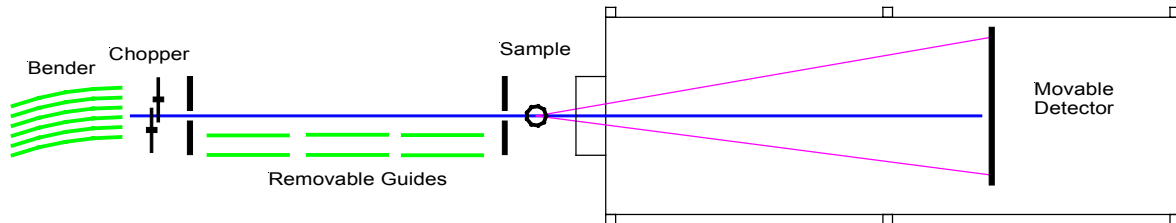
|  |   |                           |  |
|--|---|---------------------------|--|
| moderator:   | multi-spectral, coupled thermal cold combination  |                           |  |
| moderator to sample distance:                      | 90.5 m  |                           |  |
| beam delivery:                                     | curved ballistic guide,<br>biggest cross section: 7 cm x 18 cm  |                           |  |
| primary resolution chopper:                        | parallel rotating disc pair at 45 m,<br>max. speed 20000 RPM  |                           |  |
| secondary resolution chopper:                      | counter-rotating disc pair at 90 m,<br>max speed 20000 RPM  |                           |  |
| frame overlap choppers:                            | 5 single discs between 6 and 70 m,<br>speeds between 1000 – 10000 RPM   |                           |  |
| pulse rep. rate on sample:                         | variable between 16.67 and 333.33 Hz  |                           |  |
| sample to detector distance:                       | 3 m   |                           |  |
| detector area:                                     | 15 m <sup>2</sup>   |                           |  |
| scattering angle range:                            | 2° – 140°   |                           |  |
| incident wavelength:                               | 1 – 20 Å  |                           |  |
| beam size at sample:                               | 2.5 cm x 6 cm   |                           |  |
| high intensity setting:                            | average $\lambda$ :   | elastic resolution:       | flux at sample:                          |
|  | 2 Å   | 10 % (2 meV)              | $3 \times 10^7 / \text{cm}^2 \text{s}$   |
|  | 4 Å   | 5 % (0.25 meV)            | $3 \times 10^7 / \text{cm}^2 \text{s}$   |
| high resolution setting:                           | average $\lambda$ :   | elastic resolution:       | flux at sample:                          |
|  | 2 Å   | 3 % (0.7 meV)             | $2 \times 10^6 / \text{cm}^2 \text{s}$   |
|  | 4 Å   | 1.5% (80 $\mu\text{eV}$ ) | $2 \times 10^6 / \text{cm}^2 \text{s}$   |
|  | 10 Å  | 0.7% (6 $\mu\text{eV}$ )  | $1.5 \times 10^5 / \text{cm}^2 \text{s}$ |
| <i>Flux comparison with existing spectrometers</i> | <i>IN5, ILL (status 2000):<br/>flux at sample (<math>\lambda=4 \text{ \AA}</math>, 5 % resolution): <math>5 \times 10^4 / \text{cm}^2 \text{s}</math><br/>detector area: 6 m<sup>2</sup>, sample-detector distance: 4 m</i> |                           |  |

# HIGH INTENSITY SANS INSTRUMENT

**Location:** LPTS, LM04

**Moderator:** multi-spectral, coupled thermal cold combination

Schematic setup:



## Instrument description:

Viewing the multi-spectral coupled cold H<sub>2</sub> moderator, a supermirror bender reduces fast neutron background, a pair of variable opening counter-rotating choppers at 6m select a neutron wavelength band appropriate for the chosen sample-detector distance. Optional polarising filter and "guide field" will allow for detail investigations of magnetic systems.

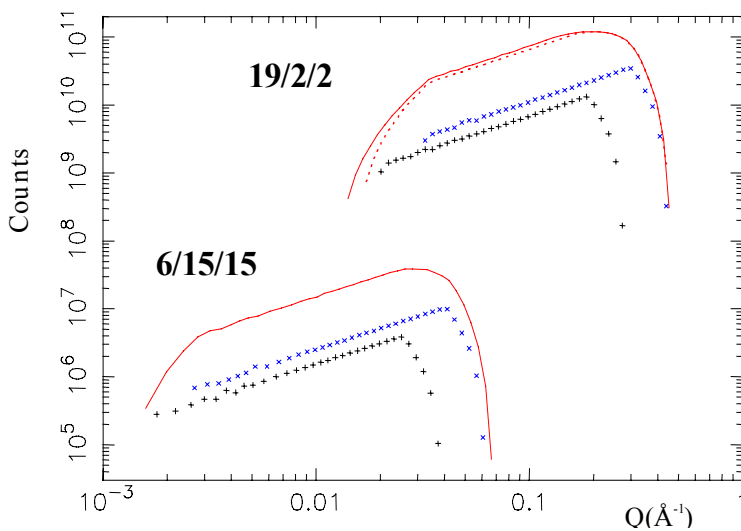
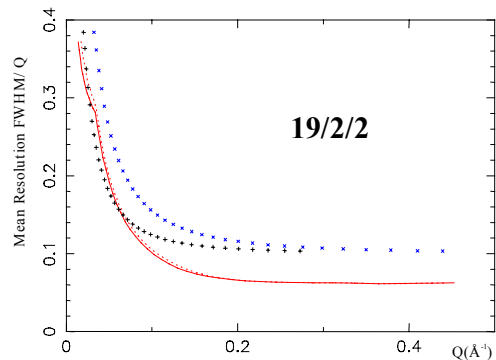
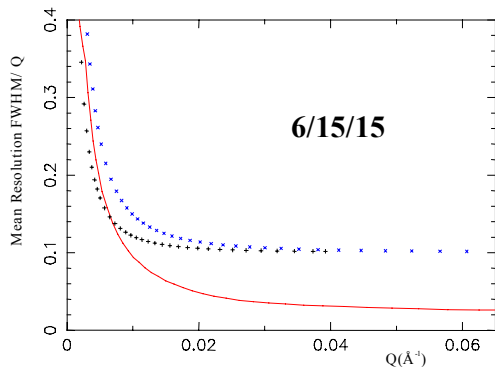


**Figure 2-8:** SANS at 36m (6/15/15) and 24m (19/2/2), collimation and sample-detector distance of 15 m & 2 m, counts for 1 cm<sup>2</sup> flat scatterer and mean resolution FWHM/Q (below)

5MW long pulse ESS, **line** 6/15/15  $\lambda=4.4 - 9.2\text{\AA}$  (including prompt spike at 6.6 - 7.0  $\text{\AA}$ , ignoring here 9.2 - 11 $\text{\AA}$  due to inelastic from hydrogen); **line** 19/2/2  $\lambda=4.6 - 12\text{\AA}$ , **dots** 4.6 - 9.9  $\text{\AA}$  (excluding prompt spike after 9.9  $\text{\AA}$ ).

Fixed wavelength comparisons ~ILL reactor: **xxx**  $\lambda=5\text{\AA}$ ; **+++**:  $\lambda=8\text{\AA}$ , 10% FWHM



Adjustable pinhole collimation and removable guide sections together with a large (>1 m square) movable area detector (at 2 – 30 m) tailor the overall Q range and Q resolution to suit particular experiments. Compared to the best available reactor instrumentation the simultaneous Q range is greatly expanded and Q resolution considerably improved over most of the range. This is illustrated for 2 m and 15 m sample-detector distances. By using a 30 m sample-detector a minimum Q of  $\sim 3 \times 10^{-4} \text{ \AA}^{-1}$  may be reached. Typical count rates will be 5-10 times improved over the current "world's best", before allowing for increased detector areas. The "fall off" in count rates of the pulsed source at small Q is due to only the longer wavelengths contributing at the smallest Q's, this is often compensated by increasing SANS cross section.

### Applications:

SANS instruments traditionally cover an extremely wide range of science from biology and soft matter through colloid science to polymers, metal alloys, magnetic systems, porous materials and geology. Many new opportunities will be presented by the increased count rates, improved resolution and expanded Q range offered by a flexible state of the art pulsed source SANS machine. Increasing use of non-equilibrium environments for the *in-situ* study of reactions and dynamics via structural changes will be important. Such studies benefit particularly from a wide simultaneous Q range as the most appropriate Q range may change rapidly or not be known prior to the experiment. Running at half the source frequency will expand the simultaneous Q range still further. Another key area will be greater use of selective deuteration to allow neutron contrast variation to reveal internal structure of systems. An increased flux will permit smaller quantities and lower concentrations of precious samples to be used.

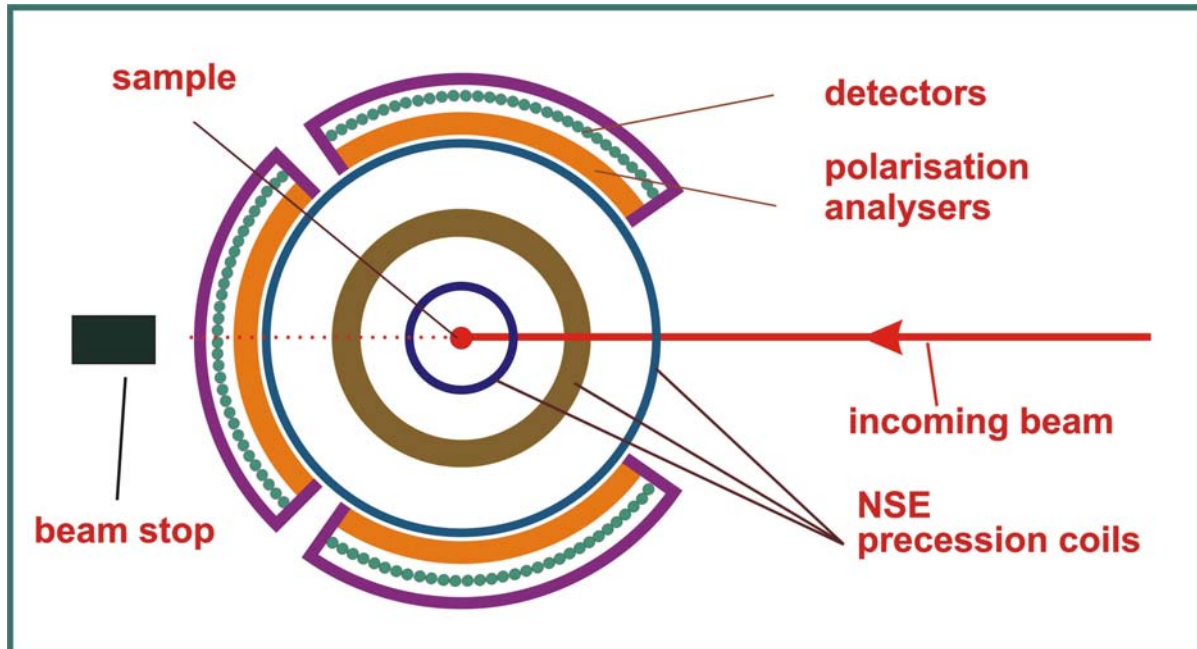
### Instrument data:

|                              |   |
|------------------------------|---|
| moderator:                   | multi-spectral, coupled thermal cold combination  |
| neutron guide:               | multi-channel bender, polarised filter, removable guide sections  |
| neutron guide cross section: | to be determined  |
| chopper distance:            | 6 m   |
| wavelength range:            | $0.2 < \lambda < 1.2 \text{ nm}$  |
| distance sample detector:    | $\sim 2$ to $\sim 30 \text{ m}$   |
| Q-range:                     | $\sim 3 \times 10^{-4}$ to $\sim 1 \text{ \AA}^{-1}$  |
| detector:                    | at least $1 \text{ m}^2$ , 5 mm resolution  |
| sample environment:          | range of temperature controlled sample changer, furnace, cryostat, shear flow / simultaneous rheology, linear flow, stop-flow, extensiometer etc. |

## WIDE ANGLE NSE SPECTROMETER / DIFFUSE SCATTERING (D7)

**Location:** LPTS, LM16

**Moderator:** multi-spectral, coupled thermal cold combination



### Instrument description:

Efficient use of the pulsed beam structure of spallation sources implies measuring with an as broad as possible wavelength band, which then requires the maximum possible solid angle for simultaneous measurements especially at high  $Q$ 's. These requirements are met by the Wide-Angle Neutron Spin Echo technique, first developed with the spectrometer SPAN at the HMI. On the basis of this design a new instrument is proposed for the ESS with an improved resolution capability and the largest possible detection solid angle. The spectrometer will also be used for diffuse scattering studies and should have the option for XYZ polarisation analysis and/or direct geometry time-of-flight (TOF) measurements. Optimum neutron economy and advanced neutron optical elements (guide, polariser, analyser) will lead to an impressive gain of more than two orders of magnitude in data collection rate compared to that presently obtained at the highest flux reactors available. Furthermore, the combination of NSE and TOF on the one side and of the broad wavelength range of the source on the other side will lead to a very wide dynamic range of at least 6 orders of magnitude making the spectrometer particularly attractive for studies of complex and disordered systems with a broad distribution of relaxation times.

The choice of excellence for the Wide-Angle NSE spectrometer is the long pulse station with a multi-spectral, coupled thermal cold combination or a coupled cold moderator and a long moderator – sample distance of at least 70 m. This

long distance is dictated by the large diameter of the spectrometer ( $\sim 8$  m) and also leads to a good monochromatisation and Q-resolution, a high TOF resolution and reduces magnetic cross talk with other instruments and with the shielding of the moderator.

For a moderator-detector distance of 74 m the wavelength band will cover 0.32 nm and the monochromatisation will be 0.011 nm FWHM. For typical measurements around the first maximum of a glass structure factor at  $Q=11 \text{ nm}^{-1}$  using wavelengths ranging from 0.4 up to 0.72 nm the scattering angles will vary from 41 up to 78 deg and an effective use of all neutrons implies an angular opening of at least 40 deg for each detector bench of the spectrometer. The goal would be to reach the largest possible angular range with e.g. an opening of 90 deg per detector bench and a total of three benches as illustrated in the figure. The detectors will be positioned at around 4 m from the sample and will move between  $-150$  deg and 150 deg of scattering angle.

Optimum conditions for NSE and polarisation analysis experiments will be assured by a curved neutron guide a polariser and supermirror analysers, which will be located in front of the detectors. For measurements without polarisation analysis the spectrometer should also offer the option of replacing the analysers in front of the detectors by radial collimators.

The main NSE precession field will be created by three pairs of coils schematically shown in the figure. Each pair will be mounted in an anti-Helmholtz fashion one coil above and one coil below the horizontal scattering plane with the electric currents oriented oppositely to each other.

The instrument will also give the option for direct geometry TOF measurements. A multichopper cascade will give full control over the resolution and will also allow for a repetition rate multiplication of 2 to 4. TOF measurements will be then performed under the same conditions as NSE, i.e. with polarisation analysis. This is particularly interesting when it comes to magnetic systems or to systems with coherent and spin incoherent contributions to the scattering cross section and will lead to a direct comparison of spectra obtained by NSE and TOF. This combination will lead to a very wide dynamic range of at least 6 orders of magnitude and will make the spectrometer particularly attractive for studies of complex and disordered systems which usually show a broad distribution of relaxations times.

## **Applications**

Phase transitions, disordered magnetic systems, dynamics of the glass transition, lifetime of elementary excitations, transport phenomena in porous materials, quantum diffusion.

## Instrument Data

|                                |  |
|--------------------------------|--|
| moderator                      | multi-spectral, coupled thermal cold combination                               |
| sample-moderator distance      | ~ 70 m   |
| beam cross section             | 120 x 60 mm <sup>2</sup>   |
| incident wavelength            | between 0.2 nm and 1.5 nm  |
| beam monochromatisation        | 0.011 nm FWHM, 5 % at 0.2 nm and 0.7% at 1.5 nm                                |
| wavelength band per pulse      | 0.32 nm  |
| detectors                      | single detectors at ~ 4 m from the sample                                      |
| angular range                  | between -150° and 150°   |
| momentum transfer range        | at 0.2 nm: 0.6 – 61 nm <sup>-1</sup> ,<br>at 1.5 nm: 0.07 – 8 nm <sup>-1</sup> |
| magnetic field integral        | from 10 <sup>-4</sup> up to 0.2 Tm   |
| NSE Fourier time range         | at 0.2 nm: 0.15 - 300 ps,<br>at 1.5 nm: 63 ps – 126 ns                         |
| NSE energy range               | at 0.2 nm: 2.2 μeV - 4.4 meV,<br>at 1.5 nm: 5 neV - 10 μeV                     |
| best time of flight resolution | at 0.2 nm: 1.5 meV, at 1.5 nm: 4 μeV   |
| chopper cascade                | to be defined  |
| sample environment             | cryostat, cryofurnace, furnace (1.5 K ≤ T ≤ 2000 K)                            |

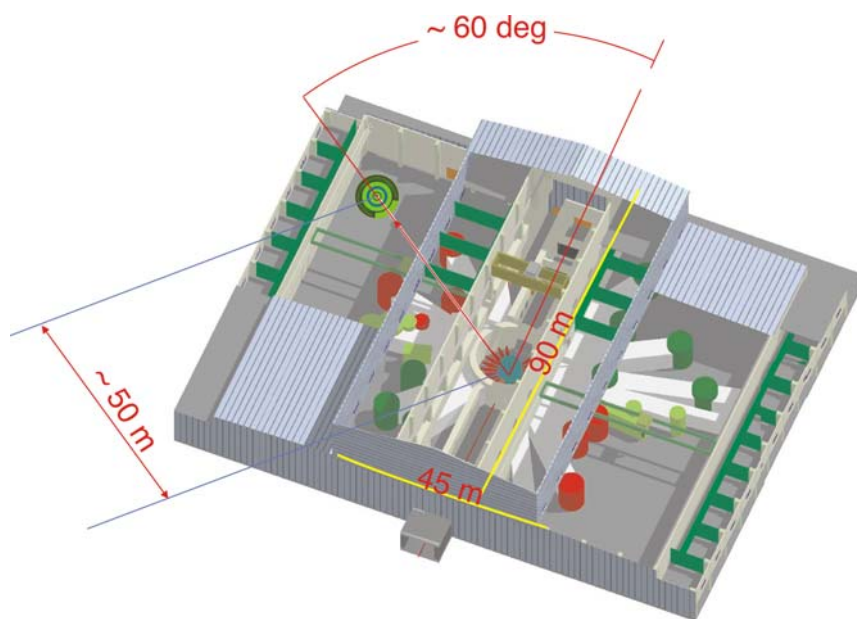


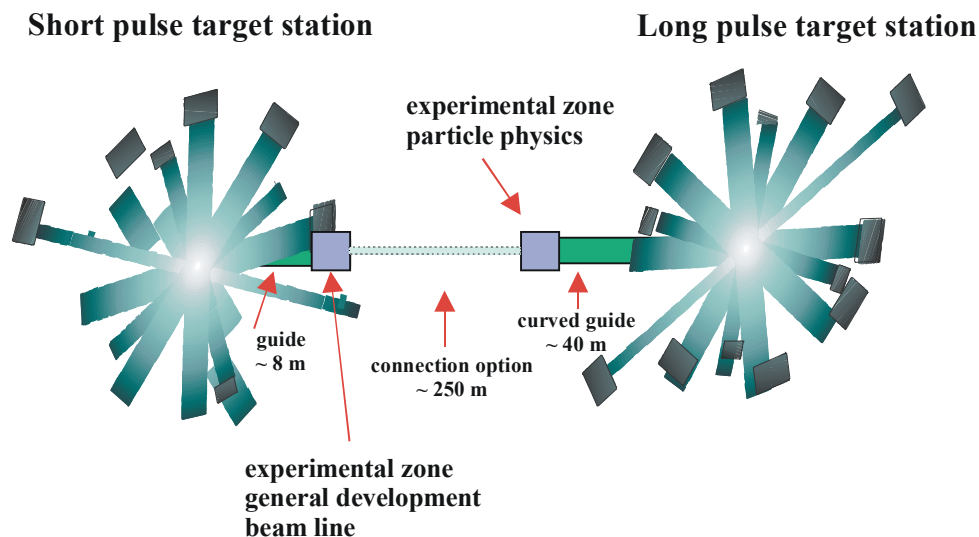
**Figure 2-9:** Possible location of the wide angle NSE spectrometer at the LPTS



## PARTICLE PHYSICS BEAM LINES

**Location:** LPTS, LC19 and/or SPTS, SM07  
**Moderator:** coupled cold hydrogen /multi-spectral, coupled thermal cold combination

Schematic setup:



### Instrument description:

Instruments used for research in fundamental physics and particle physics need a high total neutron intensity at lowest reachable background. By curved neutron guides direct view of the cold moderator is avoided. For the first beam line the guide should be about 40 m long coated with supermirror guides with a cross section of minimum 6 cm width and 16 cm height (see guides for fundamental physics application at ILL). Due to the required low background the experimental area should be located in a separate hall outside the normal instrument hall. Area required for the experiments should be about 10 m in width, 15 m in length and 6 m in height, floor load approx.  $10 \text{ t/m}^2$ , crane load of 5t. The experimental hall needs the usual supply with electricity (30 kW), water, pressure, helium etc.

The second beam line will be used for the development of long term experiments. The experimental zone is within the target station hall, with a neutron guide of about 8 m length. The two beam lines should be located in between the two target stations, LPTS and SPTS, to allow the option of cross-beam neutron-neutron experiments with an intense cold and a well focussed dense cold neutron beam in a single interaction volume (see schematic setup). For such crossed beam experiments, a connection of the two zone with ~250 m supermirror guides would be installed.



## Applications:

The intense pulsed cold neutron beam at the ESS will be used for studies in particle and fundamental physics. One important experiment will be the study of the two-body  $\beta$ -decay of unpolarized neutrons into hydrogen atoms and anti-neutrinos to clarify the origin of handedness of nature. It will also be used to study the electric dipole moment of the neutron in order to investigate the matter-antimatter asymmetry in the universe. Neutron-neutron scattering experiments will study the charge independence of nuclear forces. Ultra-cold and very cold neutrons can be used for elastic and inelastic surface reflection experiments and neutron quantum optical experiments to study quantum gravitational states and weak gravity effects.

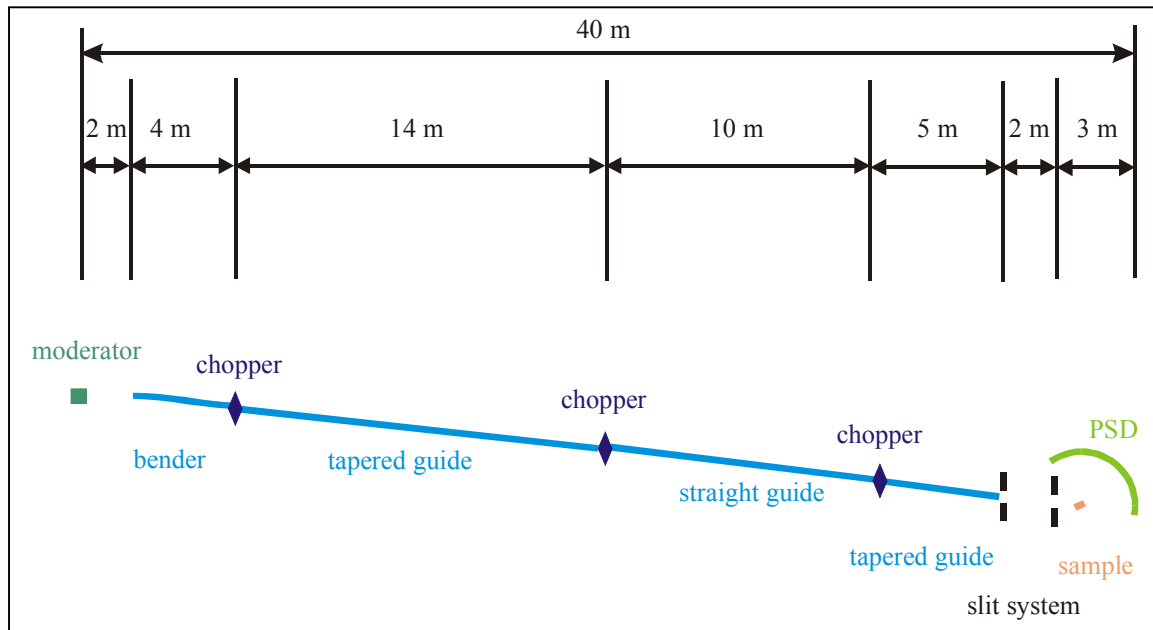
## Instrument data:

| <b>Particle Physics Beamline, Location LPTS</b>                          |   |
|--|---|
| moderator:   | cold coupled hydrogen                                 |
| supermirror guide:   | 40m, curved, cross section 6cm x 16 cm                |
| experimental zone:   | 15 m length x 10 m width                              |
|  |   |
| <b>Particle Physics Beamline for longterm development, Location SPTS</b> |   |
| moderator:   | cold coupled hydrogen                                 |
| supermirror guide:   | 8m, cross section 6 cm x 16 cm                        |
| experimental zone:   | 15 m length x 10 m width                              |
|  |   |
| <b>Equipment:</b>  |   |
| supermirror neutron guide:   | 1x 8 m, 1 x 40 m, ~250 m for crossed beam experiments |
| neutron polarizer  | 2x supermirror polarizer                              |
| polarization analysis  | 2x supermirror polarizer, $^3\text{He}$ spin filter   |
| wavelength filters   |   |
| magnetic guide fields  |   |
| superconducting magnet   | 2T, 3 m   |
| magnetic field return  | 15 t steel  |
| vacuum housing   |   |
| neutron detectors for beam measurements                                  |   |
| shielding  | $\text{B}_4\text{C}$ , Cd, Pb                         |

# HIGH INTENSITY REFLECTOMETER

**Location:** LPTS, LC21  
**Moderator:** coupled cold hydrogen

Schematic setup (side view):



## Instrument description:

Three choppers are used to get a wavelength band of  $0.25 \text{ nm} < \lambda < 0.82 \text{ nm}$  at a wavelength resolution of 8%. In order to minimise the intensity loss in the neutron guides the novel concept of a ballistic neutron guide is applied. Simulations show an increase in intensity of about 25% compared to a straight neutron guide.

In order to be able to investigate solid as well as liquid samples a vertical scattering plane is used. The exit of the bender has an inclination of  $3^\circ$  with respect to the horizontal and the tapered guide delivers a divergence of about  $6^\circ$ . Hence a range from  $0^\circ$  to  $6^\circ$  can be achieved for the angles of incidence by changing the height of the slits and the sample.

The position sensitive detector (PSD) covering a range of the scattering vector of  $150^\circ$  as well as the sample holder consisting of two tilt stages ( $\omega$ - and  $\chi$ -rotation) are novel design features. It is not only possible to investigate off-specular scattering but because of the large angular range covered by the PSD it is also possible to perform reflectometry and diffractometry with the same instrument, i.e. to determine e.g. the ferromagnetic and crystalline properties and their dependencies.

## Applications:

This reflectometer works with a resolution of about 8% and is especially dedicated for thin films (thinner than 20 nm) which do not need very high q-resolution. Because of the vertical scattering plane the reflectometer can be used for investigations of liquids as well as thin solid films. The high intensity provides the possibility to measure down to reflectivities of about  $10^{-10}$  and q-values corresponding to Bragg peaks of 1 nm thick layers.

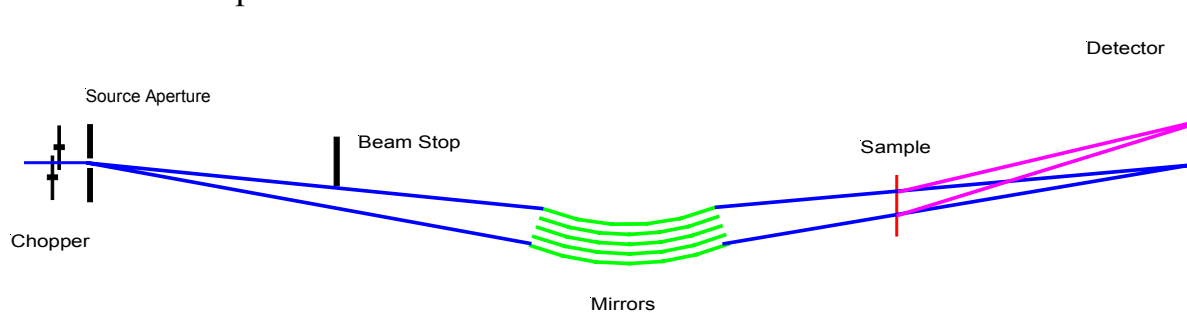
## Instrument data:

|  |   |
|--|---|
| moderator:   | coupled cold hydrogen   |
| neutron guide:   | bender (bending angle $1.5^\circ$ ) and ballistic neutron guide   |
| neutron guide cross section:   | <u>bender:</u><br>width: tapered 15 cm - 10 cm; height: 10 cm.<br><u>ballistic guide:</u><br><i>first section:</i> tapered 15 cm - 10 cm (width), 10 cm height; <i>second section:</i> 15 cm (width), 10 cm (height); <i>third section:</i> tapered 15 cm - 6 cm (width), tapered 10 cm - 3 cm (height) |
| chopper distances:   | 6 m / 20 m / 30 m from moderator  |
| chopper windows:   | $51^\circ / 172^\circ / 259^\circ$  |
| chopper speed range:   | 1000 rpm  |
| polarizer:   | Fe/Co supermirrors  |
| wavelength range:  | $0.25 < \lambda < 0.82$ nm  |
| q range for solids:  | $0.003 \text{ \AA}^{-1} - 4 \text{ \AA}^{-1}$   |
| q-range for liquids:   | $0.003 \text{ \AA}^{-1} - 0.3 \text{ \AA}^{-1}$   |
| flux at sample:  | approx. $4 \cdot 10^8$ n/s/cm <sup>2</sup> at a collimation of 1 mrad   |
| scattering angle:  | $0^\circ - 150^\circ$   |
| distance sample detector:  | 2 m   |
| detector:  | PSD covering an angular range of $150^\circ$  |
| sample environment:  | magnet, cryostat, furnace, UHV-chamber for in-situ experiments  |
| <i>Flux comparison to existing liquids reflectometers:</i>                           | <i>V6 (HMI, PG monochromator): <math>3 \cdot 10^4</math> n/s/cm<sup>2</sup> ;</i><br><i>SURF (ISIS; estimated): <math>8 \cdot 10^5</math> n/s/cm<sup>2</sup></i>  |
| <i>Flux comparison to existing reflectometers with a horizontal scattering plane</i> | <i>ADAM (ILL; PG monochromator) <math>2 \cdot 10^6</math> n/s/cm<sup>2</sup> ;</i><br><i>D17 (ILL; velocity selector): <math>4 \cdot 10^7</math> n/s/cm<sup>2</sup></i>   |
| <i>Performance gain factors</i>  | <i>V6: 13300; SURF: 500; ADAM: 200; D17: 10</i>   |

## FOCUSSING MIRROR LOW Q SANS INSTRUMENT

**Location:** LPTS, LC22  
**Moderator:** coupled cold hydrogen

Schematic setup:



### Instrument description:

At very small  $Q$  a focussing mirror will out-perform conventional pinhole SANS collimation in terms of count rate and minimum  $Q$ . [Alefeld, 1989] This is particularly attractive for a pulsed neutron source since the resulting relatively short beam line may use a broad range of wavelengths to simultaneously access higher  $Q$  values. A fully two dimensional SANS pattern is obtained, unlike the double crystal Bonse-Hart method which gives a one-dimensional slit-smear result.

Using a supermirror bender to suppress fast neutron background, a well collimated "pinhole" neutron source is focussed at the detector by a stack of  $\sim 1$  m long mirrors with focal length  $\sim 4$  to 10 m along the beam (but much smaller radius perpendicular to the beam). The mirrors are ideally parabolic but in practice may be cylindrical "replica" sections. The atomically smooth mirrors require "state of the art" technology (from X-ray and astronomical areas) to produce a sharp image of the source.

A minimum  $Q$  of better than  $10^{-4} \text{ \AA}^{-1}$  is the desired goal. Note that the sample must be relatively large, though smaller samples may be accommodated by sacrificing  $Q_{\min}$  and moving the detector off focus.

### REFERENCES:

[Alefeld, 1989] B.Alefeld, D.Schwahn & T.Springer, Nucl.Instr. & Meth. **A274** (1989) 210-216.

## Applications:

Many existing SANS studies could be extended towards the size rang accessible by light scattering, except of course that fmSANS works for opaque samples and allows the advantages of neutron contrast variation to be exploited. Phase separation in polymers, microporous materials and work in many other subject areas would be greatly enhanced. Studies of proteins structure and aggregation may be of special interest.

## Instrument data:

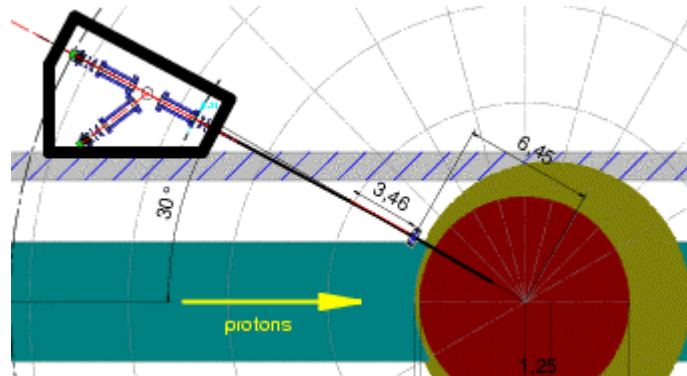
At the time of writing a prototype fmSANS instrument is under development at FZ Julich following an initial mirror used for the NSE instrument IN15 at the ILL. An optimal geometry for ESS fmSANS is yet to be defined as this depends on progress with mirror technology. Further to this development of a high count rate detector is required with better than 1 mm resolution over a reasonable area.

|                              |  |
|------------------------------|--|
| moderator:                   | coupled cold hydrogen  |
| neutron guide:               | bend polarised guide   |
| neutron guide cross section: | bender, guide section to "source pinhole" ~1 to 2 mm   |
| chopper distance:            | 6 m  |
| wavelength range:            | $0.6 < \lambda < 1.2$ nm (depending on mirror properties)  |
| distance sample detector:    | ~4 to ~10 m (fixed)  |
| Q-range:                     | $\sim 1 \times 10^{-4}$ to $0.1 \text{ \AA}^{-1}$  |
| detector:                    | central detector with < 1 mm resolution and high count rate capability,<br>outer detector at least 1 m square, ~3 mm resolution                        |
| sample environment:          | full range of temperature controlled sample changer, furnace, cryostat, shear flow / simultaneous rheology, linear flow, stop-flow, extensiometer etc. |

## HIGH RESOLUTION NSE SPECTROMETER

**Location:** LPTS, LC24  
**Moderator:** coupled cold hydrogen

Schematic setup:



### Instrument description:

The high resolution NSE will view the coupled cold H<sub>2</sub> moderator at ESS LPTS via a neutron guide containing a polarizer that bends the direction of the beam and avoids a direct sight of the moderator from the sample.

A wavelength band of  $\Delta\lambda=0.6..0.9$  nm with a range  $0.3 < \lambda < 2..2.5$  nm(+) is selected by a disc chopper placed at a distance of 6-6.5 m from the source (eventually a second chopper must be placed at a distance between 10-20 m. A primary and a secondary precession coil are placed before and after the sample respectively. A 2D multidetector is placed after the second precession coil in a distance of about 3 m from the sample. It will probably consist of an array of single detectors to cope with maximum rates of a few KHz per cm<sup>2</sup>. The secondary coil and the 2D-detector will be moved up to a mean scattering angle of 90°.

New design features in combination with the usage of very long wavelengths from the cold source will extend the range to very long Fourier times, i.e. to very high resolution. The generic design still follows that of IN11.

The major novel design feature is the use of superconducting main solenoids that provide a field integral  $J > 1$  Tm (IN15  $J_{\max}=0.2$  Tm).

*The maximum Fourier time is given by  $t \sim J_{\max} \lambda^3$ . Superconducting solenoids will also allow for optimal compensation of stray fields and thereby enable efficient magnetic shielding from external field fluctuations. To realize the resolution corresponding to  $J=1$  Tm all over the 2D detector massive highly precise correction elements will be utilized. Note that the above innovations are independent from the time structure of the source!*

*To cope with the varying wavelength within each pulse frame only the flippers have to be operated with ramped currents.*

### **Applications:**

The high resolution neutron spin echo instrument will cover a broad range in energy and momentum transfer and will be particularly attractive for studying the dynamics of polymer and glassy materials, phase transitions, disordered magnetic systems and transport phenomena.

### **Instrument data:**

|   |   |
|---|---|
| moderator:  | coupled cold hydrogen   |
| neutron guide:  | <sup>58</sup> Ni guide + bender/reflection polarizer  |
| neutron guide cross section:                            | 6 cm x 6 cm   |
| chopper distance:                                       | 6-6.5 m, ((&) ~15m)   |
| chopper windows:  | 6 cm x 6 cm   |
| chopper speed range:                                    | 16.66 Hz / 2 = 8.333 Hz = 500 RPM   |
| polarizer:  | CoTi or FeGe SM (refl. or transm.)  |
| wavelength range:                                       | 0.3 < $\lambda$ < 2.5 nm  |
| Fourier time range:                                     | 5 ps ... 1000 ns (depends on current development.)  |
| energy resolution:                                      | 0.13 meV ... 0.7 neV)   |
| momentum transfer range:                                | 0.1 nm <sup>-1</sup> – 30 nm <sup>-1</sup>  |
| momentum transfer resol.:                               | 0.05 nm <sup>-1</sup> – 4.5 nm <sup>-1</sup>  |
| flux at sample (t-average):                             | 1-2 x 10 <sup>7</sup> n/cm <sup>2</sup> /s @ 0.8 nm   |
| scattering angle:                                       | 0...90 <sup>0</sup>   |
| distance sample detector:                               | ~3 m  |
| detector:   | 2D 30 cm x 30 cm, $\Delta x < 2$ cm   |
| sample environment:                                     | cryostat, cryofurnace, furnace (1.5 ≤ T ≤ 2000 K)   |
| <i>Flux comparison with existing NSE spectrometers:</i> | <i>FZJ-NSE: ~0.8 x 10<sup>6</sup> n/cm<sup>2</sup>/s @ 0.8 nm, 10% FWHM</i><br><i>SPAN: ~0.5 x 10<sup>6</sup> n/cm<sup>2</sup>/s @ 0.8 nm, 15% FWHM</i> |

*Q-resolution will be superior at wavelength > 0.4 nm, however inferior or equal to reactor instruments at smaller wavelength (i.e 0.3 nm →  $\Delta\lambda/\lambda = 0.15$ ).*





Chapter 3

**FLIGHT SIMULATORS  
FOR NEUTRONS:  
VIRTUAL INSTRUMENTS  
FOR ESS**

### **3. FLIGHT SIMULATORS FOR NEUTRONS: VIRTUAL INSTRUMENTS FOR THE ESS**

Computer simulations play a major role in developing modern technology. For instance, every new car model has been designed through an extensive computer analysis, and nowadays all pilots are trained using flight simulators to obtain a 'real-time' experience before being responsible for a real aircraft. Similarly, the planning and design process of a large scale facility such as the ESS needs to be based on detailed and accurate "flight simulation" studies – using Monte Carlo (MC) methods – in order to be able to find the best solutions and highest performance.

'Virtual instruments' may be modelled on the computer, and through MC simulations, the flight path of many neutrons can be followed. In this way, the instrument performance can be evaluated allowing an optimisation before the construction.

Once the ESS instruments are built, real and virtual experiments can be performed in parallel in order to make the use of neutrons more efficient. MC methods are also very well suited to model the interaction of the neutron with the sample, and to evaluate the experimental data.

The simulation packages used for the design of the ESS instruments are primarily McStas [McStas] and VITESS [VITESS]. Inter-comparison efforts between these and other packages (NISP, IDEAS, Restrax) show the high precision of the simulation results [Seeger, 2002]. Another important validation is the agreement between MC simulations and experimental results [Wildes, 2002; Zsigmond, 2001].

#### **3.1 Instrument development**

As the usual analytical methods reach their limit of validity in the description of complex experimental set-ups, the use of MC simulations offer an efficient solution to reach this goal, in terms of both the computational time and the time investment for the physicists, once powerful program packages are available. MC simulations are the only way to describe conditions where analytical approaches are not exact, such as 1) realistic moderator spectra and complex geometry: comparison of the performance on different sources and moderators; optimisation of the guide and bender system; large focusing and detector systems with broad solid angles causing non-linearity; choice between different concepts and monochromating systems; and 2) non-ideal conditions: small misalignments, guide waviness and effect of gravity.

One example for using MC simulations in instrument development is the improvement of the spectrometer IN14 (see Fig. 3-1 [Wildes, 2002]).

## 3.2 Virtual experiments and data evaluation

We can envisage that in the near future all neutron instruments come with a virtual computer model that exactly reproduces all of its features and details. This "flight simulator" will provide unprecedented power for the researchers as: 1) Training and planning aids: prior to the measurement, MC simulations will provide a check of feasibility and the best instrument set-up; 2) On-line tool for set-up and error corrections; 3) Data evaluation tool: the main importance of MC simulations consists in the possibility to develop a more precise numerical technique of data reduction beside the conventional ones. This provides for the most accurate and powerful data reduction approach in experimental research: the exact assessment of the compatibility of possible models with the actual observations, taking into account the complete instrument behaviour (see Fig. 3-2 [Zsigmond, 2001]).

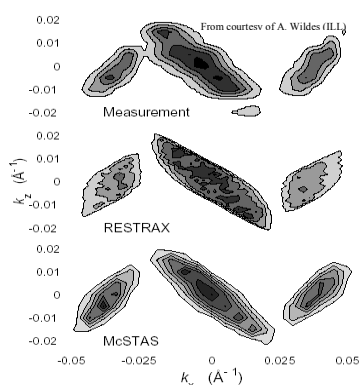


**Figure 3-1:** The effect of a converging supermirror guide inserted between a monochromator and sample on the divergence of the incident beam has been determined by using McStas and RESTRAX.

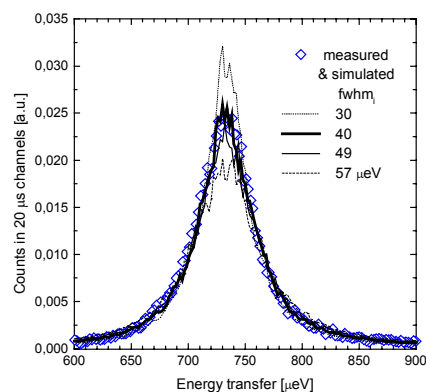


**Figure 3-2:** Evaluation of model parameters on IRIS: Determination of the roton line-width in superfluid  $^4\text{He}$  at 1.4 K by minimising the quadratic deviation between experimental and simulated data (VITESS).

### REFERENCES:

- |                  |  |
|------------------|--|
| [McStas]         | McStas web-site: <a href="http://neutron.risoe.dk/">http://neutron.risoe.dk/</a> and <a href="http://www.ill.fr/tas/mcstas/">http://www.ill.fr/tas/mcstas/</a> |
| [VITESS]         | VITESS web-site: <a href="http://www.hmi.de/projects/ess/vitess/">http://www.hmi.de/projects/ess/vitess/</a>   |
| [Seeger, 2002]   | P. Seeger <i>et al</i> , to appear in Neutron News (2002)  |
| [Wildes, 2002]   | A.R. Wildes <i>et al</i> , to appear in Applied Physics A (2002)   |
| [Zsigmond, 2001] | G. Zsigmond <i>et al</i> , Nucl. Instr. and Meth. in Phys. Res. A, 457 (2001) 299-308  |



**Chapter 4**

**NON-NEUTRON  
SCATTERING  
APPLICATIONS**



## **4. NON-NEUTRON SCATTERING APPLICATIONS**

### **4.1 RADIOACTIVE BEAM FACILITY AT ESS**

Until recently particle accelerators have been limited to accelerating stable nuclei, or electrons, and using stable targets. This imposes large restrictions on the range of nuclei, which can be produced. Stable nuclei are thought to constitute less than ten percent of all bound nuclear systems. Recent developments in the technology of ion-sources and accelerators now mean that it is possible to accelerate beams of radioactive nuclei. These radioactive beams have the potential to make major impacts in many different areas of science.

A radioactive beam facility would use a fraction of the ESS proton beam (from a position which would otherwise be occupied by a beam stop) to produce nuclear reactions in a target. The reaction products would be isotopically separated by an electromagnetic spectrometer, then captured and rapidly raised to a high atomic charge-state in an ion source, before being accelerated and used for secondary reactions. The ability to produce intense, energetic secondary beams of nuclei, with large isospin ratios, opens up large, unexplored regions of the nuclear chart for study. Understanding the structure of nuclei with extreme isospin is important not just for nuclear physics, but also for astrophysics. In addition the properties of these nuclei can be used in experiments, or applications, which will benefit areas such as material science, fundamental physics, chemistry and medicine.

#### **4.1.1 Present Radioactive-Beam Facilities**

Current "first-generation" radioactive beam facilities use fragmentation, spallation or fission reactions as mechanisms for producing the primary beam. An example of such a facility is REX-ISOLDE at CERN. This facility uses 2 micro-amps of the 2 GeV LEP proton beam. The huge increase in intensity obtained by using 100 micro-amps, or more, of the ESS beam would make the ESS radioactive-beam facility orders of magnitude more intense than any installation currently operating. Thus the performance of the ESS radioactive-beam facility would be such that it could be called a "second-generation facility". The technology for a primary target, able to withstand the heating caused by such a powerful proton beam, has already been developed in the RIST project at the Rutherford-Appleton laboratory in Britain.

#### **4.1.2. Astrophysical Studies**

Although we have a good idea about the processes responsible for nuclear reactions in stars, there is still a dearth of data on many reactions. For example very little data exist on the astrophysical rapid neutron-capture  $r$  process, which

is thought to lead to type II stellar supernovae. This  $r$  process is thought to create around half the matter in the universe heavier than iron. In this process a nucleus captures neutrons until the binding energy of the last neutron drops to around 2 MeV. At this binding energy the neutron capture cross-section is so low that beta decay becomes more probable than capture. The nuclei that participate in this reaction are extremely neutron rich. The ingredients of any  $r$ -process calculation include many nuclear structure parameters. Very little data exist on the nuclear structure parameters of very neutron-rich nuclei, and  $r$ -process calculations are at present performed using theoretically derived values, extrapolated from nuclear models of near-stable nuclei. The ability to apply these nuclear models to very neutron-rich regions of the nuclear landscape is questionable. A radioactive beam facility at the ESS would produce nuclei on, or near, the  $r$ -process path with sufficient intensity for nuclear structure studies.

Similarly other processes such as the rapid proton-capture  $rp$  process in supernovae are poorly understood, as are the proton/neutron -capture cross-sections and resonance energies in many stellar reactions are not known. Investigations into processes such as these will give us a greater understanding into the workings of stars, and our sun, the power source that sustains life on this planet. These experiments can only be performed with intense radioactive beams.

#### 4.1.3. Nuclear Structure Studies

The nucleus is a fundamental building block of the universe. Although the structure of the nucleus has been studied for many years no model exists that can fully describe the properties of nuclei throughout the whole nuclear landscape. Nucleus is a quantal, many-body system whose constituents interact through the short-range strong force. The nuclear force is too strong to be modeled using the perturbation techniques of atomic physics, and there are too few constituents to apply the semi-infinite techniques used in solid state physics. The force between the nucleons can be thought of as a van der Waals-type residual strong force, generated by quarks and gluons. This force is different for nucleons in a nucleus, and free nucleons. There is no precise analytical form of this *effective* interaction, and hence no solution to the nuclear many-body problem. The main approaches to modeling nuclei are self-consistent many-body mean-field theories. The effective interaction between nucleons in a nucleus generates a potential and the characteristics of this field reveal themselves in the experimentally observed quantal states. The key to understanding nuclear structure is to know the correct form of the effective interaction. The manifestation of this effective interaction at large values of isospin is unknown.

Examples of the surprises that arise in nuclear structure studies are the very neutron-rich "halo" nuclei, such as  $^{11}\text{Li}$ . The wavefunction of the outer two



neutrons extends a long way outside the nuclear core. These two neutrons spend most of their time far from the normal-density core of the nucleus. Halo nuclei are also the first examples of a Borromean system found in nature and can be treated as a three-body problem. The forces of attraction between any two of the components is not sufficient to bind them. At present there are only two known halo nuclei,  $^{11}\text{Li}$  and  $^6\text{He}$ , an intense radioactive-beam facility would give access to a large region of light mass neutron-rich nuclei predicted to contain more of these halo nuclei.

The best current methods of producing very neutron-rich nuclei are by fragmentation and fission, which yield nuclei no more than about ten neutrons in excess of stability, only radioactive-beam facilities can produce neutron-rich nuclei with more extreme isospin ratios. The limits of nuclear existence on the neutron-rich side of the nuclear landscape unknown, except for the very lightest nuclei. As neutrons are added to a nucleus the binding energy of the last nucleus gradually drops until it is at such a value that the next neutron added is unbound, and the nucleus decays by neutron emission. This defines the neutron drip-line. The neutron drip-line is much further from stability than the proton drip-line, due to the lack of Coulomb repulsion. Predictions for the location of the neutron drip line vary wildly.

Radical new features are also expected to manifest themselves in very neutron-rich nuclei such as neutron skins, phase transitions, rapid shape transitions and nuclear superfluidity. The structure of these nuclei is also expected to deviate strongly from that close to stability. It is thought that shell gaps will be drastically reduced, this has already been observed in the very neutron-rich light-mass region where  $^{32}\text{Mg}_{20}$  and  $^{44}\text{S}_{28}$  appear to have lost their  $N=20$  and  $N=28$  shell gaps respectively. A radioactive beam facility at the E.S.S will allow these postulates to be verified or refuted.

The theory of isospin invariance (where protons and neutrons are postulated to behave as different sub-states of the same particle, the nucleon) can be tested by observations of mirror nuclei ( $Z_1=N_2$   $Z_2=N_1$ ). The Coulomb force is expected to break isospin symmetry, but this is difficult to observe at low masses, due the quenching of the Coulomb force by large neutron excesses. At regions of higher mass, attainable by radioactive beams, this problem will diminish.

In addition to the proton and neutron drip-lines the third frontier in nuclear science is the maximum proton and mass number that a bound atom can reach. This is limited by the increasing probability of spontaneous fission, alpha decay and proton emission. It is thought that new proton shells may exist at proton numbers 114 and 126. The nuclei here are predicted to live longer than several seconds, thus allowing them to undergo observable chemical reactions. With such high proton numbers highly relativistic inner electrons will increase their

screening effect, leading to know chemical properties. Production of these super-heavy elements could be possible using radioactive beams of very neutron-rich nuclei.

Data could also be obtained for accelerator-driven nuclear power systems, which it is hoped would safely produce power whilst transmuting long-lived trans-actinide waste products from current nuclear reactors. The idea behind accelerator driven system is to use a proton-induced spallation reaction as a neutron source for a sub-critical reactor. Present knowledge of the reaction mechanism is not accurate enough for a technical application. Two critical pieces of information are missing, the neutron and residual-nuclei yields. These accelerator driven power systems would thus be able to transmute dangerous waste, and would be inherently safe, as a sub-critical nuclear reaction takes place, driven by an accelerator that can easily be halted.

#### **4.1.4. Fundamental Physics**

The atomic nucleus provides a unique laboratory to test fundamental interactions and the standard model. An example of this is conserved vector-current hypothesis in the theory of the weak interaction. The best test of this theory comes from the strength of super-allowed beta decays in specific nuclei. Although beams of stable nuclei have allowed this effect to be investigated, the production of heavier nuclei will allow proton-number dependent systematic variations to be corrected.

Intense beams of francium isotopes will also be available at a radioactive-beam facility, permitting atomic physics experiments into the investigation of parity violating reaction between atomic electrons and the nucleus. Exchange of a  $Z^0$  boson between electrons and the nucleus can give rise to a parity non-conserving neutral current, which leads to a mixing of opposite parity states. Thus otherwise forbidden electric-dipole transitions between states of the same parity are possible. These measurements can be performed with unprecedented precision (1%), rivaling the accuracy of high-energy experiments into parity violation.

#### **4.1.5. Material Science**

Implanting radioactive "spy" nuclei into materials allows the observations of atomic environments, using methods analogous to those presented in the muon facility section of the ESS Report. Perturbed angular correlations of radiation emitted from the spy nuclei will give information on the atomic impurity hyperfine-field or the atomic electric-field gradient of the sample. Diffusion rates of the radioactive spy atoms in the sample could also be obtained. These data are important for accurate modeling of solid-state systems as well as being useful to the semiconductor industry. What is particularly useful about these

beams is that they change their chemical properties as they radioactively decay. Approximately thirty percent of the beam time at the REX-ISOLDE radioactive beam facility is devoted to studies of this type.

Intense beams of mono-energetic position beams will also be available for Positron Emission Tomography (PET). These positrons would be produced on a scale orders of magnitude more intense than present sources, in the energy range 1 eV to 400 keV, and could be used to investigate sub-surface regions, thin films, surface spectroscopy and microscopy.

#### **4.1.6. Medicine**

Isotopically separated nuclei, produced at a radioactive-beam facility could be collected, and used as tracers in medical analysis. These nuclei decay would by positron emission. The positrons would then annihilate with an electron, producing two 511 keV gamma rays which can be detected, thus allowing the position of the nucleus to be determined. The large range of radioactive nuclei produced at a radioactive beam facility would allow nuclei with shorter half-lives and lower decay-energies to be used than at present, minimizing the dose to the patient.

Nuclei far from stability could be used in cancer therapy. Attaching these nuclei to drugs will allow a larger dose of radiation to be administered than at present, as nuclei far from stability would undergo more decays than near-stable nuclei. The large range of nuclei produced at a radioactive-beam facility could again be used to select nuclei with low-energy decays that would further localize the area of treatment. Radioactive beams could also be used to study the effects of radiation in biological systems, in particular radiation damage induced by heavy ions on cells and in DNA.

#### **4.1.7. Conclusion**

A radioactive beam facility at the ESS would constitute another large-scale facility in addition to the ESS itself able to answer crucial questions in nuclear physics, whilst also providing unique facilities for research in materials science, chemistry, fundamental physics and medical treatment. The range and intensity of nuclear species produced would make it a truly world-class facility, orders of magnitude better than any facility currently operating.

## 4.2. ULTRA-COLD NEUTRON SOURCE AT ESS

Ultra-cold neutrons (UCN) can be stored inside material or magnetic bottles when their kinetic energy  $E$  is below the optical potential  $\bar{V}$  representing the wall material  $E < E_c = \bar{V} = 2\pi\eta N b_c/m$  or the magnetic confinement field  $E < E_c = \bar{V} = \pm \mu B$ , where  $N$  and  $b_c$  denote the particle density and the coherent scattering length,  $B$  the magnetic field strength and  $m$  and  $\mu$  the mass and the magnetic moment of the neutron [Steyerl, 1977; Golub, 1991]. They are produced within cold moderator sources as a small part of the whole Maxwellian distribution ( $f = (E_c/k_B T)^2/2$ ). The most efficient ultra-cold neutron source exists at the high flux reactor of the Institut Laue-Langevin in Grenoble and it delivers a neutron density of about  $50 \text{ cm}^{-3}$  where an additional phase space transformer in form of a neutron turbine shifts very cold neutrons to ultra-cold ones [Steyerl, 1989].

More recently it has been shown that cooled solid  $D_2$  and  $CD_4$  moderators can cool neutrons more effectively than other moderators mainly due to many low lying energy levels existing in such solid material [Serebrov, 2000]. This can provide a gain factor of about 30 compared to liquid moderators.

In connection with neutron spallation sources Serebrov et al. [Serebrov, 2000] made an interesting proposal for an UCN factory where neutrons are produced in a separate spallation target during a rather short period (several seconds), and they are moderated in a surrounding  $D_2O$  moderator and then cooled by a dedicated solid  $D_2$  or  $CD_4$  cold source (Fig. 4-1). Neutrons leaving this source are accumulated within an UCN storage vessel and after density saturation the source is closed by a movable reflecting shutter. Then the UCN's can be used for a while (100 - 500 seconds) which is determined by the half-life of the neutron and the loss rate of the storage vessel. Thus such an UCN factory uses the beam power of a spallation source for about 1% of the time leaving the rest for the main spallation target. A rather detailed proposal for such an UCN source has been worked out for the continuous operating spallation source SINQ at the Paul Scherrer Institute (PSI) in Switzerland [Daum, 2000]. The expected UCN density is  $4000 \text{ cm}^{-3}$ .

When the whole 10 MW beam of the accelerator is used with a duty cycle of 1% for such an advanced UCN source one can expect UCN densities up to  $40.000 \text{ cm}^{-3}$ , a value which results from the extrapolation of the proposed PSI-UCN source. An even more effective mode of operation can be chosen when the shutter operation is adapted to the pulse structure of the source where phase space densities up to the peak flux from the converter can be obtained [Rauch]. In this case the 16  $\mu$  Hz, 5 MW beam would be the optimal choice for such an UCN factory where densities up to  $6 \cdot 10^5 \text{ cm}^{-3}$  become feasible. In this case low repetition rates are advantageous reaching a maximum gain for single shot

systems [Pokotilovski, 1995]. Thus ESS offers the opportunity to install an UCN factory, which produces 3 - 4 orders of magnitude higher UCN densities.

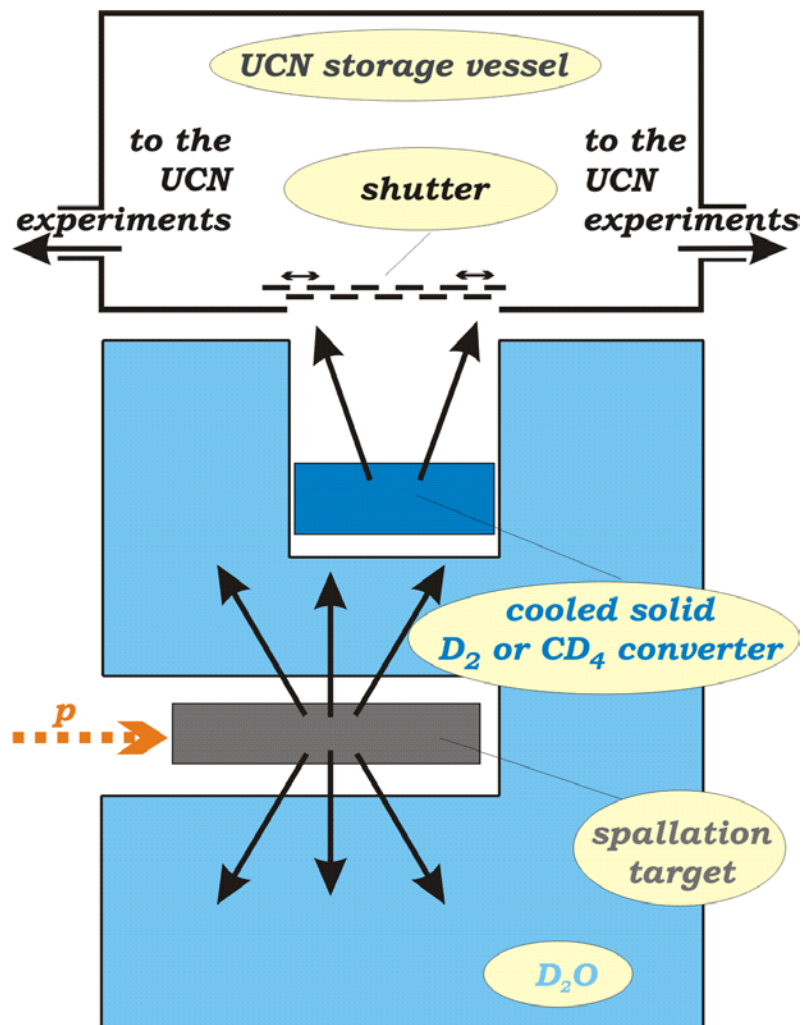


**Figure 4-1:** Sketch of the experimental arrangement of the UCN source and a feasible pulse sensitive shutter system

## REFERENCES

- [Steyerl, 1977] A. Steyerl, in: "Neutron Physics", Springer Tracts in Modern Physics 80 (1977) 57
- [Golub, 1991] R. Golub, D. Richardson, S.K. Lamoreaux: "Ultra-Cold Neutrons", Adam Hilger, 1991
- [Steyerl, 1989] A. Steyerl, A.A. Malik: Nucl. Instr. Meth. A284 (1989) 200
- [Serebrov, 2000] A. Serebrov, V. Mityukhklyayev, A. Zakharov, A. Karitonov, V. Shustov, V. Kuz'minov, M. Lasakov, R. Tal'daev, V. Varlamov, A. Vasil'ev, M. Sazhin, G. Greene, T. Bowles, R. Hill, P. Geltenbort: Nucl. Instr. Meth. A440 (2000) 658
- [Daum, 2000] M. Daum: AIP-Conf. Proc. 549 (2000) 888
- [Rauch] H. Rauch: Phys. Lett. A (in print)
- [Pokotilovski, 1995] Y.N. Pokotilovski: Nucl. Instr. Meth. A356 (1995) 412

### 4.3 MUON FACILITY FOR ESS

$\mu$ SR is a universal acronym for muon beam studies. It stands for muon spin rotation, relaxation or resonance. In context the appropriate acronym is usually clear, however we can briefly define the terms here:

*rotation* describes the dephasing of implanted muon spins by local fields within the sample in the presence of a field transverse to the muon spin direction.

*relaxation* defines the time-dependent loss of polarisation of the implanted muon spins caused by site-to-site variations of the internal fields either in zero applied field or in a field applied parallel to the initial muon spin direction

*resonance* is observed in the presence of an applied radio frequency magnetic field, corresponding to nuclear magnetic resonance detected by nuclear radiation.

In each case the precessional or relaxational behaviour of the muon spin is determined by measuring a time differential histogram of the positrons that are preferentially emitted along the muon spin direction at the time of muon decay.

Perhaps the overriding strength of the  $\mu$ SR technique is that it is a uniquely sensitive probe of extremely small magnetic fields, and the distribution and dynamics of such magnetic fields within a sample, both in zero and applied magnetic field. Indeed the sensitivity of  $\mu$ SR is such that fields generated by nuclear moments are easily measured, whilst the dynamical response ( $10^{-12}$ - $10^{-4}$  s) bridges the gap that separates, for example, neutron spin echo from bulk measurements such as magnetisation and susceptibility methods. The field dynamics measured by the muon can be related either to intrinsic internal field fluctuations, or to the apparent fluctuations caused by a muon diffusing through a lattice. The latter case is often of key interest, as the muon itself behaves like a light isotope of hydrogen ( $M_{\mu}=1/9\text{amu}$ ) and therefore can be used to probe hydrogen-like diffusion processes.

The unique sensitivity of  $\mu$ SR has secured its role as an indispensable tool in the armoury of the condensed matter scientist. Successful and often pioneering exploration of phenomena as diverse as spin glass dynamics, spin fluctuations in itinerant electron systems, heavy fermions, magnetic ordering in ultra-small moment systems, critical dynamics, flux line lattices in superconductors, hydrogen mobility, passivation in semiconductors, muonium formation and dynamics in proteins, and, more recently surface and near surface effects, is a testimony both to the wide applicability of muon beam techniques and to the breadth of the muon beam user community.

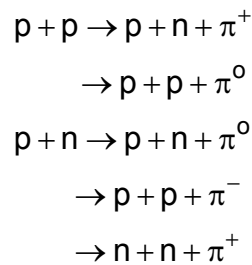
The overlap between the condensed matter science studied using  $\mu$ SR and that studied using neutron scattering is clearly considerable, and there is a growing range of applications in which the information gained by the complementary use

of muons and neutrons provides far greater insights than either technique alone can offer. In particular, over the last decade the juxtaposition of the world's most powerful pulsed neutron facilities and pulsed muon facilities at ISIS has enabled such complementarity to be explored and exploited in greater depth than ever before, whilst also exposing a wider scientific community to the enormous potential of muon beam techniques. Without doubt it is the ISIS model of adjacent muon and neutron facilities that the ESS should seek to emulate, thereby ensuring the continuing cross fertilisation of the European muon and neutron communities and enhancing the impact of both techniques in condensed matter studies.

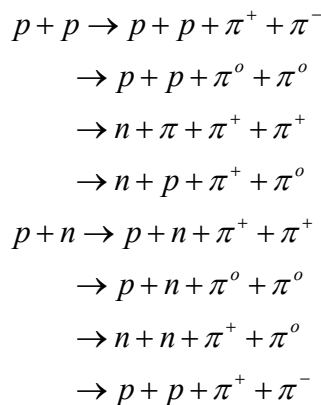
Equally importantly, ESS will be able to provide muon beams of unprecedented intensity and quality, satisfying the needs of a growing community for increasingly powerful and sophisticated facilities to take  $\mu$ SR techniques well beyond the limitations of existing sources.

### 4.3.1 The production of muon beams

Muons beams are produced in pion decay, and the pions themselves are produced by nucleon-nucleon interactions, where the incident kinetic energy of the bombarding nucleons is sufficient for the available centre of mass energy to exceed the pion mass of 140MeV. Typical single pion production reactions, which have an energy threshold of 280MeV include



At higher energies it is possible to produce pions in pairs. The threshold kinetic energy in the laboratory frame for such processes is 600MeV, with associated cross sections reaching saturation levels above 1.5GeV. ESS approaches this regime and double pion contributions to the pion, and hence muon, production process will be evident. Typical double pion production reactions are

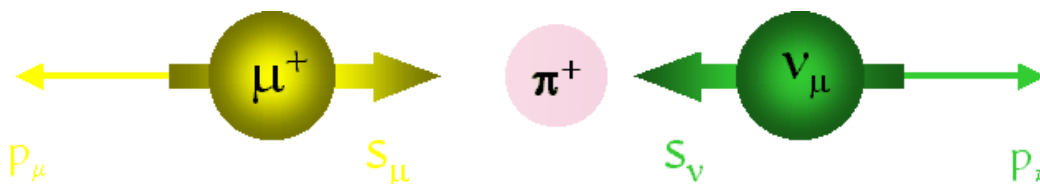


Pions are optimally produced by proton beams impacting a low  $Z$  target, such as carbon. Low  $Z$  targets are also particularly advantages in the context of pion production at ESS as multiple scattering of the proton beam is minimal, and consequently there is minimal activation of the downstream proton channel.

Muons, of both positive and negative charge, are produced from the decay of the appropriately charged pions, i.e.

| Charge state  | $\pi^+$                             | $\pi^-$                                   |
|---------------|-------------------------------------|---|
| Mean life (s) | $26 \times 10^{-9}$                 | $26 \times 10^{-9}$                       |
| Spin          | 0                                   | 0   |
| Mass (MeV)    | 139.57                              | 139.57                                    |
| Decay mode    | $\pi^+ \rightarrow \mu^+ + \nu_\mu$ | $\pi^- \rightarrow \mu^- + \bar{\nu}_\mu$ |

For muon neutrinos emitted in the decay of  $\pi^+$  the spin and momentum are antiparallel (ie the neutrino has an helicity of  $-1$ ), a consequence of parity violation in the weak interaction. When this decay process occurs at rest, the muon and neutrino must have opposite momenta, and also opposite spins to conserve angular momenta. The resulting muons must therefore be polarised with spins antiparallel to the muon momentum – a crucial requirement for  $\mu$ SR experiments.



As low energy pions come to rest and decay within the target, *fully polarised* beams of positively charged so-called surface muons are produced with energy of 4MeV. It is these intense surface muons beams that are most often used in  $\mu$ SR experiments.

A disadvantage of surface muon production is that any negatively charged muons associated with  $\pi^-$  decay are immediately captured by the target nuclei. In order to produce such negatively charged muons, which have hitherto been underused in condensed matter studies, those pions that have sufficient energy to escape the target are allowed to decay in flight in a region of high longitudinal field. The resulting muons can be selected according to momentum and charge and transmitted to the experimental station.



Surface muons rapidly thermalise within a sample (usually within a depth of a few mm) in a few nanoseconds and without any loss of polarisation. The muons decay with a time constant of  $\sim 2.2\mu\text{s}$ . Detectors positioned around the sample detect and time stamp the arrival of positrons, which in the muon decay process, are emitted preferentially in the direction of the muon spin at the time of decay. The asymmetry distribution associated with the positron emission is of the form  $w(\theta) = 1 + a_0 \cos\theta$ , where  $a_0$  depends upon the positron energy, and  $\theta$  is the angle between muon spin and the direction of positron emission. In a typical experimental set-up integration over a range of positron energies, gives  $a_0 \sim 0.25-0.30$ . From the measured time- and angle-dependent positron counts information on the muon spin relaxation or depolarisation can be extracted and the internal field profiles and dynamics with the sample determined.

### 4.3.2 Muon targets and beams at the ESS

The science that will be performed at an ESS muon facility will, of course, be determined by the characteristics of the muon source and the muon beam lines. The natural pulsed structure of ESS will afford the extremely low backgrounds that currently benefit the ISIS facility, and which enable the measurement of very small depolarisation and relaxation rates associated with very small or rapidly fluctuating internal fields. However the relatively broad proton pulse width at ESS (significantly greater than that at ISIS) presents a serious limitation to measurements of coherent muon spin rotation at frequencies greater than approximately 3MHz, corresponding to modest internal or applied transverse fields of about 0.02T. This limitation can be overcome by electronically time slicing the muon pulse, and distributing the resulting slices between several muon instruments. Such a process is technically feasible (and indeed is used at ISIS) and while pulse widths of 20ns are readily achievable, further reduction to 3ns can be foreseen if beam intensity is sacrificed. However, such narrow pulse widths still cannot provide the flexibility of a true “dc” muon beam required for several classes of experiment. It is therefore extremely important that a quasi-dc muon source is also provided at ESS.

It is suggested that the ESS design incorporates two target stations for muon production. The first, Target station  $A\mu$ , is a low power, low loss target positioned to take advantage of the beam loss at the achromat. This target would serve two quasi-dc surface muon beam lines, and would allow the partially intercepted proton beam to be transmitted, possibly to a further radioactive beam facility

Typical characteristics and operating parameters of Target A $\mu$  are:

|   |                      |
|---|----------------------|
| Target                                  | 5-10mm graphite      |
| Target type                             | water cooled at edge |
| Incident proton current                 | $\sim 75\mu\text{A}$ |
| Power generation in target              | 0.5-1.0kW            |
| Power dissipation in target environment | 4-8kW                |
| Proton loss in target                   | 2.5-5%               |
| Remote handling and rad hard components | minimal              |
| Down stream proton beam component       | minimal              |

The two resulting quasi-dc surface muon beams generated on either side of the proton beam at a  $90^\circ$  production angle will have an intensity,  $\sim 10^6\mu^+/\text{s}$ , which is comparable to that available on the continuous muon facility at PSI. However, it will be possible to utilise the small emittance of the stripped proton beam to produce small final muon spots at the sample positions, thereby affording a considerable advantage over other quasi-continuous surface muon beams. It is also envisaged that crossfield electrostatic separators would be used in both beams as  $\pi/2$  polarisation rotators in order to expand the experimental capabilities.

The second target station, Target B $\mu$ , will be a high power target station upstream of the 50Hz short pulse spallation neutron target. This will be used to generate pulsed muons for two muon channels on either side of the proton beam at  $90^\circ$  to the direction of the proton beam.

|   |                                 |
|---|---------------------------------|
| Target                                  | 2mm graphite                    |
| Target type                             | Radiation cooled rotating wheel |
| Incident proton current                 | $\sim 4\text{mA}$               |
| Power generation in target              | 12kW                            |
| Power dissipation in target environment | 80kW                            |
| Proton loss in target                   | 1.6%                            |
| Remote handling and rad hard components | mandatory                       |
| Down stream proton beam component       | mandatory                       |

The target itself will have the rotating wheel geometry, used successfully for many years at PSI. With a typical thickness of graphite of 2mm in the direction of the proton beam, a surface muon channel viewing this target would collect two orders of magnitude more muons per pulse than is currently available at ISIS (the world's most powerful pulsed muon source). Through the use of rapidly pulsed electrostatic kickers both individual muon pulses and time-sliced muon pulses can be distributed amongst a number of beam lines. In this way at least seven experimental areas can be configured to receive suitable distributed muon pulses. Once again spin rotators will introduce significantly greater flexibility to some of the experimental beam lines.

### 4.3.3 The advantages of ESS muons.

It has already been shown that the a *pulsed* muon source at ESS will be at least two orders of magnitude more intense than that currently available at the world's most powerful source, ISIS (although, because of the time structure of the beam, it may be necessary to sacrifice some of this intensity if pulses significantly narrower than those available at ISIS are required) With suitable electrostatic kickers, at least seven experimental stations can utilise a single pulsed beam.

ESS will also provide a quasi-continuous source of muons, at least as powerful as that at PSI, but with the advantage of much smaller beam profiles – a particular advantage in the study of small single crystal samples.

It should be noted, however, that the ESS provides a number of new, and extremely significant opportunities.

Firstly the orders of magnitude gain in muon intensity at ESS will facilitate the further development and much wider application of slow muon techniques, pioneered at PSI, in which muons are cryogenically moderated to energies as low as a few keV. In this way the depth of penetration within a sample to be tuned to between one and a few hundred nanometres (with 10% straggling) for studies of surface and near surface effects in metallic multilayers, superconductors, self organising systems, catalysts etc.

Secondly the tremendous gains in intensity on the pulsed beam lines will facilitate, for the first time, kinetic  $\mu$ SR studies, in which evolution of field profiles and relaxational processes with time, or under changing environment will be possible, with typical counting times of only tens of seconds per spectra

Thirdly, the development of pulsed RF techniques at ISIS suggests the possibility of effective spin-echo –like time focussing processes which will permit the full beam intensity of ESS to be utilised without recourse to electrostatic pulse shaping.

Finally the extremely efficient pion production process will enable the development of decay beams in which negative muons will be available with sufficient intensity to be used in novel condensed matter science studies, as well as in fundamental physics experiments.

### REFERENCES

For a recent discussion of the production and utilisation of muon beams in condensed matter science and fundamental physics see *Muon Science (edited by S L Lee, S H Kilcoyne, and R Cywinski, published by IOP, Bristol and Philadelphia, 1999)*



**Chapter 5**

**SAMPLE ENVIRONMENT  
AND SCIENTIFIC  
UTILISATION**



## **5. SAMPLE ENVIRONMENT AND SCIENTIFIC UTILISATION**

The ESS will offer a comprehensive range of user and programme support facilities to allow visiting scientists to use the enhanced performance of the source and the instruments most efficiently. These supports extend from the provision of a wide range of simple environment equipment through technical and computer support to comfortable accommodation arrangements.

### **5.1 Sample Environment**

The ESS instruments will be designed in such a way as to allow sample environment to be easily transferred between instruments, as familiar at the major existing neutron facilities. A wide range of general-purpose sample environment equipment will be available. These will include:

- cryostats
- furnaces (non-magnetic furnaces will be available)
- closed cycle refrigerators
- pressure systems
- gas handling equipment
- water baths
- sample Changers
- goniometers
- dilution refrigerators
- magnets

In addition, some instruments or groups of instruments will be equipped with additional special dedicated sample environment such as:

- sheer cells
- troughs for reflectometers
- very high pressure systems
- engineering stress rigs
- pulsed magnets

### **5.2. Technical Support Laboratories**

Laboratory space and equipment will be provided for the development, assembly and preparation of sample environment equipment and necessary beamline components. These laboratories will include:

**Sample Environment Laboratories:**

Separate laboratories will be available for preparing and servicing cryogenic equipment, pressure systems and furnaces, and magnets. These labs will be located close to the experimental halls.

**Detector systems:**

Detector laboratories will accommodate the support and development activities at ESS. The support laboratory will be located close to the experiment halls and carry a comprehensive supply of spares to facilitate quick response to any problems.

**Electronics:**

Like the Detector laboratories, the Electronics laboratories will provide a dedicated support and development role.

**Guides and Neutron Optics:**

The vast majority of the ESS instruments will use supermirror guides, and a large number will use various neutron optical devices. Laboratory facilities will be available for the preparation and assembly of guides and the production and maintenance of used optical devices, such as polarising mirrors.

**Polarisation Devices:**

It is envisaged that polarising filters will be used on many of the ESS instruments. Dedicated laboratories will be available for the development, production and support of polarising filter systems.

**Choppers:**

Chopper support laboratories will be available close to the instruments to provide repair, servicing and assembly and development facilities.

**5.3. Sample Preparation Laboratories**

Laboratory space and equipment will be provided for sample preparation needed by the users. These laboratories will include:

**General purpose laboratories:**

Several general-purpose laboratories containing standard laboratory equipment such as sinks, benches, water, clean water, fume hoods, balances, glove boxes etc will be available within easy reach of all instruments.

**Chemical laboratories:**

Wet chemistry laboratory facilities will also be available, situated conveniently for the instruments most likely to their required use.



**Biology laboratories:**

Similarly a dedicated biology laboratory facility will be available equipped with a cold room and a range of appropriate equipment.

**Instrument specific sample preparation space:**

Additionally to the above mentioned sample preparation laboratories some instruments or groups of instrument will require more dedicated laboratories, such as a surface techniques laboratory close to the reflectrometers and an engineering laboratory close to the engineering beam lines.

**5.4. Computing**

Effective computing facilities will be essential for instrument control, data collection, data storage and transfer and data analysis and visualisation and for the provision of office systems for both staff and visiting scientists. Computing will be supported centrally, but some systems will be tailored to specific instrument needs. Where possible standardisation of software will be employed in order to maximise the quality of support that will be available.

Simulation software will be important for both the design of instruments, but also for planning experiments and as part of the data analysis process. The ESS instrumentation development effort makes extensive use of powerful Monte-Carlo computer simulation codes to assess expected instrument performance, to develop and test new techniques and concepts, to optimise instrument layout, etc.

Powerful and in all detail realistic virtual instrument simulation codes will even gain importance once the instruments become operational. Each ESS instrument will be accompanied by its exact virtual instrument code. So experimenters will be able to plan their experiments by the use of the virtual instrument "flight simulator", optimise the choice of instrument parameters and configuration for the specific goal of the study, take best informed timely decisions on conducting their experiments and use simulation calculations for data reduction, analysis and model refinement. Such an approach will not only largely enhance the efficiency of utilisation of the beam time allocated to each study, but it will also help to gain rapidly interpret the huge quantity of data provided by ESS instruments in a short lap of time, with counting rates exceeding  $10^7$  counts/s on many instruments. ESS will support and offer the software and computer capabilities as best as possible to the users at ESS.

## **5.5. User Facilities**

The ESS user facilities will be based on the best examples of similar facilities. As the strength of the scientific culture at the ESS will depend to a large extent on the effectiveness of interactions between visiting scientists and between staff and visiting scientists, such interactions will be supported by provision of necessary office space for visitors and a suite of seminar and meeting rooms on-site. Good quality on-site accommodation and restaurant facilities will be provided.

## **5.6. Allocation of beam time**

The allocation of time on the ESS instruments will follow the best practice at existing facilities. Proposals will be peer reviewed on a biannual basis.



